Faculdade de Engenharia da Universidade do Porto

U. PORTO
FEUP FACULDADE DE ENGENHARIA
UNIVERSIDADE DO PORTO

Operation of Microgrids in Emergency Conditions

Ana Rita Dias Antunes

THESIS - FINAL VERSION

Master Thesis develop in the context of
Master in Electrical and Computer Engineering
Major Energy

Supervisor: Professor Carlos Leal Moreira
Co-Supervisor: Engineer and PhD Student Clara Gouveia

June 2014

U.PORTO

FEUP FACULDADE DE ENGENHARIA
UNIVERSIDADE DO PORTO

MIEEC - MESTRADO INTEGRADO EM ENGENHARIA ELETROTÉCNICA E DE COMPUTADORES   **2013/2014**

A Dissertação intitulada

"Operation of Microgrids in Emergency Conditions"

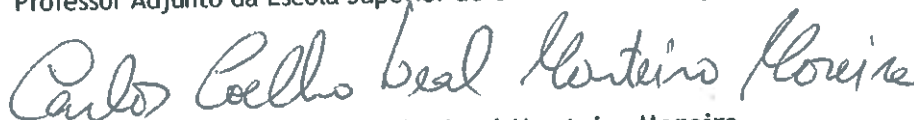foi aprovada em provas realizadas em 17-07-2014

o júri

Presidente **Professor Doutor Carlos Manuel de Araújo Sá**
Professor Auxiliar do Departamento de Engenharia Eletrotécnica e de Computadores
da Faculdade de Engenharia da Universidade do Porto

Professor Doutor Bernardo Marques Amaral Silva
Professor Adjunto da Escola Superior de Ciência e Tecnologia ISPGaya

Professor Doutor Carlos Coelho Leal Monteiro Moreira
Professor Auxiliar do Departamento de Engenharia Eletrotécnica e de Computadores
da Faculdade de Engenharia da Universidade do Porto

O autor declara que a presente dissertação (ou relatório de projeto) é da sua
exclusiva autoria e foi escrita sem qualquer apoio externo não explicitamente
autorizado. Os resultados, ideias, parágrafos, ou outros extratos tomados de ou
inspirados em trabalhos de outros autores, e demais referências bibliográficas
usadas, são corretamente citados.

Autor - Ana Rita Dias Antunes

Faculdade de Engenharia da Universidade do Porto

Abstract

This thesis presents and discusses the microgrid concept, particularly when operating in emergency conditions.

The Microgrid is a low voltage distribution network with distributed energy sources such as Microsources, inverters, storage devices and loads. Operating in a controlled and coordinated mode using an advanced management and control systems, supported by a communication infrastructure. Consequently, the Microgrid has the ability to operate as a coordinated entity, both interconnected (with Medium Voltage network) or autonomously (emergency or islanded operation mode).

For the emergency operation mode, this dissertation presents the impact of the single-phase microsources and the possible control strategies to be adopted. Taking into account the microgrid specific characteristics, namely in terms of the response of each type of Microsource, to achieve robustness of operation and to not jeopardize power quality during this operation.

The proposed microgrid control strategies consider different inverter control modes together with voltage and frequency emergency control functionalities. Given the Microgrid configuration under study this strategies are developed at the Electrical Vehicles and Photovoltaic Panels, in order to maintain a suitable local frequency and voltages magnitudes during islanding operation. The Electric Vehicle strategy it is accomplished by a coordination between primary frequency and voltage control. The Photovoltaic Panels strategy it is achieved by a primary and secondary frequency control.

It was also investigated the benefits resulting from the addition of a Balancing control functionality in the Voltage Source Inverter in order to balance the MG voltages, thus contributing to cancel the negative and zero-sequence voltage components.

Keywords Microgrid, Emergency Operation, Frequency control, Voltage control, Electric Vehicles, Photovoltaic Panels.

Resumo

A atual tese assenta no estudo das condições de funcionamento de uma Micro-rede, particularmente quando opera em condições de emergência (operação em modo isolado).

A Micro-rede é uma rede de baixa tensão com recursos de energia distribuídos como Micro-fontes, inversores, aparelhos de armazenamento e cargas. Operando de modo controlado e coordenado através da utilização de sistemas avançados de gestão e controlo suportados por infraestruturas de comunicação. Consequentemente tem a capacidade de operar como uma entidade coordenada em modo interligado (com a rede de Media Tensão) ou em modo isolado.

Para o modo de operação em condições de emergência esta dissertação apresenta o impacto das micro-fontes monofásicas e as possíveis estratégias de controlo a serem adotadas. Tendo em conta as características específicas da Micro-rede, nomeadamente em termos de resposta a cada microfonte, para atingir uma operação robusta (fiável) e não colocando em perigo a qualidade da potência durante esta operação.

As estratégias de controlo propostas consideram diferentes modos de controlos nos inversores juntamente com as funcionalidades de controlo emergência de frequência e tensão. Dada a configuração da Micro-rede estudada, as estratégias são desenvolvidas nos carros elétricos e nos painéis fotovoltaicos, tendo como objetivo manter os valores locais de frequência e tensão aceitáveis durante o isolamento. No caso dos veículos é feita uma coordenação entre o controlo de frequência primário e o controlo de tensão primário. No caso dos painéis é feito um controlo primário e secundário da frequência.

Foram ainda avaliados os benefícios resultantes da adoção de mecanismos de compensação dos desequilíbrios de tensão sobre os inversores do tipo "fonte de tensão. Estes mecanismos têm por objetivo o cancelamento da componente inversa e homopolar das tensões na micro-rede.

Palavras-Chave: Micro-rede, Condições de Emergência, Controlo de frequência, Controlo de Tensão, Veículos Elétricos, Painéis Fotovoltaicos.

Acknowledgements

This Master dissertation is the result of the work developed at the Power Systems Unit of INESC Porto during the dissertation period. It is a great pleasure for me to work in this institution, where I am having the opportunity to collaborate with people internationally recognized for their contributions to the development of the Electric Power Systems.

First, I want to express my sincere gratitude to my supervisor, Professor Carlos Coelho Leal Moreira, for his skilled guidance, valuable comments, constant support and encouragement. His focus vision and demand were fundamental in order to overcome the difficulties that came about during the development of this thesis.

I would like to thank my co-supervisor Clara Gouveia, for her fundamental help during this dissertation and to Luís Seca, INESC Power Systems Unit Coordination Assistant who made possible my integration in this project. To my Power Systems Unit colleagues I express my thankfulness for the support in the development of this dissertation: Ruben Soares, Nuno Fulgêncio, Paula and Rute. I also would like to thank Sara Costa, Renata Monteiro, Isabel Carneiro and João Santos for their friendship.

Last but not the least, a special acknowledgement to my parents, sister, brother in law, boyfriend Daniel Sousa and his mother Sheila Nolan Sousa for all the support, constant encouragement and optimism they gave me during the development of this thesis.

Contents

List of Figures

List of Tables

Abbreviations and Symbols

List of Abbreviations

MG	Microgrid
DG	Distributed Generation
CHP	Combine Heat and Power
DER	Distributed Energy Resources
MT	Microturbine
FC	Fuel Cell
MS	Microsource
CERTS	Consortium for Electric Reliability Technology Solutions
EV	Electric Vehicles
HV	High Voltage
MV	Medium Voltage
LV	Low Voltage
RES	Renewable Energy Sources
MGCC	MG Central Controller
MAS	Multi-Agent Systems
AC	Alternating Current
DC	Direct Current
DER	Distribution Energy Resources
PMSG	Permanent magnet synchronous generator
PV	Photovoltaic
SOFC	Solid Oxide Fuel Cell
SSMT	Single-shaft microturbine
PEV	Plug-in Electric Vehicles
BEV	Battery Electric Vehicles
PHEV	Hybrid Electric Vehicles

MERGE	Mobile Energy Resources on Grids of Electricity
VC	Electric Vehicles controller
V2G	Vehicle-to-Grid
FAPER	Frequency Adaptive Power Energy Reschedule
DDC	Dynamic Demand Control
AHC	Adaptive hill climbing
VSI	Voltage Source Inverter
SMO	Single master operation
MMO	Multi master operation
DDC	Dynamic Demand Control
AHC	Adaptive Hill Climbing
SM	Smart Meter
MC	Microsource Controller
VC	Electric Vehicle Controller
LC	Load Controller
MAS	Multi-Agent Systems
PCC	Point of Common Coupling
MPP	Maximum Power Point

List of Symbols

V_a; V_b; V_c	Phases voltages
V^0; V^-; V^+	Zero sequence, positive and negative voltages components
$\%VUF$	Voltage Unbalance Factor
ω	Angular Frequency
k_P; k_Q	Droop slopes (positive quantities)
P	Active power
Q	Reactive Power
ΔP_i	Active power injected by i-th
ω_{grid}	MG angular frequency
Δf	Mg frequency error
f_{ref}	Reference Frequency
f_{meas}	Measure Frequency
P_{set}	Power set-point (for frequency or voltage)
f_0	Zero-crossing frequency
V_0	Zero-crossing voltage
I	Photovoltaic Current

I_L	Light generated current
I_D	Diode current
I_0	Diode reverse saturation current
R_s; R_{sh}	Series and shunt resistances
T_1, T_2	Fuel system time constants
T_3	Load limit time constant
V_{max}, V_{min}	Maximum and minimum fuel value positions
k_t	Temperature control loop gain
L_{max}	Load limit
L_d, L_q	d and q axis inductances
R_s	Stator windings resistance
v_d, v_q	d and q axis voltages
i_d, i_q	d and q axis currents
Φ_m	Flux induced by the permanent magnets in the stator windings
p	Number of pole pairs
T_e	Electromagnetic torque
T_m	Local mechanical torque
J	Combined inertia of the load, PMSG, shaft, turbine and compressor
F	Combined viscous friction factor of the load, PMSG, shaft, turbine and compressor
P_C	Power balance in the capacitor of the DC-link
P_{MS}	Power received from the Microsources
P_{inv}	Inverter output power
V_{DC}	DC-link voltage
I_{DC}	DC-link current
v^*	Inverter internal voltage
i_{ref}	Reference current
$\bar{v}$; $\bar{\imath}$	Voltage and Current instantaneous space vectors
p	Instantaneous Active power
i_a; i_b; i_c	Phases currents
q_a; q_b; q_c	Phases reactive power
q; $\bar{q}$	Instantaneous Reactive power
$\hat{v}$; v_{RMS}	Voltage Values
$\underline{s}$	Power
db	Dead-band
P_{max}	Maximum EV Power
P_C	Dead-band EV Power
P_{min}	Minimum EV Power

$PV_n max$	Photovoltaic maximum power injection
P_{VSI}	VSI Power charging
$PV_{n\,set-point}$	Photovoltaic Power set-point
W	Watt unit
V	Volt unit
A	Ampere unit
s	Second unit
H	Henry unit
Ω	Ohm unit
Hz	Hertz unit
$rad.s^{-1}$	Radian per second unit
$kg.m^2$	Kilogram square meter unit
$N.m$	Newton meter unit
Wb	Weber unit
Var	Volt-Ampere unit

Chapter 1

Introduction

1.1 - Thesis Context

Until recently, Microgrids (MG) were used mainly in Military bases, particularly in USA Military Units, or in areas subject to natural disasters where the ability to operate autonomously (islanded operation) is of utmost importance regarding continuity of service [1].

Nowadays, the penetration of Distributed Generation (DG) at Medium and Low Voltages, both in utility networks and downstream of the meter, is increasing worldwide [2]. Consequently, it requires structural changes on the power system operation, planning and engineering.

The small Combine Heat and Power (CHP), provide by the conversion of the fuel waste heat to electricity by gas turbine, and microturbine (MT) or fuel cell (FC), together with small renewables systems, heat and electricity storage, and also with controllable loads, are expected to be important in future electricity business models. All these elements becoming nowadays available in the electric distribution grids and are usually referred as Distributed Energy Resources (DER) [2].

The connection of small generation unit—the Microsource (MS), with power ratings less than a few tens of kilowatts—to LV networks potentially increases reliability to final consumers and brings additional benefits for global system operation and planning, namely, regarding investment reduction for future grid reinforcement and expansion[3].

The Consortium for Electric Reliability Technology Solutions (CERTS) initiated the research on the impact of connecting large amounts of DER to LV networks in order to enhance the reliability of the electric power system and developed the MG concept.

Therefore, the large penetration of small and large-scale power generation units and their production variability impose additional technical challenges. For this reason, in the past

decades, a serious standardization effort was made, in order to establish interconnecting requirements for different generation technologies, addressing mainly:

- Power quality problems,
- Harmonic distribution,
- Voltage magnitude limits,
- Protection and connection requirements.

The commitment of reduce CO_2 emissions in the electricity generation field, make indispensable the utilization of DER or Renewable Energy Sources (RES) for the most developed countries.

Considering the 2050 decarbonizing objectives, the distribution network will have to deal with the increase of RES both at the transmission and distribution network and at the same time accommodate new loads such as the Electric Vehicles (EV) [3].

Therefore, in order to maintain power systems reliability further development on innovative active management and control strategies are required [3]. Coordinating the RES with flexible resources such as storage, EV and responsive loads. The development of an active distribution network is part of the Smart Grid vision [3].

The Smart Grid is defined as an electricity grid supported by a bi-directional information and communication infrastructure capable of accommodating a high share of RES based generation, EV and enables the local energy demand management to interact with end-users, through smart metering systems [3].

The following figure presents the power evolution with smart grid concepts implementation.
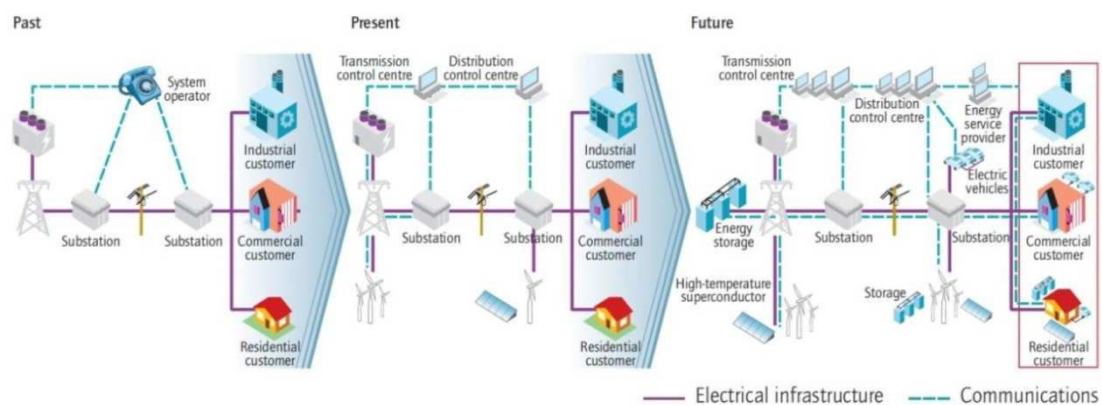
Figure 1.1 - Power Evolution with Smart Grid [4].

As the number of DER and EV increases in the distribution network, it is necessary communication and control infrastructure to support proper system operation. That will be constituted by a decentralized management system with several control levels, which

incorporate intelligent monitoring, control, and self-healing functionalities. Under this new paradigm, the LV network is managed exploiting the Microgrid structure [4].

The MG is a highly flexible, active and controllable LV cell, has at least one distributed energy resource and associated loads, which are controlled and coordinated though an appropriated network of controllers.

Within MG, loads and energy sources can be disconnected from and reconnected to the area or local electric power system with minimal disruption to the local loads, with the possibility to form small electric islands.

Any time a MG is implemented in an electrical distribution system, it needs to be well planned to avoid causing problems. When major disturbances occur in the upstream network, the MG emergency mode is activated and the MG isolates from the upstream grid, being able to coordinate local generation resources, storage devices and flexible loads, in order to operate isolated from the upstream grid, through the adoption of specific control strategies [3].

Several projects have been addressing the MG emergency operation, developing specific control strategies and in less extent through experimental laboratorial and pilot field-tests [3]. However, being one of the key pieces for the implementation of future smart distribution networks, the MG requires innovative control functionalities in order to fully integrate the EV and new demand response strategies in the emergency operation, in order to improve the MG stability when operating autonomously [3].

According to the topic of this thesis, providing a successful MG emergency operation with adequate values of frequency and voltage in the system it is essential to analyse the behaviour of the MG operating under unbalanced conditions and study new strategies to mitigate this problem.

1.2 - Motivation and Thesis Objectives

The evolution of microgeneration technologies increase the integration of Distributed Generation in High Voltage (HV) and Medium Voltage (MV) networks and consequently also at the Low Voltage (LV). Therefore, a new paradigm appears in the electric power systems operation - the Microgrid - that is growing quickly.

The MG is a LV network connected to small microgeneration units (fuel cells, microturbines, solar photovoltaic panels, small wind generators, energy storage units, etc.), and it is a system totally controlled by appropriated mechanism.

The highest integration of microgeneration in the present days it is Photovoltaic Panels and in a close future will be the electrical vehicles, which requires at certain moments of MG operation a coordination in order to maintain the operation security of the system.

The storage devices and the flexible loads are also important elements in the Microgrid that need to be coordinated with other network elements.

The MG can operate in two ways, interconnection with the medium voltage grid upstream or autonomously (operating in emergency mode) following disturbances of the upstream network.

Operating in emergency mode, the characteristics of the MG LV network- high resistance levels in comparison with the reactance - requires the identification of voltage regulation mechanisms through active power control, thus being a possible conflict with the frequency regulation. Additionally the significant number of single-phase loads and Microsources may cause significant voltage unbalances, mainly during islanding operating conditions.

In this context, the study of this thesis aims the development of the necessary control strategies, in the adequate elements of the MG. In order to coordinate the frequency and voltages at system and improve their values, particularly during emergency operation mode.

Thus, the main objectives of the thesis can be stated as follows:

- Study the mathematical models of Microsources dynamic response characteristics and respective power electronic interfaces;
- Exploit MG dynamic simulation platforms in order to address the operation of the system under severe conditions (such as unbalanced operation with high power production and low load);
- Identification of potential problems resulting from voltage and frequency control functionalities in microgrids islanding operation conditions;
- Identification of coordination actions to improve microgrid operation during islanding operation regarding the potential interaction between voltage and frequency control functionalities;
- Validation of the coordination actions through extensive simulation.

1.3 - Document Outline

The present document is organized in six main chapters, and between the second and the fifth chapter each one has a last section of *Summary and Main Conclusions*. The first one contextualizes the problem under investigation, introduces the motivation and the main objectives that this dissertation aims to achieve.

The second chapter reviews the MG concept regarding their emergency operation, starting to describe the types of micro distributed energy resources that can integrate the MG. After that, it is present the MG architecture and communication infrastructure, their problems of control and operation and penult section the MG operating in emergency conditions. In this last section it is possible to find the emergency operation control and their regulation functionalities, followed by the researchers used in this dissertations.

The Chapter 3 presents the MG dynamic models, considering both three-phase and single-phase connections to a three-phase four wire LV network. The EV single-phase dynamic model is based on the INESC research as well as the implementation of frequency regulation mechanisms.

Since one of the outlined objectives of this thesis is the development of control strategies to minimize the disturbances impact during the isolation, in the fourth Chapter it is described all the control strategies projected. The Chapter is divided in 3 major sections assigned to each type of component which performs some sort of control.

The Chapter 5 represents the simulation results with the purpose of: first understanding one of the causes that lead to the MG problems, second to build and validate the control strategies stated, in the previous chapter, and finally to see the potential of the Balancing Unit, to balance the MG operation condition.

In chapter 6 the main conclusions are made and also some suggestions for future work.

Chapter 2

Microgrids Emergency Operation

The Distributed Generation deployment can potentially reduce the demand for distribution and transmission facilities. Consequently, the distributed generation located close to the loads will [14]:

- Reduce the flows in transmission and distribution circuits - with important effects such as loss reduction and ability to potentially defer reinforcement or upgrade investment costs;
- Reduce the customer interruption times - in islanded operation following disturbances in the upstream system.

The increasing of DG penetration in Medium Voltage networks is expected to become one possible approach to face the continuous electricity demand growth.

The "fit and forget" policy it is the current practice for the DG units connection to the distribution network, but this massive integration may cause more problems.

Therefore, the MG concept presented in this chapter, appears as a DG integration strategy in order to better exploit the potential benefits that DG and other DER management may provide.

This microgrid concept, that will be presented in detail, consists in the aggregation of loads and microsources operating in a single system with appropriate management and control functionalities, providing both power and heat to local consumers, aims to be a possible solution for the referred MS integration strategy.

Moreover, the MG concept leads to the development of an active cell of the distribution network, which has the ability of autonomous operation. Exploiting such an active cell of the distribution network – the Microgrid – as an entity that is able to be operated autonomously or interconnected with the upstream MV network [14]. Providing high flexibility and contributing with important benefits to the distribution network operator and to the end-user [14].

2.1 - Types of Micro Distributed Energy Resources

The DER described below, are usually connected to the MV distribution network, or to the LV grid, and represent the possible elements that could explore better the needs of MG system. They are divided in five groups described by the next following order.

2.1.1 - Microsources

This kind of energy conversion technologies are usually available in power units with less than 100 kW and are potentially adequate to be connected to LV distribution grids.

The most typical MS are briefly described below:

- Micro-Wind: or Micro variable speed wind turbine (<5kW) is couple directly to a three-phase or single-phase squirrel-cage induction generator or to a permanent magnet synchronous generator (PMSG) mounted on the same shaft. The PMSG is more preferred because it is mounted on the same shaft as the micro-wind turbine, avoiding the need for brushes. Although, this type of generator produces variable frequency and AC (Alternating Current) voltage according to the wind speed, requiring an AC/DC/AC inverter to couple the system to the LV network.

- PV (Photovoltaic) technologies: energy production depends on the quantity of irradiation at PV and produces DC (Direct Current) voltage, being necessary a DC/AC converter connected with the PV. Based on International Energy Agency in 2030 PV power installed will reach 200GW against the 13GW of2008 [3].

- Fuel Cells: electrochemical devices that convert chemical energy directly into electricity. This system contains a stack of several fuel cells that achieve adequate DC voltage and power levels, requiring a DC/AC converter to couple them to the grid. There are many types of fuel cells, classified according to the fuel and electrolyte adopted. Though, fuel cells such as Solid Oxide Fuel Cell (SOFC) are usually considered for micro-CHP applications, since they operate with high temperatures, producing waste heat that can be used for heating purposes. High temperatures fuel cells allow the use of a great diversity of fuels, namely hydrocarbons based fuels, such as natural gas, methane and propane gases [3].

- Microturbines: small gas turbine that can operate on a great variety of fuel types, such as natural gas, biogas and diesel amongst others. Typical power outputs range from a few kW to 300kW [3]. The most common configuration, is the single-shaft microturbine (SSMT), where the turbine and the PMSG mounted in the same shaft, with air compressor.

The microsources can be classified in three ways [13]:

- Depending on their type of primary energy source: described previously;
- Depending on their control capacity to inject active power in the grid:

- o Controllable: small co-generation units and storage units (Microturbines and Fuel Cells);
- o Partially controllable: renewable sources that can reduce output only (Micro-wind);
- o Non-controllable: PV technologies.
- depending on their type of function at MG:
  - o Grid forming unit: define the grid voltage and frequency reference by assuring a fast response in order to balance power generation and loads (Diesel generation or an inverter coupled to a Storage device);
  - o Grid supporting unit active and reactive power: allow some form of dispatch upon their power production levels, according to system voltage and frequency characteristics (Microturbines and Fuel Cells);
  - o Grid parallel unit: operate in order to inject as much power into the grid as possible (non-controllable and partially controllable).

2.1.2 - Storage systems

Storage technologies can be divided according to their degree of efficiency for power or energy applications:

- Power applications - frequency regulation: built on droop characteristics and ramp rate control for variable generation, require storage technologies with the capacity of provide rapid injection or absorption of power during system transients. The technologies more adequate for this purpose are flywheels, supercapacitors and some type of batteries such as lithium.
- Energy applications - peak shifting: to complement the power generation patterns from variable generation, such as wind, which can have higher power production during off-peak hours. The technologies more suited are flow batteries (vanadium and zinc bromine), valve-regulated lead-acid and sodium batteries having higher energy capacities.

Contrarily to power applications, energy applications require storage technologies with a high energy capacity, ensuring the delivery of energy over a considerable length of time [3].

All the storage technologies referred, can be used for both power and energy applications, depending on the system requirements and economic factors [3]. The choice of the adequate technology should consider parameters such as: power capacity, energy storage capacity, response time and cost should be taken into consideration [3].

Flywheels and batteries can be used for the MG centralized storage, installed at the MV/LV substation.

However the first ones are usually considered, since they are able to provide fast power balance during system disturbances and there, life cycle is almost independent on the depth of discharge and its state of charge.

The second ones can also be used as distributed storage units connected to the DC link of several MS. Deep cycle batteries are able to provide frequency and voltage regulation and at the same time provide some energy applications.

Super-capacitors present a better performance over conventional batteries regarding their power density lifetime, cycle life and temperature sensitivity, being able to storage large amounts of energy when compared to conventional batteries (lead-acid or nickel-cadmium) [3]. However, their high initial costs and low energy density prevents them from replacing conventional batteries [3].

2.1.3 - Electric Vehicles

In the next years, the MG will have to integrate a new load resulting from the charging of the EV batteries.

Plug-in EV (PEV) family includes battery EV (BEV), hybrid EV (PHEV) and fuel cells EV. BEV and fuel cell EV are powered exclusively by electricity, while PHEV have an internal combustion engine, extending the EV autonomy [3].

The time required to fully charge the EV batteries will depend on the charging power. Under the European project Mobile Energy Resources on Grids of Electricity (MERGE) three charging levels were identified, as indicated in following Table [3].

Table 2.1 — EV typical charging levels [3].

Charging Level	Requirement	Typical charging power	Approximate charging time (35 kWh battery)
Level 1	Standard domestic outlets	3 kW	12 hours
Level2	Dedicates charging outlets	10 – 20 kW	2 – 4 hours
Level 3	Dedicates charging outlets and wiring	≥ 40 kW	≤ 45 minutes

Charging levels 1 and 2 will correspond to single-phase AC charging, most common to be perform in domestic or private charging points. Level 1 charging can be performed by connecting the EV charging plug to a standard electric outlet, while level 2 charging will require a dedicated charging interface due to the higher charging power. Charging level 3 can be performed through a three-phase AC connection or through DC dedicated off-board charger, to provide direct DC current to the EV. This level of charging can be provided by public fast charging stations [3].

Smart management system has been proposed to actively integrate the EV in the power system operation. The long period of time which EV are expected to be connected to the LV network along with the predictability of its power consumption, makes them good candidates for the development of dedicated load control strategies.

In [7], the authors classify the EV charging strategies in two main categories:

- Uncontrollable: the EV is envisioned as a conventional load, being the EV owner free to charge the vehicle in any time of the day.
- Controllable: the EV controller (VC) will receive specific control signals to control the EV battery charging. Include smart charging and Vehicle-to-Grid (V2G) strategies.

In the smart charging strategy the EV charging power can be controlled by an aggregating agent and other by the DSO, in order to reduce or increase the EV charging power [7].

In the V2G charging mode, the EV charging interface admits bi-directional power flow, enabling the EV to inject active power into the grid, with some drawbacks related with the batteries degradation. Batteries have a finite number of charge/discharge cycles and its usage in a V2G mode might represent an aggressive operation regime due to frequent shifts from injecting to absorbing modes [3]. Thus the economic incentive to be provided to EV owners must be even higher than in the smart charging approach, so that they cover the eventual battery damage owed to its extensive use [7].

When the grid is being operated near its technical limits, or in emergency operating modes, e.g. islanded operation, the system operator overrides the aggregator control signal, in order to control the EV charging. So, the flexibility of the EV loads and provision of short-term storage capacity allows an increase in the safe integration of MS and improves the frequency regulation of the MG in islanded mode, reducing the need for centralized storage [7]. The EV control strategies for emergency operation will be addressed more forward.

2.1.4 - Inverters – Grid Coupling devices

The inverters, or power electronic interface (DC/AC or AC/DC/AC), are essential to MS, storage units and EV, because the inverters convert power output into grid-compatible AC power.

As already motioned:

- Photovoltaic panels are DC sources requiring a DC/AC converter to convert their power output into grid-compatible AC power;
- Micro-wind turbines and SSMT are AC sources, requiring AC/DC/AC inverters in order to convert their power output into grid-compatible AC power.

A good way to understand the inverters characteristics is to compare with electrical machines, knowing that inverters intrinsically do not have inertia. In reference [3] the

authors compare the characteristics of conventional synchronous machines to the ones of the inverters. The main differences are pointed out in the following table.

Table 2.2 — Comparison between the characteristics of electrical machines and inverters [3].

Electrical Machines	Inverters
Operate as voltage sources. Voltage amplitude adjusted by closed-loop excitation control scheme.	Can operate as voltage or current source. Independent control of the magnitude and phase
Sine-wave voltage: dependent of the machine design and construction.	Sine-Wave can be achieved through the use a modulator, but any shape can be achieved as desired.
Low voltage harmonic distortion.	Filtering is needed to reduce the emission of high frequency distortion, produced by switching actions.
High short circuit current.	The short circuit current should be limited to avoid damaging the power electronic components.
Real power exchange is dictated by the torque applied to the shaft.	Real power exchange is dictated by the references applied to the control system.

The inverters control system is responsible for:

- Controlling the active and reactive power exchanged with the grid, ensure high quality power and grid synchronization;
- Ancillary services required by the grid operator, local and frequency regulation, voltage harmonic compensation or even active filtering.

The two most common control strategies used for the inverters connected to the power systems are:

- PQ inverter control: the inverter inject a given active and reactive power into the grid. The control is implemented as a current-controlled voltage source, with the objective of exporting a controlled amount of power (active and reactive) to the grid (these inverters are usually referred as grid tied inverters). The PQ controlled inverter does not have the ability of imposing voltage and frequency.
- Voltage Source Inverter (VSI) control: the inverter control the phase and magnitude of its output voltage. Therefore, it behaves as a voltage source and can emulate the

behaviour of the synchronous machines, through the adoption of droop characteristics.

The operational characteristics of the inverters will help understand the operation and control issues to be faced in the MG operation, particularly during emergency conditions.

2.1.5 - Microgrid Loads

The MG can supply loads such as residential, commercial or small industrial customers which could be connected to LV networks mainly by single-phase, with exception of larger loads requiring three-phase connections.

The Residential and commercial are usually constituted by smaller loads compared to the industrial ones, with larger induction motors or other types of machinery.

The majority of thermostat controlled loads such as air conditioners, refrigerators and space and water heaters have thermal storage while dish and clothes machine present long running cycles. These characteristics make them good candidates for participating in demand response schemes, where their connection/disconnection may improve the system frequency and voltage regulation capacity [3]. Increasing load flexibility particularly gives additional resources for the MG emergency operation, although this approach was not consideration, only loads with constant impedance [3].

The MG, at emergency operation, relies in local storage and generation capacity to supply the loads and maintain power balance. However, if the MG has insufficient generation reserve capacity to supply load, part of the MG loads will have to be disconnected until the MG is re-synchronized to the MV network.

The MG load shedding schemes are usually under-frequency or based on the rate-of-change-frequency relays [3]. In this case the MGCC will remotely control interruptible equipment such as electric heating load, air conditioners, swimming pool pumps or manufacturing equipment, or in case of severe disturbances disconnect customer's premises [3]. However, if the MG has sufficient generation capacity, some demand response strategies may help dealing with transient disturbances resulting from load or variable generation, compensating the slow response of MS to power control signals [3].

Demand side management strategies developed to give support to the system during transient periods are usually based on the system frequency.

In the MG case the contribution of such frequency load control methods would depend on the amount of load available for control and does not avoid load curtailment due to generation reserve shortage. However, the following cases were all tested for large power systems with sufficient generation reserve capacity to supply the loads:

- In [8] in 1980, was proposed a load reduction method based on frequency measurements: a Frequency Adaptive Power Energy Reschedule (FAPER), switch on/off one or a group of equipment installed based on the local measurement of

frequency. More specifically, the load will disconnect in case of a sudden load increase or generation loss and reconnecting after some time when the frequency of the system recovers through secondary control, providing spinning reserve to the system.

- In [9], the authors developed a Dynamic Demand Control (DDC) method dedicated in particular to refrigerators: an alternative controller to the conventional thermostat, which will connect/disconnect the refrigerator based on the frequency in addition to the freezer air temperature. This method avoids additional disturbances due to the on/off cycles of conventional thermostat controlled refrigerators. The results presented have shown that the DDC method potentially improve power system stability, when facing the sudden loss of generation, increase of load or dealing with a large penetration of variable generation.

- According to [10] a load reduction algorithm is proposed considering the local frequency measurement from smart meters. This load control method aggregates typical domestic appliances according to the level of discomfort caused to consumers due to its disconnection. Thermostat controlled loads and appliances with long running cycles will disconnect for smaller frequency disturbances (>0.3 Hz) and during longer periods of time (5 min), while resistive loads and lighting will only be disconnected for frequency disturbances superior to 0.7 Hz.

Regarding the MG operation, some demand response strategies have also been proposed [3]:

- In [11] an Adaptive Hill Climbing (AHC) load control method was proposed, in order to improve the MG voltage and frequency regulation: determines the minimum percentage of responsive loads which should be disconnected/ connected based on the MG frequency deviation. The commands will then be sent to the electric water heaters controllers. The method was tested considering a small system with a diesel generator, which ensured secondary frequency control. In order to effectively contribute to the MG primary frequency control, the system would require a robust communication network, ensuring a maximum latency of 500ms.

The frequency responsive load control methods based on local frequency measurements do not have such communication requirements and will not depend on the communication infrastructure to respond to the MG frequency changes. However, they also require an accurate local frequency measurement [3].

2.2 - Microgrids

The MG can also be defined as a low voltage distribution grid incorporating local generation, storage devices, responsive loads and in the future Electric vehicles.

Coordinate the control of the MG its realized by hierarchical control structure, develop according MG specific requirements and providing the required flexibility.

The exploitation have a centralized control strategy that require multiple high data rate bidirectional communication infrastructures, powerful central computing facilities and a set of coordinated control centres. Consequently, is not attractive for a practical realization due to the inherent high costs of a high data rate and extremely reliable telecommunication and control infrastructure.

MG control strategies should be based on a network of controllers with local intelligence, in order to guarantee an efficient and reliable control under abnormal operation conditions

The information exchange should be limited to the minimum necessary to achieve the optimization of MG operation when the MG is connected to the main grid, to assure stable operation during islanding conditions and to implement local recovery functionalities after a general failure (local Black Start functionalities).

MG operation and control specificities bring a set of issues, including safety, reliability, voltage profile, power quality, protection, unbalance/asymmetry and non-autonomous/autonomous operation.

The MG application can be divided in two major parts [6]:

- *MG operating as a MV customer*, with the main Operation objective to meet the customer's and economic requirements, while being capable of providing services to the upstream grid.
- *MG as an extension of the distribution network management system:* Ensure technical management and control of the LV network (for large amounts microgeneration technologies, EV and responsive loads).

Knowing the applications referred, the microgrid can operate in the two following ways:

- *Normal Interconnected Mode:* MG is connected to a main MV network, each being supplied by it or injecting a quantity of power into the main system.
- *Emergency Mode:* MG operates autonomously, in a similar way to a physical islands, when disconnected from the upstream MV network.

In order to be flexible and controllable, the MG power infrastructure is supported by a communication (bidirectional) and information system constituting the MG technical management and control system. This local intelligence is responsible for controlling local resources and enable innovative self-healing operation strategies [6].

2.2.1 - Architecture and Communication Infrastructure

The basic architecture of a MG have an hierarchical/decentralize structure composed by a network of local controllers connected to each MG element and headed by a central manager agent installed at the MV/LV substation, the MG Central Controller (MGCC), represents by the following figure.
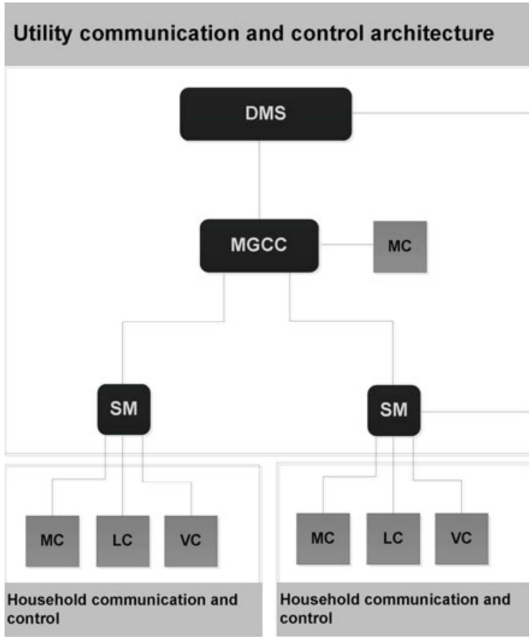
Figure 2.1 - Smart distribution network architecture based on MG concept [6].
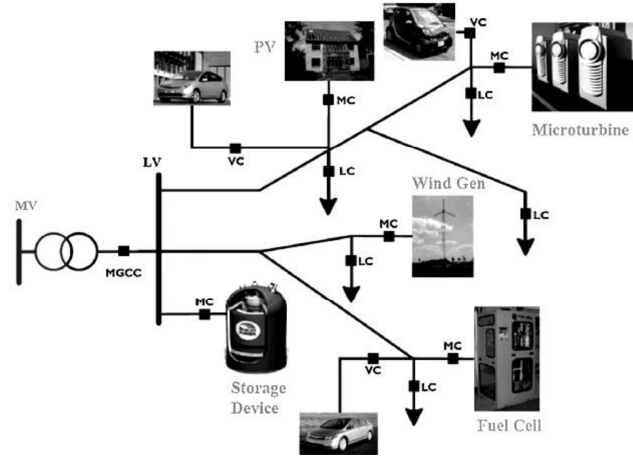
Figure 2.2 - MG architecture, comprising MS, loads and control Devices [3].

MGCC, such as first hierarchical control level, concentrates the high level decision making for the technical and economic management of the MG. Its functions are different for the each type of MG operation mode:

- _Normal Interconnection Mode_ includes: MS dispatch, voltage coordination, security assessment and load and micro-generation forecasting;
- _Emergency mode_: perform a secondary control to ensure that MG voltage and frequency are returned to their nominal values.

The MGCC also includes software modules responsible for managing restoration procedures at the MG black start [3].

The Smart Meter (SM) support bidirectional communications between the local controllers and the MGCC. Operating also as a local gateway, aggregating the information related with power consumption, generation, service interruption, voltage and other relevant data.

Given the different characteristics of the MG resources and the fact that local controllers are the second hierarchical control level, the three types represented are:

- MC- Microsource Controller: connected to the MS and to the Storage Device. It is also, responsible to control active and reactive power production levels for each MS,

- <u>VC- EV Controller:</u> connected to the EVs and responsible to control the levels of active power receive and injected for each EV,
- <u>LC – Load Controller:</u> interfaces to control loads.

They are responsible to control their own entities based on set-points received from MGCC, at Normal Interconnection mode. In emergency mode provide primary frequency and voltage regulation, ensuring the survival of the MG following islanding.

Summarizing, the amount of data exchanged between network controllers is small, since it includes mainly messages containing set-points to LC and MC, information request sent by MGCC to LC and MC about active and reactive power, voltage levels and messages to control MG switchers [3].

At *Normal Interconnection Mode* the MG distributed functionalities are based on Multi-Agent Systems (MAS) concept, which requires advanced communication infrastructures to ensure the bi-directional flow of information between all the agents, located in different nodes of the LV network [3].

The dependence on communication infrastructures associated to distributed architectures is particularly concerning for the MG emergency operation, where the stability and success of the MG autonomous operation requires fast acting controllers [3].

2.2.2 - Problems of control and Operation

The increasing trend of connecting DG to MV and LV grids brings challenging problems that will require the adoption of more ambitious concepts. That are related to active management of the distribution grids, where loads, storage devices and DG can be used together to improve the overall system efficiency, the quality of electricity supply and the overall operating conditions, leading to a fully active distribution network.

2.2.2.1 -General Technical Problems

The consequences of these DG connections arise mainly due to the changes induced in the network power flows, affecting not only its magnitude but also its direction.

In order to overcome the technical problems resulting from DG integration, several authors suggest advanced control techniques oriented to a specific technical problem at a time and not an integrated solution for all the aspects [14].

The main technical aspects that usually need to be evaluated in the grid are:
- Voltage profile;
- Steady state and short-circuit currents;
- Distribution network protection schemes;
- Power quality;
- Stability;

- Network operation;
- Islanding operation.

2.2.2.2 -Emergency Operation Problems

The MG comprises a large number of single-phase loads and generation units, requiring three-phase with neutral conductors. Therefore, depending on the distribution of DER among phases, voltage unbalance within the MG will be prone to appear.

The unbalanced voltages can be defined such as:

- Different voltages magnitudes between them at fundamental frequency of the system;
- Unequal Offsets between phases;
- Different levels of harmonic distortion between phases.

The way to detect the voltages unbalance is through the negative and zero sequence components of three-phase voltages:

- Determining the respective magnitude voltages – Measurements in unbalance system:

$$
\begin{bmatrix} V_a \\ V_b \\ V_c \end{bmatrix} = \begin{bmatrix} 1 & 1 & 1 \\ 1 & a^2 & a \\ 1 & a & a^2 \end{bmatrix} \times \begin{bmatrix} V^0 \\ V^+ \\ V^- \end{bmatrix} (V) \tag{2.1}
$$

Where:

$a = e^{j120^0}$;

V^0; V^-; V^+ are the Zero sequence, positive and negative voltages components (V)

The negative sequence component have major impacts at, LV loads, induction machines (produces a opposite torque) and power electronic converters and dives.

- Determining the voltage unbalance factor ($\%VUF$) for negative and zero sequence voltages:

$$
\%VUF_{neg.} = \frac{V^-}{V^+} \times 100\% \quad and \quad \%VUF_{zero\ seq.} = \frac{V^-}{V^+} \times 100\% \ (\%) \tag{2.2}
$$

These two factors must be below the 2% defined in the EN50160 that represent an acceptable value.

Recently, new active voltage compensation strategies have been developed to be implemented at the storage and MS grid-coupling inverters [3].

The grid side inverter can be controlled in order to minimize harmonic distortion and, if it is gifted with storage, additional control loops can be implemented in order to compensate voltage unbalance.

For adequate voltage compensation, the Voltage Source Inverter connected to the main storage can be equipped with a voltage balancing mechanism [3]. The VSI balancing unit is

able to provide three independent output reference voltages, regardless of the MG loading conditions.

Summarising, the solutions for this kind of problems are operational strategies executed by the MG inverters. So, Intended for global MG optimization will run periodically (few minutes) in the MGCC and the resulting dispatch (voltage set-points, active and reactive power set-points, loads to be shed or deferred in time, etc.) will be communicated to local controllers (MC and LC) in a second stage corresponding to a larger time frame. The model and implementation of the controllers will be discussed in detailed in 0.

2.3 - Microgrid Operating in Emergency Conditions

The MG islanding concept is emerging in the electrical power systems domain. The establishment of an autonomous MG by exploring the MS generating capabilities installed at a certain LV area is the main concept that is explored within this thesis.

The conventional idea about MG emergency mode is when major disturbances occur in the upstream network, where the mode is activated and the MG isolates from the upstream grid. Being able to coordinate local generation resources, storage devices and flexible loads, in order to operate isolated from the upstream grid, through the adoption of specific control strategies, to maintain suitable voltage and frequency levels in the system.

Without synchronous machines, to balance demand and supply through its frequency control scheme, the inverters are responsible for frequency control during islanded operation and furthermore a voltage regulation strategy is required. Otherwise, the MG might experience voltage and/or reactive power oscillations.

2.3.1 - Emergency Operation Control

With a considerable group of MS operating in MG and the main power supply (the MV network) is available and all the inverters can be operated in PQ mode, because there are voltage and frequency references.

In this case, during shift to islanding operation, thanks to VSI, that provide a reference for voltage and frequency, the MG is not lost. Consequently, it is possible a load/generation balancing and a frequency and voltage control without changing the control mode of any inverter.

After identifying, the key solution for MG islanded operation, two main control strategies must be defined: the single master operation (SMO) and the multi master operation (MMO).

2.3.1.1 -**Single Master Operation**

In the Single Master Operation, the VSI (acting as master) is used as voltage and frequency reference and all other inverters are operated in PQ mode. These PQ inverters receive the MGCC information and control the LC and update their one set-point. The SMO control scheme is represented by the following figure.
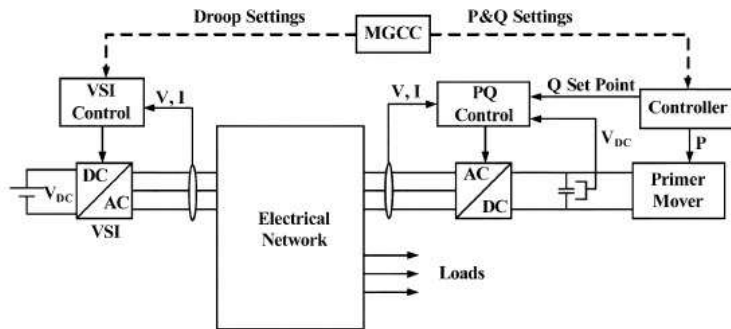
Figure 2.3 – Control scheme for SMO [3].

2.3.1.2 -**Multi Master Operation**

In the MMO, the MG operates with several inverters in a VSI mode using pre-defined frequency/active power voltage/reactive power characteristics.

The VSI is attached to storage devices (batteries or flywheels) or to MS with storage devices in the dc-link (batteries, super capacitors), which are continuously charged by the primary energy source.

With the possibility of other PQ-controlled inverters may coexist, the MGCC can modify the generation profile by changing the idle frequency of VSI and/or by defining new set points for controllable MS connected to the grid through PQ-controlled inverters. The MMO control scheme is represented by the following figure.
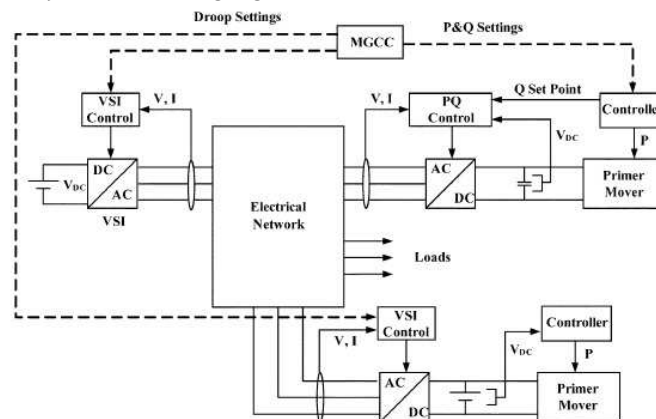
Figure 2.4 – Control scheme for MMO [3].

The MMO is more robust than the SMO, because in case of a major communication failure between the MGCC and the MS or in case of losing the MG main storage unit and the

associated VSI, the MG continues operative since voltage and frequency regulation relies in several (distributed) VSI units [4].

Summarizing, in emergency operation the output power control of the MS change and require a controlling frequency and voltage of the islanded section of the network. Therefore, the MGCC performs an equivalent action to the secondary control loops existing in the conventional power systems: after the initial reaction of the MC and LC, which should ensure MG survival following islanding, the MGCC performs the technical and economical optimization of the islanded system.

In this thesis, the SMO approach will be use, where the storage device acts as the "master-VSI" and all other sources are operated in a PQ mode.

2.3.2 - Emergency Regulation Functionalities

The DER must be able to supply the active and reactive power requirements during islanded operation and react if a fault current has occurred downstream of the switch location.

When VSI react to network disturbances, based only in information available, this inverter provides a primary voltage and frequency regulation in the islanded.

So, in order to provide power balance between generation and loads and restore frequency to adequate values, the MG requires a specific the following specific control strategies:

- Primary Control: Stabilize frequency oscillations and maintain the balance between the load and generation, in a local level;
- Secondary Control: to maintain voltages and frequency at acceptable limits, ensuring the electric variables regulation;

The implementation of frequency regulation strategies have to consider the MG resources controllability, namely [4]:

- The main storage device response;
- EV charging controllability;
- Controllable MS response;
- Load shedding schemes.

The SSMT, a controllable MS, is dispatchable source being adequate for the provision of secondary frequency regulation or voltage control. In the order non-controllable and controllable units are controlled with a PQ control strategy.

The MG forming elements are fast-responsive storage unit(s), such as flywheels, super-capacitors or batteries [4]. Their capacity of providing fast power balance makes them the devices more adequate for fast frequency and voltage regulation, being their coupling inverters controlled as VSI [4].

2.3.2.1 -**Primary Voltage and Frequency Regulation**

The voltage and frequency primary regulation is done using a storage unit grid coupling inverter control by the VSI device, with external droop control loops.

The control is usually performed through droop compensation methods, as present in the next figures, and define the MG voltage and frequency references as a function of the grid operating conditions, as in following equation.
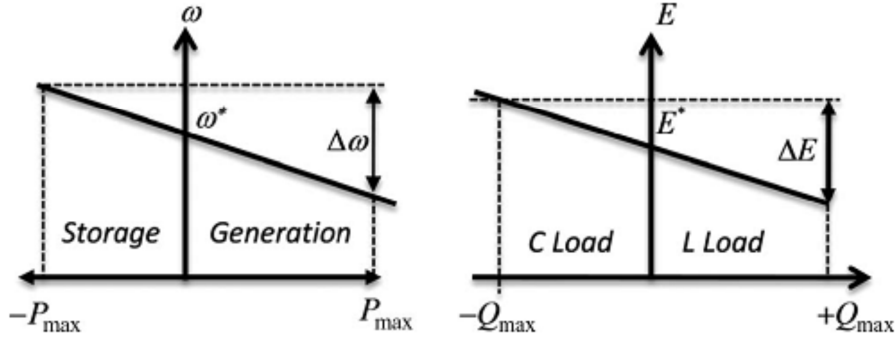
Figure 2.5 – P/Q droop characteristics [4].

$$\omega = \omega_0 - k_P \times P \ (rad.s^{-1}) \tag{2.3}$$

$$V = V_0 - k_Q \times Q \ (V) \tag{2.4}$$

where P and Q are the inverter active and reactive power outputs, k_P and k_Q are the droop slopes (positive quantities) and ω_0 and V_0 are the idle values of the angular frequency and voltage (values of the inverter angular frequency and terminal voltage with no load conditions) [3].

In this kind of regulation and for a MMO, when a disturbance occurs, the storage units will respond to the power imbalance according to their droop characteristics, as in the next equation.

$$\Delta P = \sum_{i=1}^{n} \Delta P_i \ (W) \tag{2.5}$$

where ΔP is the unbalance between the MG generation and load and ΔP_i is the active power injected by the i-th VSI connected to the MG. The MG frequency deviation can be determined by the system of equations represented in the following equation.

$$
\begin{bmatrix}
1 & k_{P1} & 0 & \cdots & 0 \\
1 & 0 & k_{P2} & \cdots & 0 \\
\cdots & \cdots & \cdots & \ddots & \vdots \\
1 & 0 & 0 & \cdots & k_{Pn} \\
0 & 1 & 1 & \cdots & 1
\end{bmatrix}
\times
\begin{bmatrix}
\omega' \\
\Delta P_1 \\
\Delta P_2 \\
\vdots \\
\Delta P_n
\end{bmatrix}
=
\begin{bmatrix}
\omega_{grid} \\
\omega_{grid} \\
\vdots \\
\omega_{grid} \\
\Delta P
\end{bmatrix}
\tag{2.6}
$$

Where ω' is the post-disturbance MG angular frequency and ω_{grid} is the pre-disturbance MG angular frequency (see Eq. (2.3)). Using the last equation it is possible to compute MG frequency deviation and the power sharing among the VSI following a generation or load variations during ΔP islanding conditions.

Both cases SMO and MMO can be implement at this primarily control, but a convenient secondary load-frequency control during islanded operation must be considered to be installed in controllable MS after this regulation.

Some storage units can be connected to controllable MS, such as SSMT or fuel cells. As an UPS solution and in normal operating conditions, the controllable MS injects power into the grid according to the droop characteristic in next equation.

$$\Delta\omega = \omega_{0i} - k_{Pi} \times P_i - [\omega_{0i} - k_{Pi} \times (P_i + \Delta P_i)] = k_{Pi} \times \Delta P_i \ (rad.s^{-1}) \qquad \textbf{(2.7)}$$

As shown in Eq. (2.3) to Eq. (2.7), during a transient the power balance is assured by the MG energy storage devices, which would keep on injecting or absorbing active power during the time of response of the secondary frequency control, to correct the frequency deviation [4].

2.3.2.2 - Secondary Load-Frequency Control

The main target of secondary frequency control is to guarantee that after a disturbance the frequency returns to its nominal value, by increasing the power output of controllable MS such as Microturbines and/or fuel cells.

This control its divided in two strategies:

    A. Local implementation at each MS controllable;

    B. Centralized and mastered by the MGCC.

In both cases, target values for active power outputs of the primary energy sources are forward defined based on the frequency deviation error [3].

For SMO, the target value is the direct active power set-point sent to the prime mover of a controllable MS, while for MMO, the target value can be both an active power set-point for a controllable MS connected to a PQ inverter or a new value for the idle frequency of a VSI.

Particularly, the local secondary control (A) is implemented as an external control loop of active power control for controllable MS, as seen in the next figure.
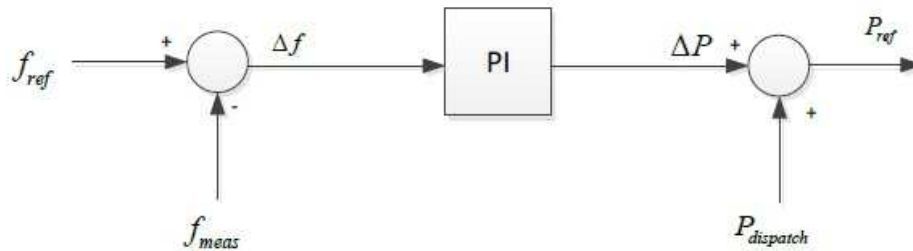
Figure 2.6 – Local secondary frequency control of PQ controlled MS [4].

Consequently, if the MS inverter is controlled with a PQ strategy, the reference active power (P_{ref}), to be injected by the MS, is determined by a PI controller based on MG frequency error $\Delta f = f_{ref} - f_{meas} \ (Hz)$.

For MS inverter controlled as VSI, local secondary control can be performed by updating the idle frequency ω_{0i} of the MS P/f droop function, as represented next figure.
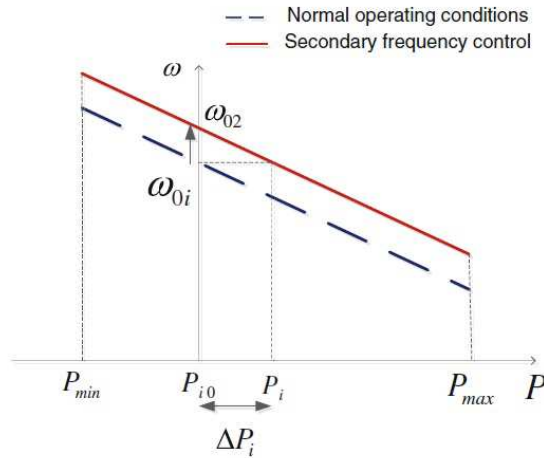
Figure 2.7 – Local secondary frequency control for VSI controlled MS [4].

According to the equation (2.7) the VSI active power output is proportional to the MG frequency deviation. Therefore, when a disturbance occurs the VSI operate in agreement with the droop characteristic.

In the PQ control strategy the PI controller can be used to determine the new idle frequency (ω_{02}), based on the MG frequency deviation [4]. As represented in following figure, based on the local measurement of frequency, the frequency deviation is determined and corrected through a PI controller ($Gfsec$).
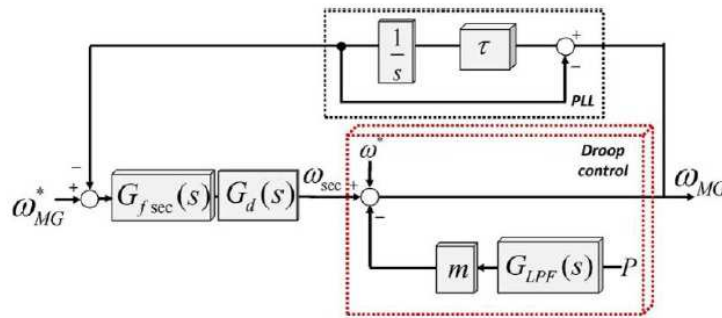
Figure 2.8 – Block Diagram of VSI local secondary frequency control [4].

The resulting signal (ωsec) is added to the initial idle frequency (ω^*) in order to update the active power droop characteristic [4].

The main advantage of local secondary frequency control is that it only relies on local measurement to define the new reference power. However, the MS active power response will also depend on the PI controller parameters.

The centralized secondary control determines the new MS active power set-points at MGCC, based on the overall state of the MG, and sends to the respective local controllers.

The active power set-points aforementioned are determined considering the MG frequency deviation and an economic dispatch algorithm, which are based on pre-defined cost functions or on the MS capacity. The next figure reflects what was previously mentioned.
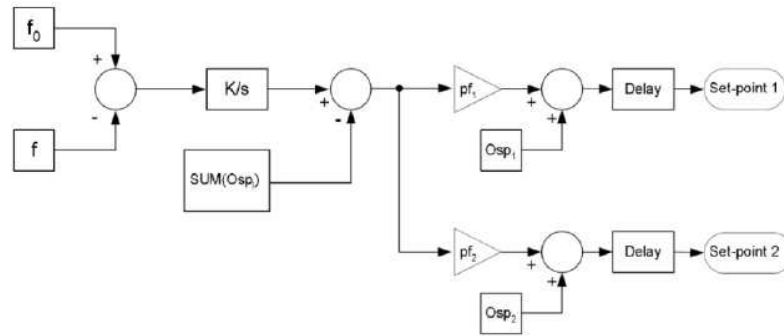
Figure 2.9 – MG centralized local secondary frequency control based on participation factors [4].

In the reference [4], a centralized secondary frequency and voltage restoration loop was use, considering only the VSI controlled droop. As shown in the next figure, based on the MG voltage and frequency measurements at the Point of Common Coupling (PCC) the frequency and voltage error are corrected through PI controllers and the obtained control compensation signals are sent to each VSI.
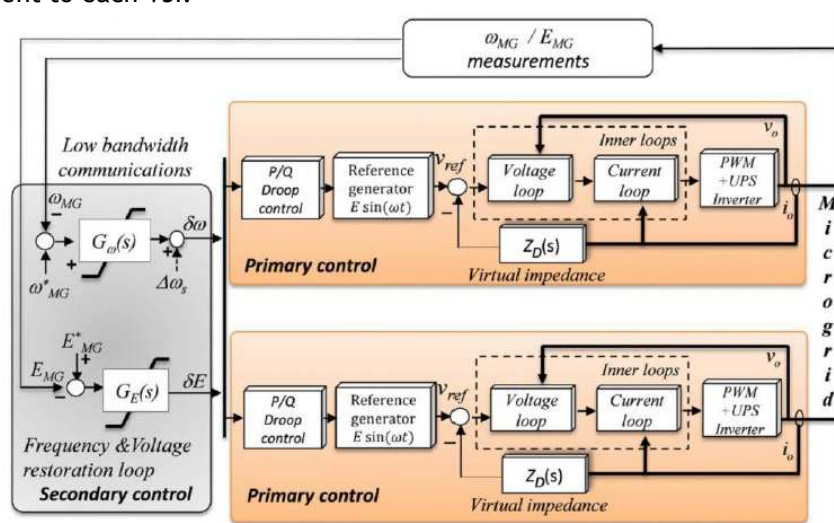
Figure 2.10 – MG centralized frequency and voltage restoration loop [4].

The frequency compensation signal has also a synchronization term which measures the phase between the MG and the upstream MV network, otherwise when the grid is not present it will be zero.

The active power injected by the storage device as a result of the MG primary frequency response is used to determine the MS power set-points. The MS will increase its output, decreasing the power injected by the storage unit and correcting the MG frequency deviation.

2.3.2.3 -**Regulation with EV**

With the adopting of the innovative EV control strategy it is possible to take advantage of the EV flexibility, acting both as a controllable load or storage device depending on the MG frequency and local voltages, in the case of this thesis.

Reducing the central storage capacity it is required to assure MG system robustness, during islanding conditions, and to provide additional resources that can be exploited for MG frequency regulation purposes.

In [3], [4] and [7]the authors propose a P-ω droop control strategy implemented at the EV charger (see following figures). Where the EV will modify their power exchange with the LV grid based on the MG frequency.
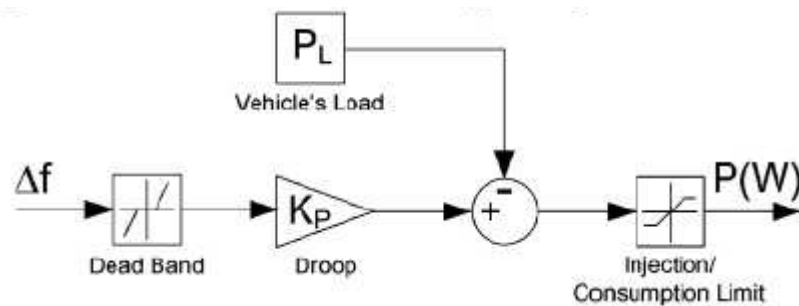
Figure 2.11 – Control loop for the EV active power set_point [4].
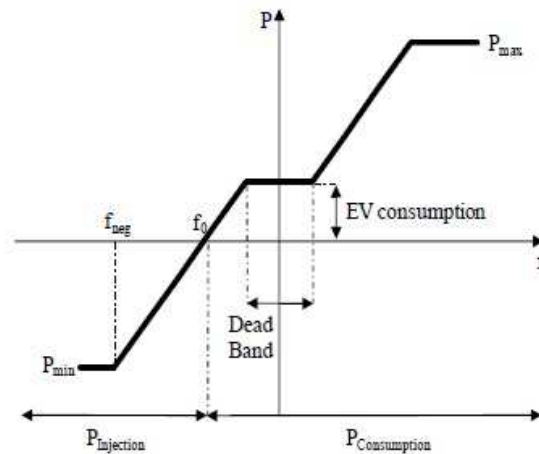
Figure 2.12 – EV Frequency-Droop characteristic [4].

The EV Frequency-Droop characteristic shows that frequency:

- In the Dead-Band - the EV will charge the battery at a pre-defined charging rate;
- Bigger then dead-band maximum value - the EV can also increase its power consumption;
- Lower the dead-band minimum value, if occurs an acceptable disturbances - the EV reduces its power consumption, reducing the load of the system;

- Below to the zero-crossing frequency (f0), for large disturbances - the EV starts to inject power into the grid (Vehicle-to-Grid-V2G functionality);
- Out of the pre-defined frequency range, make the vehicle inject/absorb a fixed power.

The EV control parameters depend on the EV charger characteristics and on the disposition of EV owners to participate in such services. These parameters may differ from grid to grid and can be changed remotely by the MGCC, in order to promote adequate coordination with the MG frequency regulation mechanisms (load shedding schemes, availability of energy storage devices and their state of charge) [4].

For the local voltage regulation, the authors in the reference [7], recommend a similar approach as described above for frequency. Because the LV networks are resistive and the regulation of voltage cannot be solved only by the injection of reactive power [4].

Consequently, for voltage variations the EV absorbs (voltage increase) or injects (voltage decrease) power into the grid.

To make possible a commitment between the voltage and frequency voltage in EV, the authors in [7] suggest to use the following control:

$$P_{set} = \begin{cases} P_{set\_f}, P_{set\_f} < P_{set\_V} \\ P_{set\_V}, otherwise \end{cases} (W) \tag{2.8}$$

$$P_{set\_f} = \frac{1}{k_P} \cdot (f_{grid} - f_0) \ (W) \tag{2.9}$$

$$P_{set\_V} = \frac{1}{k_V} \cdot (V_{phase} - V_0) \ (W) \tag{2.10}$$

Where:

$k_V = $ slope of the $P - V$ characteristic, $\qquad V_{phase} = $ measured voltage (V), $V_0 = $ the zero$-$crossing voltage (V);

$k_P = $ slope of the $Q - V$ characteristic, $\qquad f_{grid} = $ measured frequency (Hz), $f_0 = $ the zero$-$crossing frequency (Hz);

The zero crossing frequency/Voltage defines the point where the EV starts to inject power to the grid and becomes a V2G.

In islanded conditions, both frequency and voltage characteristics will produce different active power set-points in the EV charger and this control give priority to load balancing.

2.4 - Summary and Main Conclusions

This chapter gives a general overview about the scientific, technic and theoretic concepts associate to Microgrids, including all the projects or researches use or related.

With the increasing of DG in LV networks and the consequent problems that they bring, the Microgrid is one viable solution.

Under this scenario, the types of micro distributed energy resources and their architecture at MG are crucial for the good operation mode.

Their essential components are:

- Microsources - can be classified by: their type of primary energy source, control capacity to inject active power in the grid and their type of function;
- Storage system – divided in power application (frequency regulation) or energy application (peak shifting);
- Electric Vehicles – classified by the charging strategy;
- Inverters - defined by the control strategy PQ inverter control or VSI;
- MG loads.

The MG incorporate these components with a hierarchical control structure according with their specific requirements. Where the exploration have a centralized control, made by the MGCC, a bidirectional communications support, made by SM, and a Local control, made by MC, VC and LC.

The MG can operate connected with the MV network or in isolate mode. In the isolate mode the operation problems are: different voltages magnitudes at fundamental frequency of the system, unequal offsets between phases and different levels of harmonic distortion between phases.

Therefore, the strategies of operation control and regulation functionalities are required for the isolate mode. The operational control can be Single master operation or multi master operation. In the first one only exists one VSI and the others are PQ inverters and in the second one has a number of VSI inverters.

In order to provide power balance between generation and loads and restore frequency to adequate values, the MG requires primary and secondary frequency control strategies, proportional to active power. Additional of these control strategies is the primary voltage control, proportional to reactive power. The EV characteristics make possible that EV contribute for the regulation of grid frequency or local voltage magnitude, depending on the rule of Power Set study for the authors [14].

Finishing, the MG inverters operate in order to provide stable voltage and frequency in the presence of arbitrary varying loads or power production. The reduced global inertia and high resistance compared to the reactance of LV lines in MG, requires the development of specific strategies for voltage and frequency control. In addition to that, the larger number of MS makes the communication of information impractical and implies the inverter control system based on terminal quantities.

Chapter 3

Microgrid Dynamic Modelling

Regarding the main objectives of this thesis, the study of the MG dynamic behaviour became essential. Over the development of full dynamic simulation models with the capacity to answer under several conditions.

The integration of these models is done in a *Matlab Simulink* simulation platform, using *SimPowerSystem* toolbox, and in user defined models. In order to analyse the steady state and dynamic stability of the MG operation.

This simulation platform was developed at INESC Porto [4], under the European project Microgrids, which can be considered as a reference point for the first generation development of new architectures for electricity grids at EU level. Therefore, the platform incorporates the dynamic models of the MG components, described in Chapter 2, including their power electronic interfaces and control strategies. However, the LV distribution network was modelled considering only three-phase balanced operation, despite the fact that this is not the most common situation in LV distribution networks [4].

The following organization of this chapter is divided in three major groups that associate the MG elements with similar roles.

3.1 - Distributed Energy Resources Modelling

This section describes the dynamic behaviour of the distribution energy resources under consideration in this thesis.

Regarding DER modelling it is important to consider the following issues [4]:

- Development and implementation of models that represent the behaviour of single-phase power electronic interfaces, both for EV and microgeneration units;
- Development and implementation of the control model that enables EV contributing for improving MG operating conditions through active (dis)charging control depending on MG operational issues;

- Identification and development of additional control mechanisms to be placed at the power electronic converter level, in order to improve MG operating conditions during islanding in case of excessive voltage unbalance;
- Development and implementation of the control model that enables or reduces PV contributing for improving MG operating conditions through active power injection control depending on MG operational issues.

3.1.1 - Storage Devices Modelling

The storage devices in the MG are responsible for the provision of some form of energy buffering capabilities in order to ensure the system stability compensating the power unbalance between the MG generation and load.

Following MG islanding operation, storage devices have the capacity of quick charge or discharge in order to provide balance power to the MG. Regarding the typical time frame of these phenomena, storage devices can be regarded as an ideal dc voltage sources that make use of power electronic interfaces to be coupled with the electrical network (AC/DC/AC converters for flywheels and DC/AC inverters for batteries and supercapacitors) [14].

These electrical interfaces act as controllable AC voltage sources (with very fast output characteristics) to face sudden system changes such as load-following during islanding conditions and have physical limitations and thus a finite capacity for storing energy [14].

It is possible to find in the reference [17] the literature models for analysing the behaviour of storage devices such as batteries, flywheels or supercapacitors. However, the nature of the research developed within this dissertation does not require a deep knowledge about the behaviour of the internal variables of storage devices.

Further explanations on the use of storage devices for MG operation and control will be presented, where their main utility is done in the VSI.

3.1.2 - Microsources Modelling

According to the author in [4], the main components of the MS dynamic models are represented in following figure.
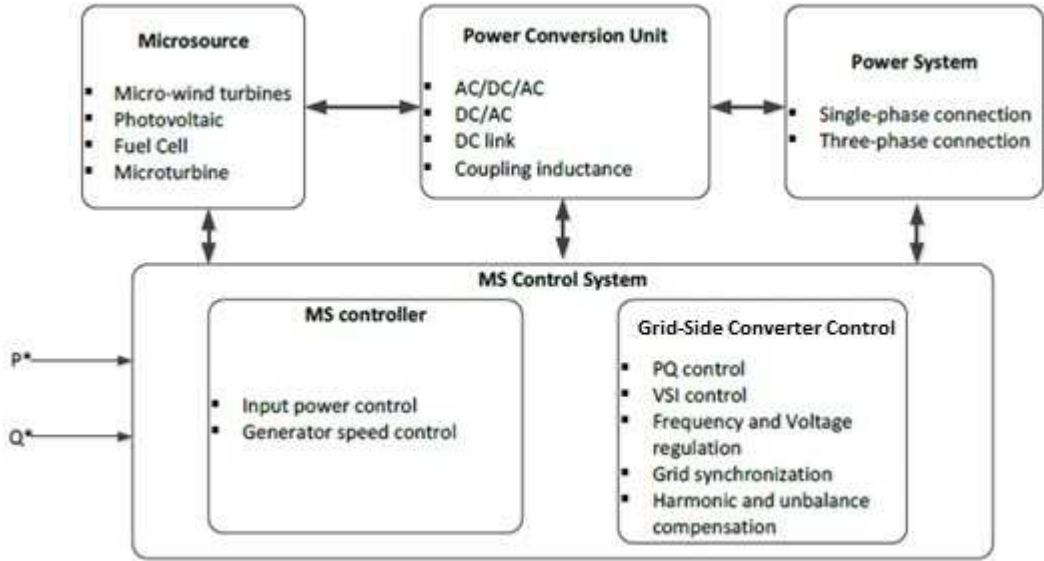
Figure 3.1 – General structure of the Microsource models [4].

In MS models, the dynamic behaviour of the generation units are represented regarding their power response to voltage and frequency disturbance and the external control signals sent from the MS controller, responsible for the MS power output control.

As illustrated and referred in Chapter 2 the MG use four types of MS. However, in this thesis only two were used: the PV and the Microturbine.

3.1.2.1 -Photovoltaic Panel

The most common model of the PV cell is the single diode that reflects the current/voltage characteristic of the cell (in the next equation) and can be represented by the equivalent electric circuit (in the next figure). According to Figure 3.2, the output current is given by:
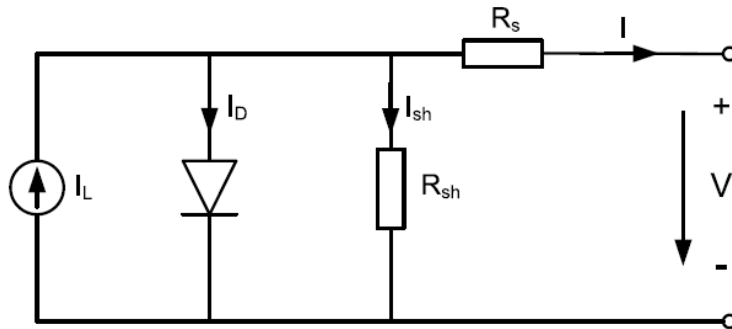
Figure 3.2 – PV cell equivalent circuit [4].

$$I = I_L - I_D - I_{sh} = I_L - I_0 \left\{ \exp\left(\frac{Q(V + R_S L)}{A.K.T} \right) - 1 \right\} \tag{3.1}$$

Where:

I (A) and V (V) are the current and load voltage,

I_L is the light generated current (A), I_D is the diode current (A), I_0 is the diode reverse saturation current (A),

R_s and R_{sh} are the series and shunt resistances (Ω),

Q is the electron charge, A is the curve fitting constant, T the cell absolute temperature and K the Boltzmann constant.

The five parameters of the model (I_L, I_0, R_s, R_{sh} and A) depend on the weather conditions (cell temperature and solar radiation) [14].

The PV cell manufactures usually provide a set of data which can be used in order to compute the parameters of the mathematical model, defined in the previous equation [14]. This is based on cell data: such as short-circuit current (I_{SC}^C), open circuit voltage (V_{OC}^C) and maximum power for a given set of references (P_{max}^C) [14].

Through the typical PV cells current–voltage (I-V) and power-voltage (P-V) characteristics it is possible to observe that the maximum power, which can be extracted from the PV cell, depends on the operating point.
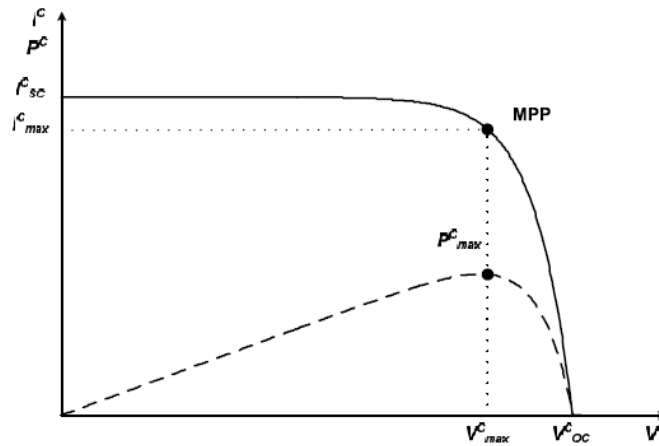
Figure 3.3 – I-V and P-V Characteristics of a solar cell [14].

The point which maximum power P_{max}^C is extracted from the cell is denominated by Maximum Power Point (MPP) and it is reached with a cell terminal voltage V_{max}^C and an output current I_{max}^C [14].

As demonstrated in the following two figures in the Photovoltaic the MPP influence depend also on the solar radiation GT, that for:

- A GT fixed value the temperature decrease and the V_{max}^C increase;
- A temperature fixed value the GT decrease and the V_{max}^C remains almost constant.
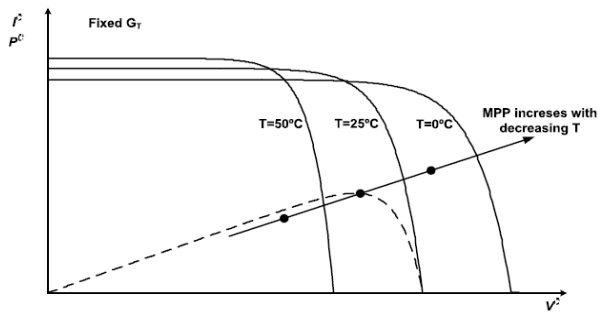
Figure 3.4 – Influence of cell temperature in the I-V characteristics [14].
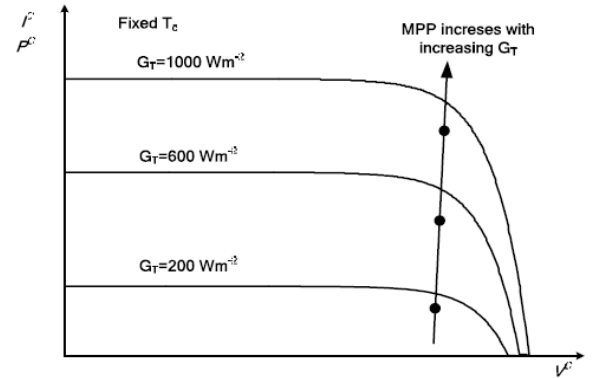
Figure 3.5 – Influence of solar radiation in the I-V characteristics [14].

The solar PV system is composed by, Photovoltaic panels, DC/DC converter controlled by the MPPT algorithms and the DC/AC inverter grid-coupling inverter, as show in the next figure.
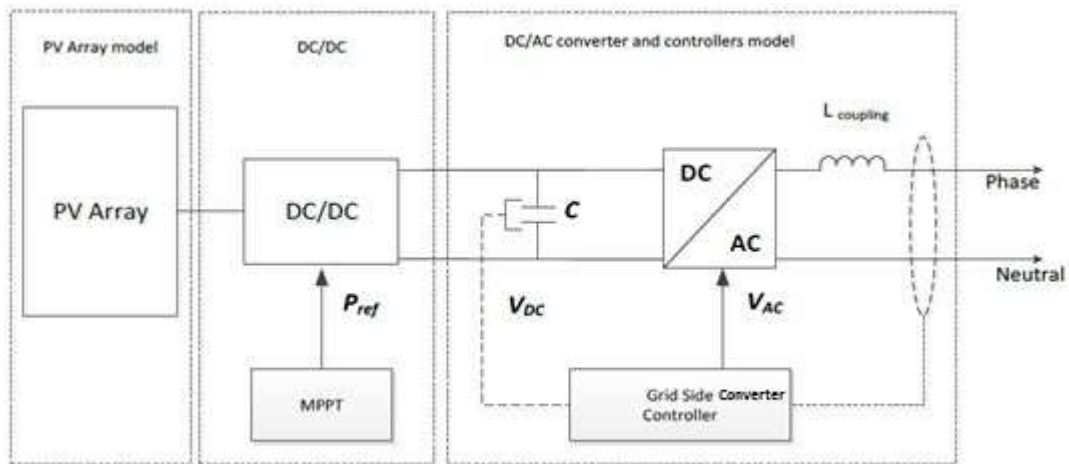
Figure 3.6 – Basic configuration of the solar photovoltaic system [4].

The DC/DC MPPT converter are relatively slow acting devices which may be ignored in transient stability studies [4]. Therefore, PV panels can be modelled as a constant DC power source for dynamic stability assessment [4].

3.1.2.2 - Microturbine

The microturbines are controllable MS that participate in the MG secondary frequency control. Their reaction to the active power control signals will have a great impact on the MG transient behaviour.

As described in [14], the modelling of the SSMT assume that there is an AC to DC uncontrolled rectifier (full wave three-phase diode bridge rectifier) connected to the Permanent Magnet Synchronous Generator, a DC-link with a capacitor and a DC/AC inverter.

Technically speaking, based in reference [14] for the SSMT its necessary to consider:

- A small size SSMT engine, similar to conventional combustion gas turbines;
- A representation of the electric and mechanic behaviours model for the microturbines in an electric network from a dynamic point of view;
- An Exclusion of the hot exhaust gases in the recuperator as the exclusive device used to increase microturbine global efficiency;
- A speed and acceleration control system – that will be important for conditions during start-up or loss of power, but it will have very little influence during normal operating conditions.

For this dissertation the SSMT dynamic model configuration is represented in the next Figure.
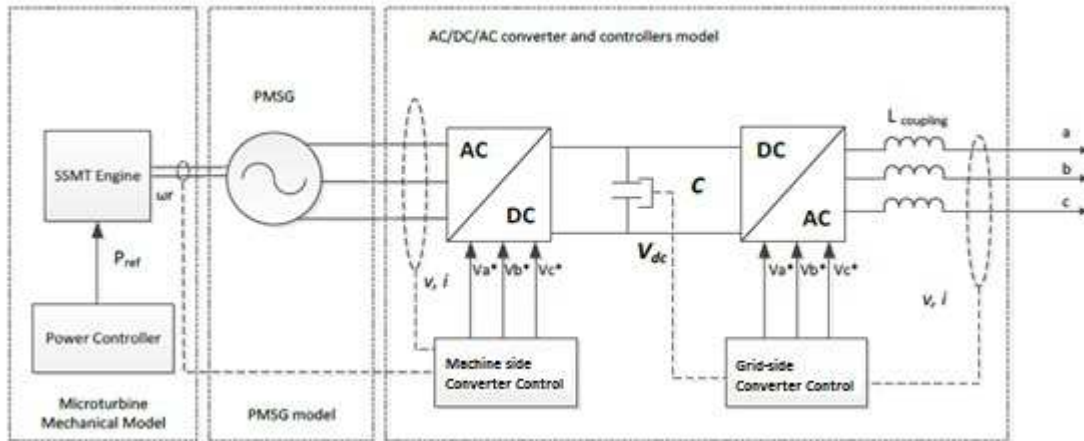
Figure 3.7 – Basic configuration of a single-shaft microturbine [4].

Composed by the SSMT mechanical model, the PMSG generator and the power conversion unit, with a rectifier and a grid-synchronizing DC/AC inverter [4]. Where the SSMT nominal power can range to 100 kW for LV applications, being connected to the three-phases of the system [4].

The power produced in the electric generator (the PMSG) is variable frequency AC power due to the variable speed operation characteristic of the microturbine [14]. A more detailed description of the SSMT engine and PMSG can be found in [14].

To control the power output of the SSMT was done an **Active Power Control,** in other words, an external control loop that defines the mechanical power reference of the turbine.

As show in the next figure, the reference power (P_{in}) is determined by a PI regulator corrects the error (ΔP) between the power measured at the SSMT output (P) and the reference value ($Power\ set - point = P_{ref}$), which can result in a set-point sent by the MGCC [4].
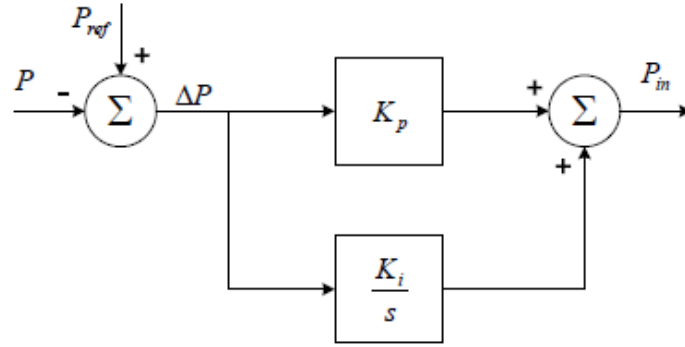
Figure 3.8 – SSMT active power control **[4].**

The mechanical part of the SSMT (**SSMT engine**) is represent through the conventional model commonly use to represent the dynamics of simple cycle single shaft gas turbines, usually known as the GAST (GAS Turbine) model, without the droop control [14].
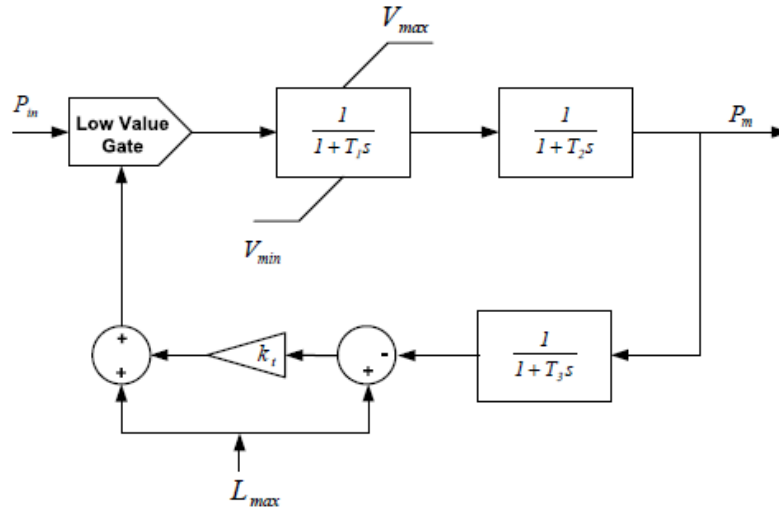
Figure 3.9 – Dynamic model of the SSMT engine **[14].**

The parameters in the microturbine engine model are:

$T_1, T_2 = fuel\ system\ time\ constants\ (s);\ T_3 = load\ limit\ time\ constant(s);$

$V_{max}, V_{min} = maximum\ and\ minimum\ fuel\ value\ positions\ (V);$

$k_t = temperature\ control\ loop\ gain;\ L_{max} = load\ limit\ (W).$

The PMSG dynamic model is represented in the rotor d-q reference frame and can be described by the electrical and mechanical equations [4].

$$v_d = R_s.i_d - p\omega L_q i_q + L_d \frac{di_d}{dt} \tag{3.2}$$

$$v_q = R_s.i_q - p\omega L_d i_d + L_q \frac{di_q}{dt} + p\omega \Phi_m \tag{3.3}$$

$$T_e = \frac{3}{2}p[\Phi_m i_q + (L_d - L_q)i_d i_q] \tag{3.4}$$

$$T_e - T_m = J\frac{d\omega}{dt} + F\omega \tag{3.5}$$

where:

$L_d, L_q = d\ and\ q\ axis\ inductances\ (H);\ R_s = stator\ windings\ resistance\ (\Omega);$

$v_d, v_q = d\ and\ q\ axis\ voltages\ (V);\ i_d, i_q = d\ and\ q\ axis\ currents\ (A);$

$\omega = angular\ velocity\ of\ the\ rotor\ (\text{rad}.\,s^{-1});$

$\Phi_m = flux\ induced\ by\ the\ permanent\ magnets\ in\ the\ stator\ windigns\ (Wb);$

$p = number\ of\ pole\ pairs;$

$T_e = electromagnetic\ torque\ (N.m);\ T_m = \text{Local mechanical torque}\ (N.m);$

$J = combined\ inertia\ of\ the\ load, PMSG, shaft, turbine\ and\ compressor\ (kg.m^2)$

$F = combined\ viscous\ friction\ factor\ of\ the\ load, PMSG, shaft, turbine\ and$

$compressor\ (N.m.s.rad.\,s^{-1}).$

The **Machine Side Converter** or input side controller is responsible for controlling the SSMT angular velocity and the power factor of the PMSG [4]. Their general structure is represented in the next figure.
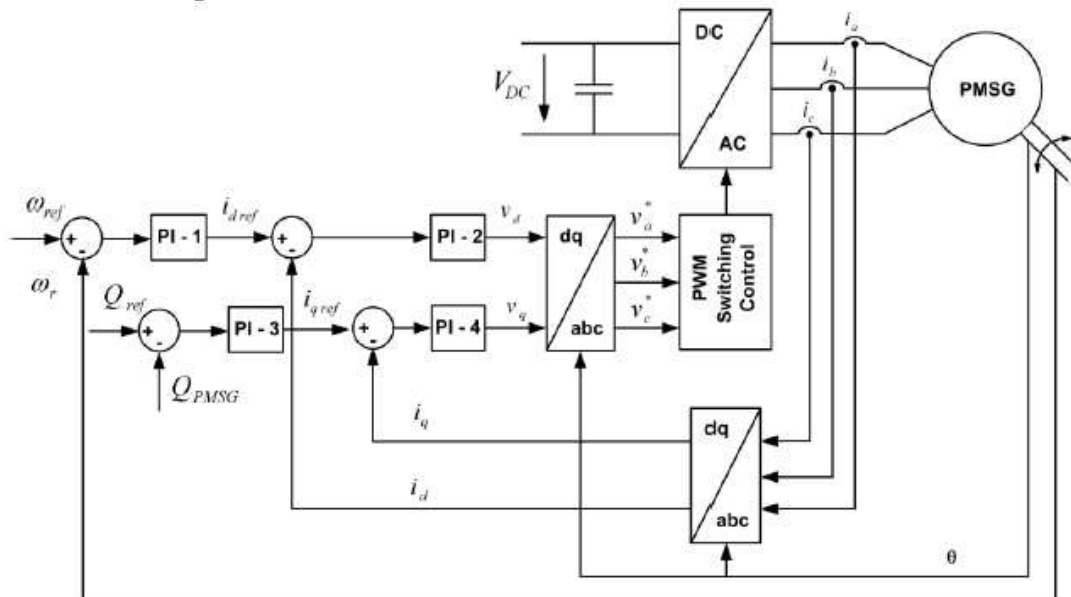
Figure 3.10 – General structure of the input-side controller of the SSMT **[14].**

To regulate the direct axis voltage vd and consequently the microturbine angular velocity, the microturbine reference speed (determined according to the machine P-f characteristic) is compared to the shaft speed and the resulting error is corrected through a PI controller [4]. On the other hand, the quadrature axis voltage vq can be regulated in order to assure a unit power factor for the PMSG.

3.1.3 - **Electrical Vehicle Modelling**

As mentioned in Chapter 2 the EV has a single-phase connection with the grid, therefore the subsequent figure represent their dynamic model.

Figure 3.11 – Block diagram of EV dynamic model **[4].**

Some blocks of the EV diagram model represented, are as follows:

- EV battery charging, as a DC voltage source coupled to a DC-DC converter - controls the (dis)charging current on the battery side;
- AC-DC converter - assures the link between the grid and the DC-link capacitor;
- Capacitor Voltage - controlled to be constant by an adequate adjustment of the power flow with the AC grid.

A possible variation in the DC-link capacitor voltage are due to the power demand/injection on the battery side [4]. Consequently, the general control approach that is followed in the operation of the DC/AC EV power electronic interface is the same presented for single-phase PQ controlled inverters [4]. However, the main differences rely in the external control loop which determines the EV charging power based on P-f droop characteristic [4]. The EV charging power is determined based on the local frequency or voltage measurements.

3.2 - Grid Coupling Modelling

As described in the previous chapter, the MS, EV and other devices are coupled to the grid through power electronic devices (inverters), which can be single-phase or three-phase depending on the MS nominal power.

In the case of the MS, depending on their control functionalities, the inverter can be controlled with a PQ strategy or with a VSI, with additional external droop controllers in order to provide frequency and voltage regulation.

Given the fast response of power electronic converters, they can be modelled from the network point of view by a controllable AC voltage source. The control strategies demand the magnitude and phase of this voltage source, particularly when the inverters are modelled based only on their control functions. Consequently, fast switching transients, harmonics and inverter losses are neglected.

3.2.1 - PQ inverter Modelling

The PQ inverter, under grid-connected mode, control their injection of active and reactive power flow and is also responsible for the control of the DC-Link of the cascading DC/AC/DC system [14].

Consequently, the internal voltage of the inverter is controlled in order to maintain the DC-link voltage at a specified reference and the reactive power output at the desired set-point, as showed in the following figure [14].
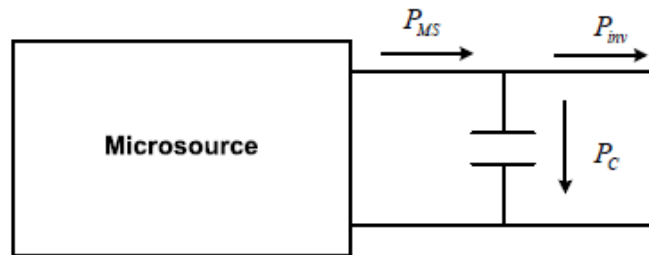
Figure 3.12 – **DC-link Capacitor power Balance [14].**

3.2.1.1 - Grid-side inverter

The grid side controller main functionality is to control the MS exported power, in other words, to maintain the DC-link voltage at a specified reference and the reactive power output at the desired set-point.

Ignoring losses, the power balance in the capacitor of the DC-link (P_C) is the difference between the power received from the MS (P_{MS}) and the inverter output power (P_{inv}) [4].

$$P_C = P_{MS} - P_{inv} \ (W) \tag{3.6}$$

$$P_C = V_{DC} \times I_{DC} \ (W) \tag{3.7}$$

$$V_{DC} = \frac{1}{C} \int I_{DC} \cdot \mathrm{dt} \ (V) \tag{3.8}$$

The second equation represents the power delivered by the capacitor depending on the DC-link voltage (V_{DC}) and current (I_{DC}). The equation (3.8) shows the DC-link voltage, where C is the value of the capacitance in the DC-link.

Combining all three equations and taking the Laplace transformation, the DC-link dynamics can be modelled as the following figure.
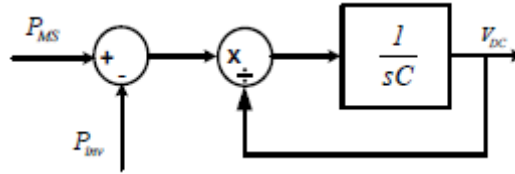
Figure 3.13 – **DC-link dynamic model** [4].

Neglecting losses, the power balance in the capacitor of the DC-link (P_C) is the difference between the power received from the MS (P_{MS}) and the inverter output power (P_{inv}) [14].

For this thesis the PQ inverter is the grid-coupling inverter of the MS and is modelled as a current controlled voltage source with single-phase or three-phase connection, depending on the nominal power of the units [4].

The MS power variations cause voltage error in the DC-link, previously constant, in order to control active power which will be corrected through PI controller using the correction of active power delivered to the grid [4].

The reactive power control is done through the error correction (between the reactive power measured and their reference) by PI controllers, in order to change the reactive current delivered to the grid. This control system (PI-2) is composed by two cascaded loops, where the inner most control loop regulates the inverter internal voltage (v^*) to meet a desired reference current (i_{ref})[14].

$$v^* = v + k(i_{ref} - i) \ (V) \tag{3.9}$$

The majority of the MS are single-phase and based on variable RES, so the next block diagram is a single-phase DC-AC grid-coupling inverter that will inject the power available at its input.
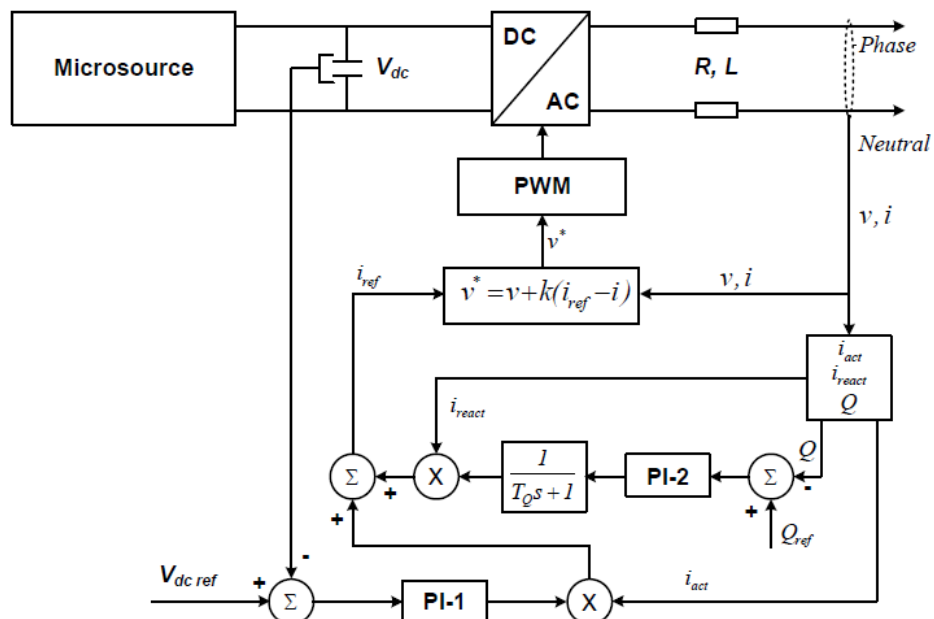
Figure 3.14 – **Single-phase grid coupling inverter PQ control [14]**.

For the other cases, the three-phase controllable MS, the PQ control strategy has the ability to change their power output when participate in secondary regulation schemes.

This three-phase is a three-leg DC-AC inverter PQ control that performs in a d-q reference frame, as represented in the next figure [4].
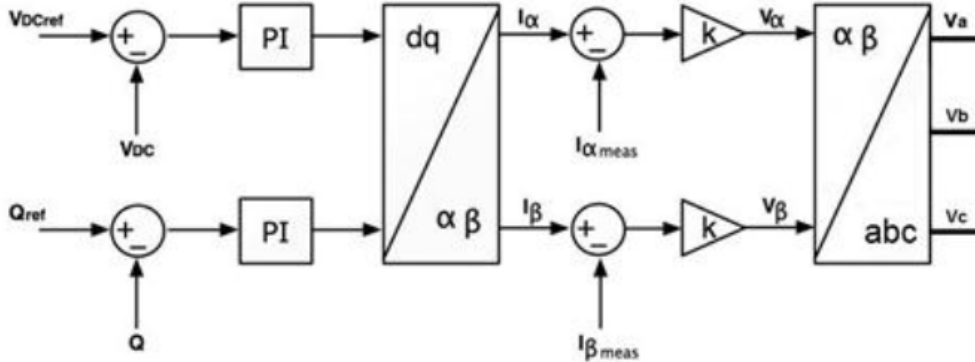
Figure 3.15 – Three-phase grid coupling inverter PQ control [14].

The active power exported to the grid is controlled by the direct component of the reference current, generated by the DC voltage error [4]. On the other hand, the reactive power output will be controlled by the quadrature component of the reference current resultant from the error between the measured value and the reference reactive power set-point [4]. Therefore, the d-q reference currents are then transformed to the α-β stationary reference frame. Consequently, the inner current control loop based on a proportional controller is used in order to generate the converter output voltages [4].

3.2.2 - **Voltage Source Inverter Modelling**

The Voltage Source Inverter acts as an ideal dc voltage source, due to their fast charging or discharging capability [4]. As described in Chapter 2 at the Primary and Secondary Frequency Control section, the VSI has their magnitude and frequency of the output voltage controlled by droops.

The VSI is used in order to interface a storage device (such a flywheel or a battery) with the AC grid. Making use of the energy stored in such devices, VSI acts as a voltage source, with the magnitude and frequency of the output voltage controlled through droops, as described in the chapter 2.

For this thesis the VSI is use interconnected to the medium voltage network and in isolate mode, so the following sections described the dynamic model for both situations.

3.2.2.1 -Medium Voltage Interconnection Operation

The VSI interconnected mode with stiff ac system is characterized by an angular frequency and terminal voltage and their references are externally imposed [3].

According to the authors in [4], the VSI three-phase balanced model has an external droop concept shown by the following image.
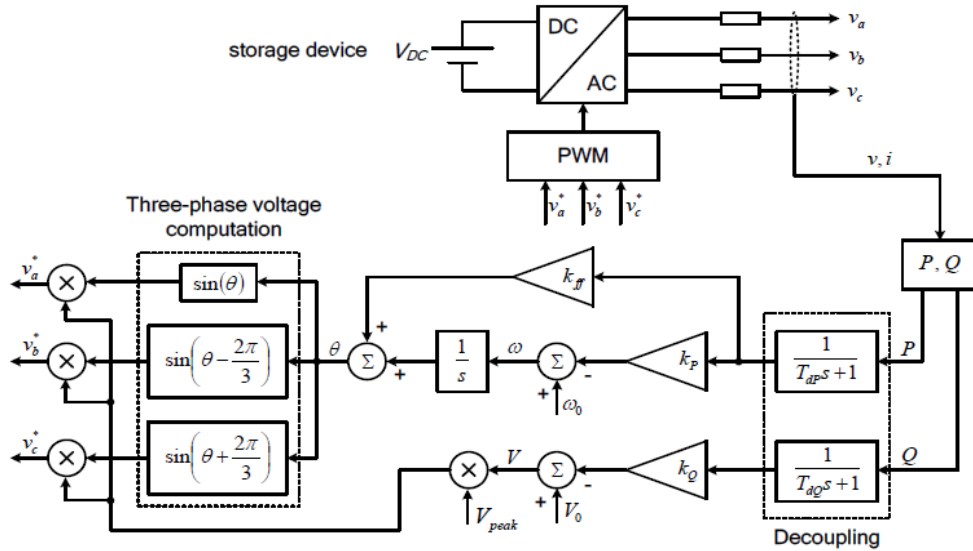
Figure 3.16 – Three-phase balance VSI control model **[4].**

The VSI terminal voltage and current are measured in order to compute the active and reactive powers, which will be described ahead in section 3.3.2 - . This measuring stage introduces a delay for decoupling purposes [4]:

- T_{dP} for the active power measurements – that determines the frequency of the output voltage by the active power/frequency droop;
- T_{dQ} for the reactive power measurements – that determines the magnitude of the output voltage by the reactive power/voltage droop.

A phase feed-forward control was included for stability purposes, corresponding to the k_{ff} gain in the previous figure [4]. The output voltages are the reference signals that control the VSI switching using a PWM modulation technique [3].

Based on the information in [3], the standalone ac system operation control principle allows the VSI to react to system disturbances (for example, load or generation changes) based on information available at its terminals. The disadvantage of this fact is the inability to accelerate the communications between the MS controllers. However, the MG communication infrastructure has the purpose of allowing an optimal management, not requiring the fast communication capabilities [3].

3.2.2.2 -Emergency Operation with Balancing Unit

As referred the microgrids operate under three-phase unbalanced conditions (due to the connection of single-phase loads and/or microgeneration units). A three-phase VSI with a voltage balancing control mechanism is adopted in this Thesis to improve system operation regarding system voltage unbalancing.

The VSI interfaces with a storage device (such as battery or flywheel) and the MG has the ability to produce three independent output voltages, regardless of loading [15]. Still, the balancing unit cancels all unwanted negative and zero-sequence voltage-current components.

For the MG emergency operation is necessary provide a variable-frequency operation mechanism, which can be delivered by the utilization of droop control concepts (active power versus frequency droop and reactive power versus voltage droop), as described in Chapter 2. The utilization of droop control concepts allows the definition of the voltage reference for the voltage balancing unit [15].

Considering what was previously mentioned, it is necessary to assume that the VSI will be based on a four-legged inverter, since it is the only power converter structure that allows an independent control of all the single-phase voltages [4]. These four-leg inverters are able to produce three independent phase voltages, while conventional 3-leg inverter produce two independent voltages [4]. The next figure represent general block diagram of the VSI model.
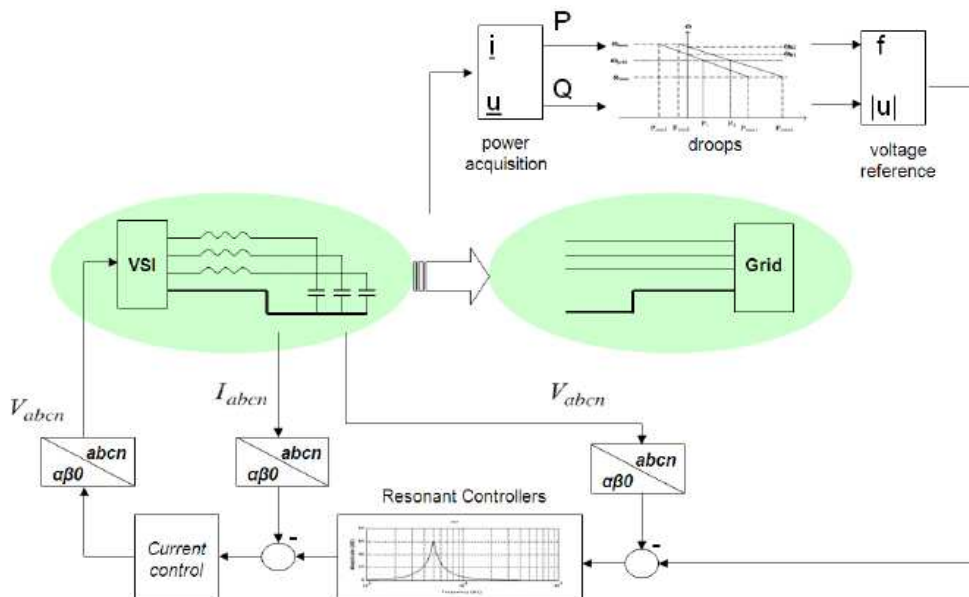
Figure 3.17 – General block diagram of the three-phase VSI with voltage balancing mechanism **[4].**

As shown in the previous figure, the droop control block provides the frequency and positive-sequence voltage reference for the voltage-current regulation block [4]. Where the control is implemented in the $\alpha\beta0$ reference frame, avoiding frame transformations for the positive, negative and zero sequence voltage components [4]. On the other hand, $\alpha\beta0$ frame requires the utilization of resonant controllers, expressed in the next equation, since the PI

controllers (associated to d-q control) are not able to remove steady state errors of sinusoidal waveforms [4].

$$G(s) = K_P + \frac{K_i.s}{s^2 + 2.s.\omega_{cut} + \omega^2}$$ (3.10)

Where:

$\omega = resonance\ frequency\ of\ the\ controller\ (rad.s^{-1})$;

$\omega_{cut} = low - frequency\ cutoff\ (\omega_{cut} \ll \omega)\ [rad.s^{-1}]$;

$K_p\ and\ K_i =\ the\ proportional\ and\ integral\ gains, respectively.$

The balancing unit resonant frequency is the reference frequency set by the active power/frequency droop characteristic, avoiding the need of a mechanism to track the grid frequency [4]. Therefore, in frequencies around ω, a more practical implementation form can be written according to the previous transfer function, which approximates the ideal integrator [4].

According to the next figure [4]:

- The resonant controller is used in each of the $\alpha\beta0$ coordinates;
- The inner current control block is a proportional controller, since any steady state error in this loop would not affect the outer voltage loop accuracy substantially;
- The output signal of the current block is then transformed in the abc frame by the inverse Clarke transformation.
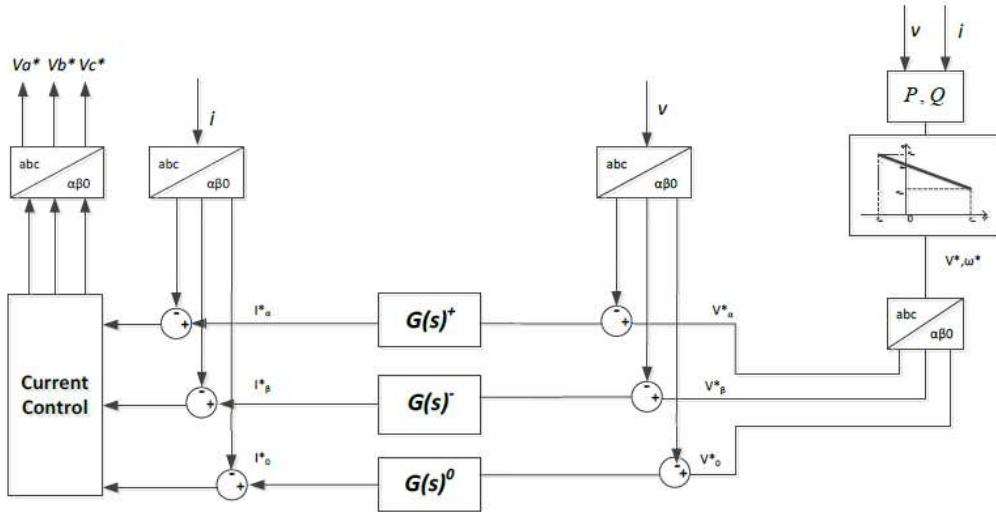
Figure 3.18 – General block diagram of the three-phase VSI with voltage balancing mechanism **[4].**

Due to stability problems, for the emergency operation, the MG:

- Would only be stable for higher values of proportional gain, cut-off frequency (ω_{cut}) and integral gain (K_i);
- If K_p is chosen rather low, the dynamic simulations also collapse.

The **MG interconnected operation mode** has a set of control parameters, adopted to allow the microgrid operation under interconnected or isolated mode [4].

3.3 - Network Modelling

The LV network study in this thesis is a three-phase unbalanced system with neutral, as represented in the following figure.
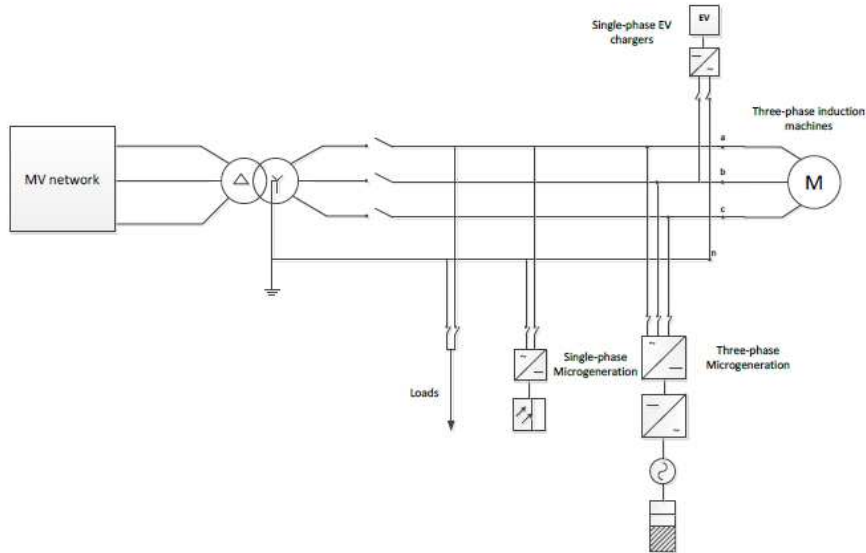
Figure 3.19 – LV network three-phase four wire representation [4].
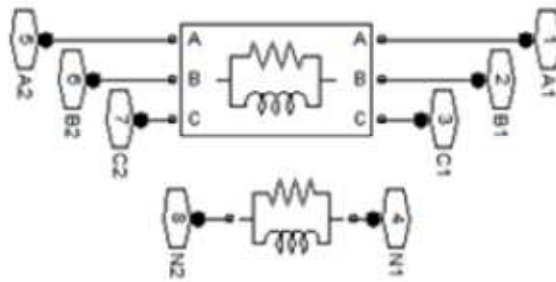
Figure 3.20 – Four-wire line model [4].

The figure 3.20 represent the LV lines and cables model correspondent to a simple parallel RL. This is preferred to other models that would cause significantly lower simulation speed [4].

The phase's impedances were considered to be equal, while the neutral impedance may vary depending on the cable/line section [4].

3.3.1 - Loads Modelling

The loads can be constant impedances (depending on frequency and voltage) or motor and also-both single and three-phase.

Excluding the induction machines, the following figure represents the MG loads modelled by static constant impedance model.
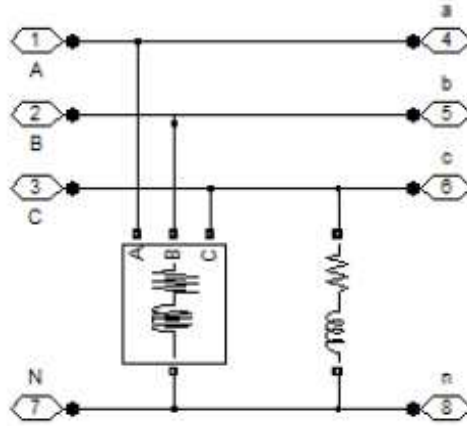
Figure 3.21 – Three and single-phase loads **[4].**

The active and reactive power absorbed by the load, which varies with the square of the MG voltage, will produce acceptable results when not considered the presence of larger induction machines.

According to the author in [4], the induction motor loads may compromise the MG stability particularly during unplanned islanding due to faults in the MV network. Being more accentuated by the voltage unbalance which is more critical when the MG operates autonomously.

3.3.2 - **Power measurements under unbalanced conditions**

For a balanced three-phase system the measurement of P and Q are well defined. Otherwise, if the system is unbalance, the measurement of P appears with an oscillatory component. Under these conditions, it is necessary to make power measurements, in order to turn the MG operation more robust.

For the MG in study, a three-phase system with zero sequence voltage/current components, the generalized instantaneous reactive power theory, was use as the measurement in [4]. This theory is proposed for three-phase systems with neutral and it is valid for sinusoidal or non-sinusoidal, balanced or unbalanced three-phase systems, with or without zero-sequence currents and/or voltages [4].

Consequently, the measurements for a three-phase power system are made in the following way [4]:

1. Instantaneous voltages on each phase (v_a, v_b, v_c) and instantaneous currents (i_a, i_b, i_c) can be expressed as instantaneous space vectors:

$$\bar{v} = \begin{bmatrix} v_a \\ v_b \\ v_c \end{bmatrix} (V) \; \bar{\iota} = \begin{bmatrix} i_a \\ i_b \\ i \end{bmatrix} (A) \qquad\qquad (3.11)$$

2. The instantaneous active power, can be determined by the internal product of the voltage and current vectors:

$$p = \overline{v}.\overline{i} = v_a \times i_a + v_b \times i_b + v_c \times i_c \ (W) \tag{3.12}$$

3. The instantaneous reactive power vector determined, from the (3.12) equation, which it will be possible to determine the instantaneous reactive power:

$$\overline{q} = \overline{v}.\overline{i} = \begin{bmatrix} q_a \\ q_b \\ q_c \end{bmatrix} = \begin{bmatrix} \begin{vmatrix} v_b & v_c \\ i_b & i_c \end{vmatrix} \\ \begin{vmatrix} v_c & v_a \\ i_c & i_a \end{vmatrix} \\ \begin{vmatrix} v_a & v_b \\ i_a & i_b \end{vmatrix} \end{bmatrix} \ (Var) \tag{3.13}$$

$$q = \|q\| = \|\overline{v} \times \overline{i}\| = \sqrt{q_a{}^2 + q_b{}^2 + q_c{}^2} \ (Var) \tag{3.14}$$

For the single–phase connection is necessary apply the Burger and Engle methodology used by the authors in [4]. This method determines the instantaneous values in a single-phase system, based on the d-q coordinated system used for three-phase system.

The following equation expresses the single-phase voltage and currents in two fictitious orthogonal components.

$$\underline{v} = \hat{v}e^{j\omega_N} = v_r + jv_s \tag{3.15}$$

$$\underline{i} = \hat{i}e^{j\omega_N} = i_r + ji_s \tag{3.16}$$

Where $\underline{v}$ and $\underline{i}$ are the instantaneous voltage and current space vectors represented in the r and s fictitious components, where r has the same phase as the input signal (single phase voltage or current) and the s component is shifted by 90° [4].

Based on the previous equations the peak value of voltage is determined by the next equation.

$$\hat{v} = \sqrt{v_r{}^2 + v_s{}^2} \ (V) \tag{3.17}$$

$$v_{RMS} = \frac{\hat{v}}{\sqrt{2}} \ (V) \tag{3.18}$$

The power is computed by using the complex apparent power split up in its real and imaginary part [4].

$$\underline{s} = p + jq = \frac{1}{2}\underline{v}.\underline{i}^* = \frac{1}{2}(v_r + jv_s)(i_r + ji_s) \ (W) \tag{3.19}$$

This approach is simple and fast not requiring zero crossing detection and enabling a decoupled control of active and reactive power [4]. The generation of the r and s components is obtained using the block diagram in the next Figure.
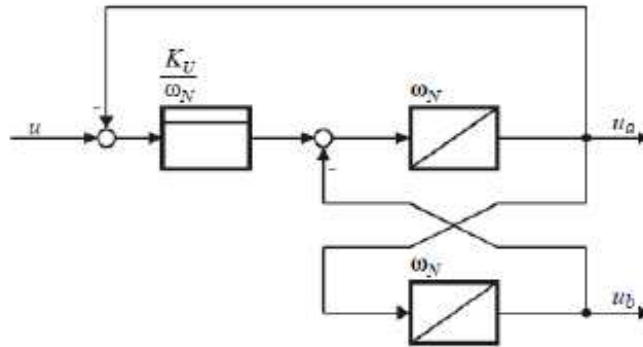
Figure 3.22 – Block diagram of the decomposition of signal u into the a, b components [4].

3.4 - Summary and Main Conclusions

This chapter presents and describes the dynamic models of the MG components used for an emergency unbalanced operation.

The appropriate dynamic models of the MG resources, such as the microsources (photovoltaic Panels and microturbines), EV and the control of grid-coupling inverters are crucial for the MG operation control at isolating mode.

In addition of that, to compensate the system voltage unbalance a control mechanisms was placed at the power electronic converter level, in order to improve MG operating conditions during islanding in case of excessive voltage unbalance.

Based on the work developed in INESC Porto, under the European project Microgrids, for the steady state and dynamic stability of the MG operation under unbalanced conditions analyse, the models presented and described were integrated in a *Matlab Simulink* simulation platform using *SimPowerSystem* toolbox.

Chapter 4

Microgrid Emergency Control Strategies

Regardless of the MG operation mode, this LV distribution system is a three-phase with neutral under unbalanced conditions of operation. Additionally to that, for the MG in emergency operation the single-phase MS and loads carry problems in maintaining suitable voltage and frequency levels in the system.

To solve this kind of problems, based on previous INESC Porto researches, specific control strategies were developed, in order to coordinate local generation resources, storage devices and flexible loads. Where the MG concept integrates EV has an implementation of the smart grid functionalities.

When the active power at the microsources and loads varies, the system frequency and local voltages also diverge from their nominal values. The frequency is directly proportional to the active power in the system and the unbalance between voltages is directly proportional to the system reactive power. Consequently the approach passes through the study of the active and reactive power in the system having knowledge of the power variation in microsources and loads. This is only possible through the communication infrastructure between the MGCC and the local controllers in each distributed generation.

In this study, a SMO approach was used, where the storage device acts as the "master-VSI" and all other sources are operated in a PQ mode. In the PQ inverts of PV and EV are implemented control concepts where the active power is regulated depending on frequency or voltage local values. If it is a primary control the information about the frequency is provided by the MGCC, and the voltage magnitudes are measured locally. If it is a secondary control, used in PV, an intersection of information from the local controllers and their own measurements is made in the VSI (in MGCC). Then, the MGCC demand the control parameters to the local controllers.

Therefore, the first section of this chapter review briefly the EV frequency control strategy and describe the EV voltage control developed. In the second section the PV

frequency control strategy is presented and also their additional secondary control strategy developed.

4.1 - Electrical Vehicle control Strategies

The EV control parameters depend on the EV charger characteristics and on the disposition of EV owners to participate in such services.

4.1.1 - Primary frequency control

In this study, based on the research made by the authors in [4], the P-f droop control strategy implemented at the EV charger has the following evolution and parameters.
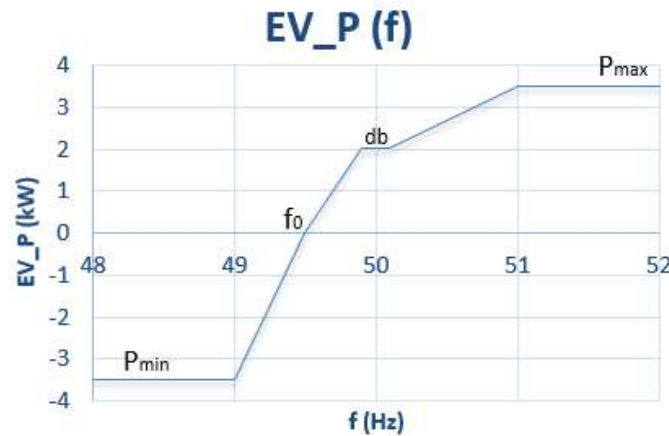
Figure 4.1 – EV Frequency-Droop characteristic.

Parameters:

$Zero - crossing\ frequency - f_0 = 49.5\ Hz;$

$Frequency\ dead - band - db = 0.2\ Hz;$

4. **Period of EV consumption** $[f_0, P_{max}]$

$Maximum\ EV\ Power - P_{max} = 3.5\ kW;$

$Dead - band\ EV\ Power - P_C = P_{nominal} \times 0.58 = 2.03\ kW$

(0.58 *was chosen in based of simulations being the value with more charging power*);

5. **Period of EV Injection** $[P_{min}, f_0]$

$Minimum\ EV\ Power - P_{min} = -3.5\ kW.$

4.1.2 - Primary voltage control

As referred in the Chapter 2 for the local voltage regulation, it is recommend a similar approach as used in frequency control.

Therefore, in the **EV voltage control** a P-V droop control strategy is implemented at the EV charger (see following figures), where the EV will modify the power exchange with the LV grid based on the voltage phase node of EV connection.
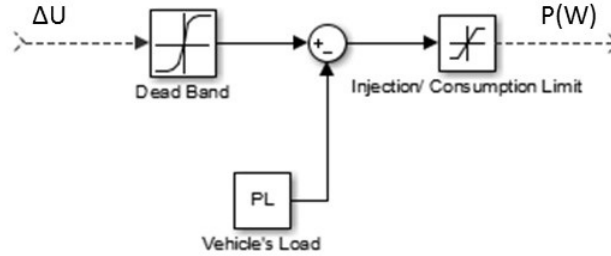
Figure 4.2 – Control loop for the EV active power voltage set_point.
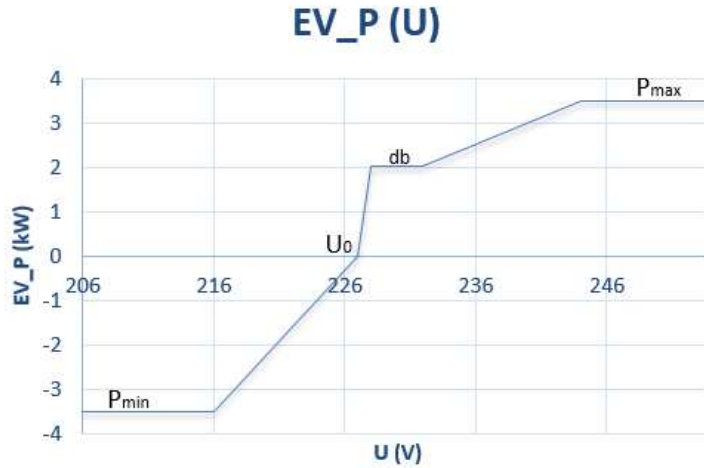
Figure 4.3 – EV Voltage-Droop characteristic.

In order to reach the appropriate parameters, represented in the previous figure, and using the EV node voltages, some simulations were done. Starting with the simulations of the microgrid only with the primary frequency control and then only with the primary voltage control. In each simulation the following considerations were made:

- U_{min} represents an approach of the minimum voltage value in the node
- U_{max} represents an approach of the maximum voltage value in the node
- U_{db_min} represents an approach of the minimum voltage value from the group of the maximum node voltages;
- U_{db_max} represents an approach of the maximum voltage value from the group of the minimum node voltages;
- U_0 represents an approach of the biggest voltage value smaller than U_{db_min}.

Therefore, evaluating these consideration, the parameters of the EV Voltage-Droop characteristic were adapt in each simulation until the voltages in the EV node present similar results to the previous simulation.

The simulations results and parameters will be presented in the next chapter with an evaluation of this control strategy developed.

More precisely the parameters not visible in the figure are:

$$Zero-crossing\ frequency-V_0 = 227\ V;$$

$$Voltage\ dead-band-db = 4\ V;$$

- **Period of EV consumption $[f_0, P_{max}]$**

$$Maximum\ EV\ Power-P_{max} = 3.5\ kW;$$

$$Dead-band\ EV\ Power-P_C = P_{nominal} \times 0.58 = 2.03\ kW$$

$$0.58\ was\ chosen\ based\ on\ simulations, being\ the\ value\ with\ more\ charging\ power)$$

- **Period of EV Injection $[P_{min}, f_0]$**

$$Minimum\ EV\ Power-P_{min} = -3.5\ kW.$$

The EV Voltage-Droop characteristic shows that:

- Voltage around the nominal value (in this case, 230 V) - the EV will charge the battery at a pre-defined charging rate;
- Voltage higher than the dead-band maximum value - the EV can also increase its power consumption;
- Voltage lower than the dead-band minimum value - the EV reduces its power consumption, reducing the load of the system;
- Grid Voltage below the zero-crossing voltage (V0): for large disturbances - the EV starts to inject power into the grid (Vehicle-to-Grid-V2G functionality);
- Voltage becomes out of the pre-defined frequency range the vehicle will inject/absorb a fixed power.

4.1.3 - **Coordination of Primary frequency and voltage control**

For the MG under study, through some simulations, it was possible to validate the following role for the commitment between the voltage and frequency control in EV, referred in the Chapter 2. This consideration is based on rehearse made in the reference [7].

$$P_{EV} = \begin{cases} P_{EV\_f}, & P_{EV\_f} < P_{EV\_v} \\ P_{EV\_V}, & otherwise \end{cases} (W) \qquad\qquad \textbf{(4.1)}$$

Where:

P_{EV_f} is the power that the primary frequency control assume depending on the system frequency

P_{EV_V} is the power that the primary voltage control assume depending on the phase voltage

P_{EV} is the power that the eletrical vehicle assume

This role evaluates the power output in each primary control and give priority to the lower one. The least favourable situation (lower power) is assumed as primary control strategy in electrical vehicle, the frequency or voltage.

4.2 - Photovoltaic Panel control Strategies

The fact that before, PV was only controlled by injecting their maximum active power it became a problem mainly for the frequency suitable levels in the system.

Therefore, in order to mitigate this problem, two methods were developed to control the active power injection. The first one depending on the MG frequency and the second on the active power at the VSI.

4.2.1 - Primary frequency control

The PV primary control depends on the system frequency, because their active power contribution is one of the big influences for the deviation in the nominal frequency value.

Therefore, taking into account the PV characteristics, the frequency control approach used in EV, is also adopted in the PV in order to provide primary frequency control. The P-f droop control strategy is implemented at each PV inverter (see following figures), where the PV modify the power exchange with the LV grid based on the MG frequency.
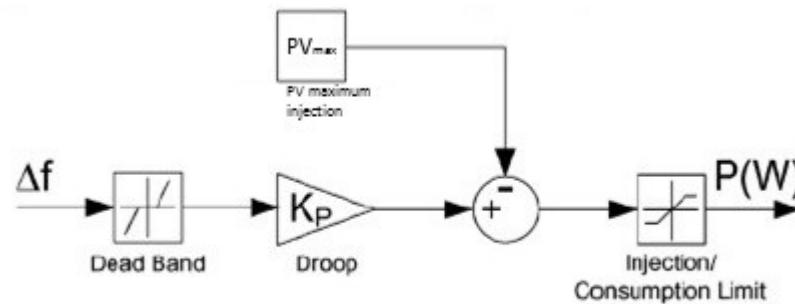
Figure 4.4 – **Control loop for the PV active power set_point.**
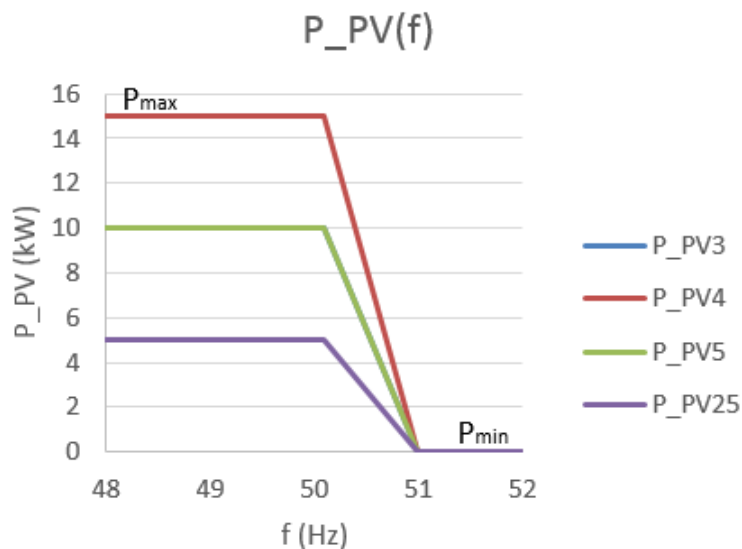
Figure 4.5 – P**V Frequency-Droop characteristic.**

The figure 4.5 shows each PV frequency-droop characteristic in the MG, where the frequency value of 50.1 Hz (maximum frequency in a possible dead-band) defines the moment when each PV must decrease their active power injection depending on the MG frequency. In the frequency of 51 Hz it is defined that the PV contribution most be over.

The maximum active power injection of each MG PV is:

$$PV3_{max} = PV5_{max} = 10 \ kW; \ PV4_{max} = 15 \ kW; \ PV25_{max} = 15 \ kW.$$

4.2.2 - Secondary control – global coordination

Contrarily to primary frequency control, made autonomously and locally, during MG islanding transition, the secondary control happens after this transient and is done following the orders of the central control.

As result the PV secondary control was developed because the simulations feedback from their primary frequency control showed that the system frequency could be improved and the photovoltaic panels had the capacity to decrease their power injection.

Therefore, the strategy developed consists on sending the power set points to each PV by the Central control (the MGCC). In the MGCC the procedure is:

- Measure the active power of VSI injection (P_{VSI});
- Determine the proportion (P_{b_n}) of P_{VSI} that each PV will decrease in their power set point:

$$P_{b\_n} = P_{a\_n} \times P_{VSI} \ (kW) \tag{4.2}$$

  - The following equations are pre-determined:

$$PV_t = \sum_{i=1}^{4} PV_{max} \ (kW) \tag{4.3}$$

$$P_{a\_n} = \frac{PV_n}{PV_t} \tag{4.4}$$

- Determine power set-point of each PV:

$$PV_{n \ set-point} = PV_n - P_{b\_n} \ (kW) \tag{4.5}$$

Where:

$PV_n = active \ power \ value \ of \ particular \ PV;$

$(the \ value, correspondent \ to \ the \ control \ instant, reported \ by \ the \ local \ controls)$

$PV_t = Total \ maximum \ power \ of \ PV;$

$P_{a\_n} = Proportion \ of \ each \ PV \ in \ the \ total \ value.$
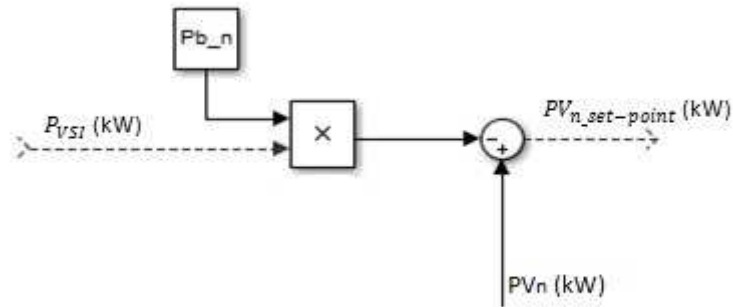
Figure 4.6 – Secondary Control at VSI for the PV active power set_point.

4.3 - Summary and Main Conclusions

This chapter presents all the control strategies studied in this thesis for the MG Emergency Operation.

A relevant fact is the development of these control strategies which were designed for any MG, but some adjustments of control parameters have been adapted to the specific MG under study.

For a MG with Single-Master Operation, photovoltaic panels, electrical vehicles and without the microturbine, the control strategies were implemented on the components with capacity to improve problems such as voltage and frequency suitable levels (the EV and PV).

For Electrical Vehicle there were projected two primary controls, one depending on the frequency system and other on the local phase voltage. The intention is to coordinate both, so that in the desired moment the most appropriate is applied.

The primary and secondary controls were developed for the Photovoltaic Panels, the first dependent on the frequency system and the other on the VSI active power. In this case knowing that the PV active power injection has a big impact on the frequency system value, the intention was to mitigate, in the best way, this impact.

The EV and PV control strategies developed will be evaluated in the following chapter, in order to understand if their strategies are adequate. Including the combination of both components strategies.

Chapter 5

Evaluation of Microgrid Emergency Operation

The previous chapter presents and describes the control strategies developed for the Microgrid operating in emergency conditions. The main objective of this Chapter is to evaluate the behaviour of the proposed control strategies through extensive numerical simulations.

The simulation platform was developed under the *MatLab®/Simulink®* environment, where it is possible to analyse the dynamic behaviour of several Microsources and storage devices (described in Chapter 3) connected to a Low Voltage network, together with the proposed control strategies for MG emergency operation conditions.

This chapter starts by presenting and describing the microgrid configurations under study, where each one is associated to the type of evaluation made in the different simulations.

The evaluations, described in the following sections, are divided in three major parts and reflect the type of methodology developed to answer the goals of this thesis. So, the first section begins to study the impact of generation variation in the microgrid with or without microturbine (controllable microsource).

The second section studies the impact of the control strategies described in the Chapter 4 and is divided in two parts. One related to the electrical vehicle control strategies and the other to the photovoltaic control strategies. The EV part starts to evaluate their primary frequency control, developed by INESC in other researches. Then to build and validate the EV primary voltage control and in the end to combine and coordinate the both control strategies.

Having knowledge that one of the causes for the development of the control strategies is the presence of single-phase microsources, the PV part builds and validates their primary and secondary control strategies.

The last section represents the balance between the system phases voltages influenced by the balancing unit.

5.1 - Microgrids System Test

As previously stated, the single line diagram of the LV system was adapted from an INESC TEC study case. In this thesis the microgrid system tested has three types of configurations:

1. The **first** used to assess the Impact of the Single-phase Generation (second section) including or not one microturbine (SSMT);

2. The **second** used to assess the Impact of the Control Strategies Proposed (third section), based on the first one but with more photovoltaic panels, the electrical vehicles and control functionalities;

3. The **third** used to assess the Impact of the Balancing Unit (fourth section), based on the first configuration and with the addiction of the Balancing Unit at the VSI (Balancing Unit model presented in the Appendix A).

An important parameter that is used in all the MG configurations is the time of isolation during simulation. When this time is achieved the MG operate in island mode, being necessary that all MG variables are stable at this moment. So, in order to maintain this stability some simulations were performed and the appropriate times were determined: 20 seconds for the first and third configurations and 5 seconds for second configuration.

In the first configuration the following components were adopted:

- MV/LV distribution transformer with the MG separation device;
- Three groups of loads (darker green blocs), in different nodes, composed by constant single and three-phase impedance;
- Three single-phase Photovoltaic Panels (blue square blocs) in two different nodes (PV3, PV4 and PV25);
- Three-phase Microturbine (purple bloc) with (SSMT_25);
- One Voltage Source Inverter (orange bloc) associated to the central control;
- One single-phase Electrical Vehicle operating (lighter green bloc) as a load (Node 69 in Phase A).

The next figure represents the *MatLab®/Simulink®* simulation environment for the first MG configuration with SSMT. The MG configuration without SSMT is presented in the Appendix A.

Figure 5.1 – First MG configuration topology with SSMT simulated in *Matlab®/Simulink®*.

The next table 5.1 presents the most relevant parameters considered in the previous MG configuration topology. These components parameters are associated to their connection phase and grouped by their power influence in the grid (Load or Generation).

Table 5.1 — First MG Configuration Parameters

	Load (W)			Generation (W)				Load (W)
Node	15	25	69	15		25	69	69
				PV3	PV4	Microturbine	PV25	EV
Phase A	5500	2747	2747	2000	0	0	0	7000
Phase B	1150	500	4828	0	5000	0	0	0
Phase C	1150	800	1.28	0	0	0	2000	0
Three-Phase	1250	1200	1943	0	0	7500	0	0
MG Total (W)	30816.28			16500				

The values presented in the previous table show that the starting point of this microgrid configuration is a scenario with higher load comparing with the generation. One of the big contributions is the fact that the electrical vehicle is operating as a load.

Using the first configuration and the feedback of their simulations results, presented in the next chapter section, it was possible to create the second configuration. In order to have a more significant scenario in terms of generation and consequently a significant impact from the control strategies.

Therefore, the second MG configuration has the following components by the order shown in the Figure 5.2:

- MV/LV distribution transformer with the MG separation device;
- Three groups of loads (darker green blocs), in different nodes, composed by constant single and three-phase impedance;
- Four single-phase Photovoltaic Panels (blue squares blocs) in two different nodes (PV3, PV4, PV5 and PV25);
- Two single-phase Electrical Vehicles (lighter green blocs) with 3.5 kW each and in the same node 69 in different phases (EV1 and EV2).
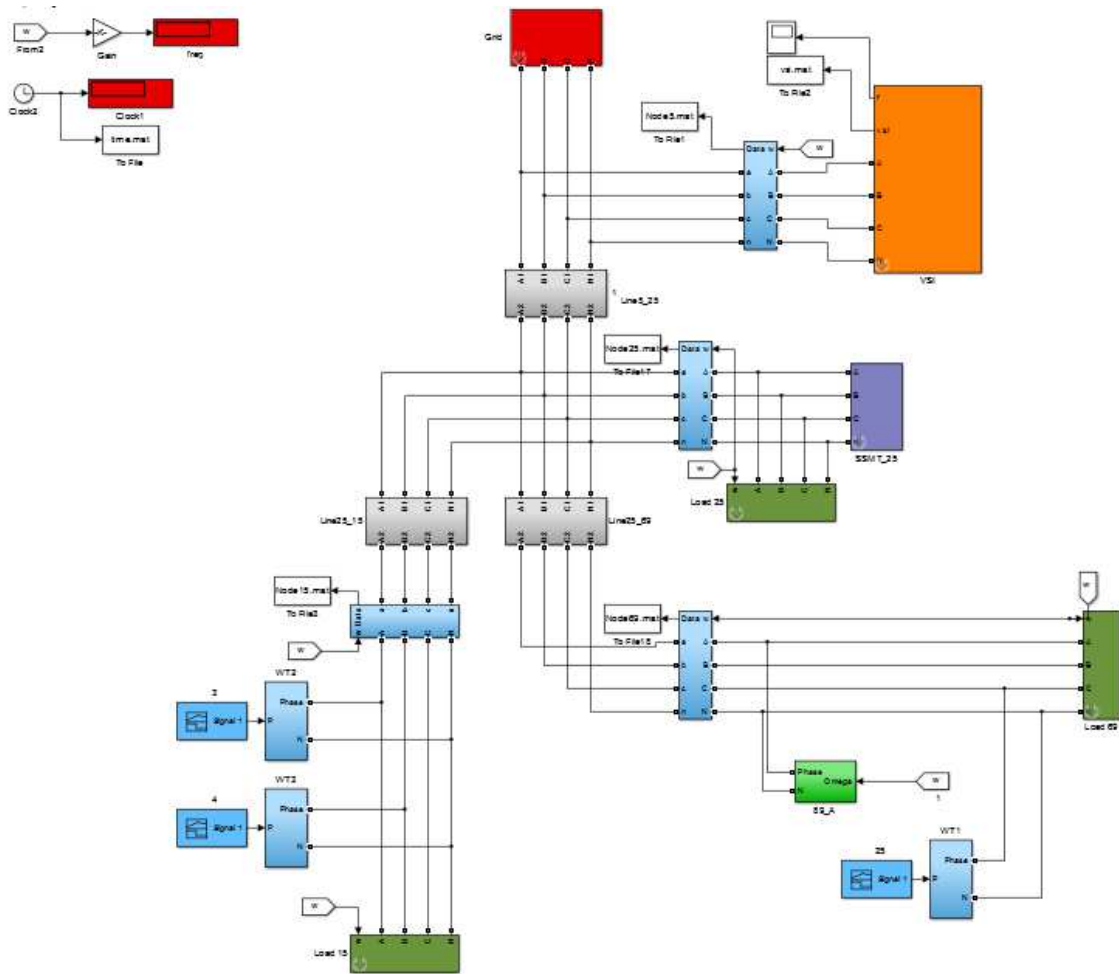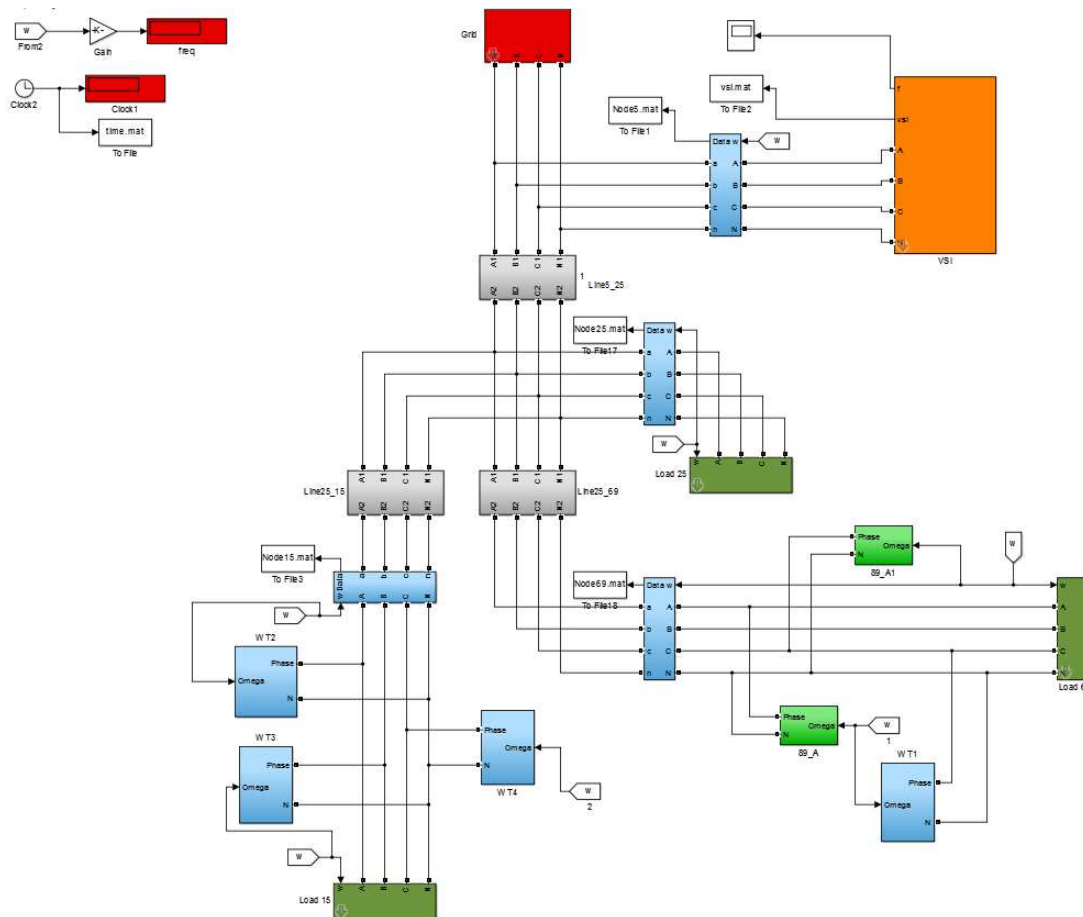

Figure 5.2 –Second MG configuration topology simulated in **Matlab®/Simulink®**.

The next table presents the most relevant parameters considered in the second MG configuration topology, where they are associated to their connection phase and grouped by their power influence in the grid (Load or Generation).

Table 5.2 — Second MG Configuration Parameters

Node	Load (W)			Generation (W)				EV
	15	25	69	15			69	69
				PV3	PV4	PV5	PV25	
Phase A	5500	2747	2747	10000	0	0	0	3500
Phase B	1150	500	4828	0	15000	0	0	0
Phase C	1150	800	1.28	0	0	10000	5000	3500
Three-phase	1250	1200	1943	0	0	0	0	0
MG Total (W)	23816.28			40000				7000

The values presented in the previous table show that the generation is always bigger than the load in the grid, for the case of maximum charging from EV (Load=30 816.28W and Generation=40 000W) or for the EV injection active power in the grid (Load=23 816.28W and Generation=47 000W).

In the next evaluation sections the simulations are followed by graphics that represent the MG electric parameters variation during the time of simulation. Therefore, it is possible to find the subsequent graphics:

- MG frequency;
- VSI active and reactive power;
- Microturbine active and reactive power;
- EV active power;
- For each node the phases voltages magnitudes;
- For each node the voltage unbalance factor ($\%VUF$) for negative and zero sequence voltages.

5.2 - Impact of the Single-phase Generation

For a MG emergency operation the single-phase MS and loads carry problems to maintain a suitable voltage and frequency levels in the system. Therefore, in this section only the increasing of the generation in the MS is evaluated.

Another aspect studied is the influence of the microturbine, given their capacity to regulate their power injection as function of the system frequency.

For the case scenarios described below, the Electrical Vehicle operates as a load (without any control strategy). Thus, the study cases and their predicted results are:

1. The first MG configuration using microturbine:
    1.1. With double generation in all Photovoltaic Panels;
    1.2. With triple generation in all Photovoltaic Panels;
2. The first configuration without microturbine:
    2.1. With double generation in all Photovoltaic Panels;
    2.2. With triple generation in all Photovoltaic Panels;

2.3. With quadruple generation in all Photovoltaic Panels.

Table 5.3 — Simulation Scenarios Overview

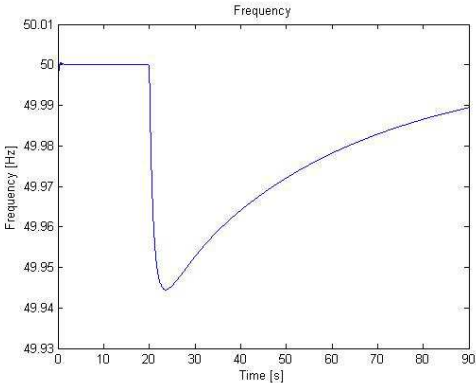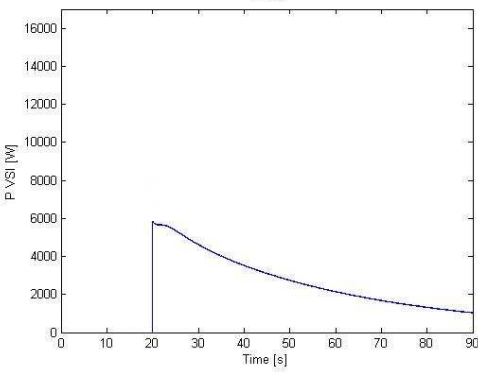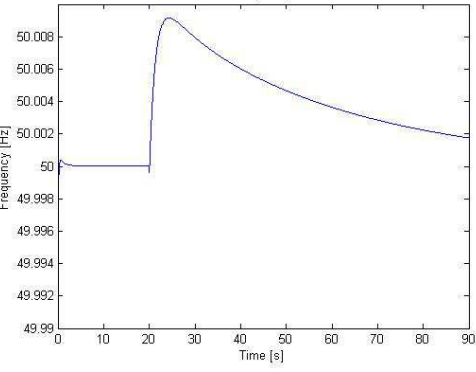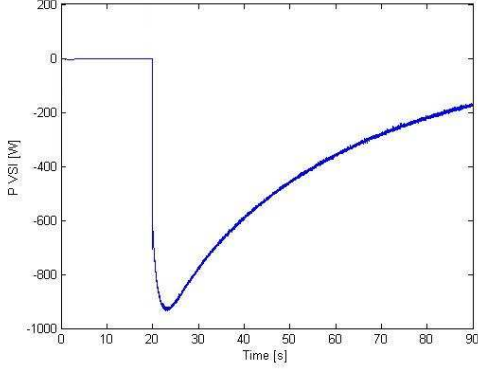| Scenario		Phase A (W)	Phase B (W)	Phase C (W)	Microgrid (W)
1.1	Load	19458.333	7942.3333	3415.6133	30816.28
	Generation	6500	12500	4500	23500
	Total	**-12958.333**	**4557.6667**	**1084.3867**	**7316.28**
1.2	Load	19458.333	7942.3333	3415.6133	30816.28
	Generation	8500	17500	4500	30500
	Total	**-10958.333**	**9557.6667**	**1084.3867**	**316.28**
2.1	Load	19458.333	7942.3333	3415.6133	30816.28
	Generation	4000	10000	4000	18000
	Total	**-15458.333**	**2057.6667**	**584.38667**	**12816.28**
2.2	Load	19458.333	7942.3333	3415.6133	30816.28
	Generation	6000	15000	6000	27000
	Total	**-13458.333**	**7057.6667**	**2584.3867**	**3816.28**
2.3	Load	19458.333	7942.3333	3415.6133	30816.28
	Generation	8000	20000	8000	36000
	Total	**-11458.333**	**12057.667**	**4584.3867**	**-5183.72**

The **highlighted** values represent the difference between the MG generation and the MG load, which become the active power in VSI.

Analysing the prediction results is possible to understand which scenarios have excess of production (generation) or load, depending on the PV generation increasing. The ones with positive value have excess of Load, the others with negative value have excess of production. The best case scenario will be a value closer to zero (scenario 1.2), meaning that the difference between Load and Generation is minimum and the MG will become more stable.

For these simulations only the following graphics are needed to analyse the single-phase generation impact. Therefore, it was considered that the VSI active power is related to the MG frequency and VSI reactive power is related to the voltages magnitudes in the node 15, where the increasing of generation is more significant.

For simulations of 90 seconds (horizontal axis) in the scenarios 1.1 and 1.2, and 40 seconds (horizontal axis) in the scenarios 2.1, 2.2 and 2.3, the analysis of the MG frequency and VSI active power are achieved by the subsequent graphics.

Table 5.4 – MG Frequency and VSI Active Power Graphics for the Firs MG configuration with microturbine

	MG Frequency	VSI Active Power
1.1	 Figure 5.3 –Time Evolution of the Frequency in Scenario 1.1.	 Figure 5.4 –Time Evolution of the Active Power in Scenario 1.1.
1.2	 Figure 5.5 – Time Evolution of the Frequency in Scenario 1.2.	 Figure 5.6 – Time Evolution of the Active Power in Scenario 1.2.

Table 5.5 — MG Frequency and VSI Active Power Graphics for the Firs MG configuration without microturbine

	MG Frequency	VSI Active Power
2.1	Figure 5.7 – Time Evolution of the Frequency in Scenario 2.1.	Figure 5.8 – Time Evolution of the Active Power in Scenario 2.1.
2.2	Figure 5.9 – Time Evolution of the Frequency in Scenario 2.2.	Figure 5.10 – Time Evolution of the Active Power in Scenario 2.1.
2.3	Figure 5.11 – Time Evolution of the Frequency in Scenario 2.3.	Figure 5.12 – Time Evolution of the Active Power in Scenario 2.2.

Analysing the graphics above, for all case scenarios, it is possible to observe the following similarities:

- For the MG frequency (directly proportional to the increasing of generation):

- o If the Generation Power is bigger than the Load Power the frequency is higher than the nominal value (50 Hz);
  - o If the Generation Power is smaller than the Load Power the frequency is lower than the nominal value (50 Hz);
  - o Although it is not observed, if the Generation Power is equal to the Load Power the frequency will have its nominal value (50 Hz).
- For the VSI active power:
  - o Inversely proportional to the increasing of generation – because the function of the VSI is to compensate the excess or deficit of active power in the system using their storage capacity;
  - o If the Generation Power is smaller than the Load Power the VSI active power is positive;
  - o If the Generation Power is equal to the Load Power the VSI active power is zero (or with a small value that can't be observed in the graphics);
  - o Although it isn't observed, if the Generation Power is bigger than the Load Power the VSI active power will be negative.

The main difference between the scenarios with microturbine (the 1.1 and 1.2) and the ones without it (the 2.1, 2.2 and 2.3) is the frequency and active power evolution during the period of isolated operation.

The microturbine has the capacity to react to the system frequency droop by readjusting their active power contribution in the MG system. Consequently, in the 1.1 and 1.2 scenarios, the MG frequency tends gradually to their nominal value (50 Hz) and the VSI active power to zero.

In the scenarios with the microturbine absence (the 2.1, 2.2 and 2.3) the responsibility, to improve the MG frequency and the VSI active power, belongs only to the VSI. However, for all the scenarios seen the VSI acts by the following way:
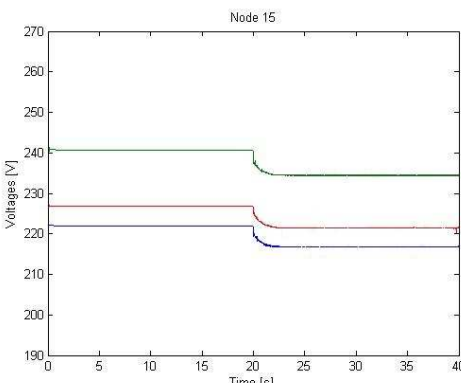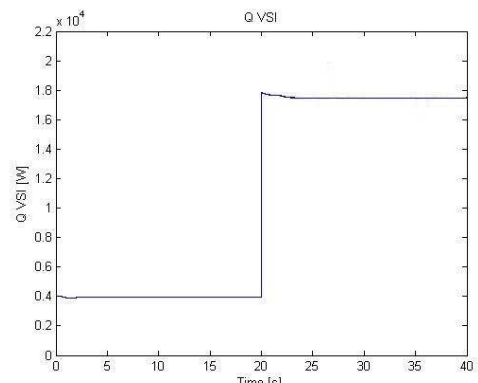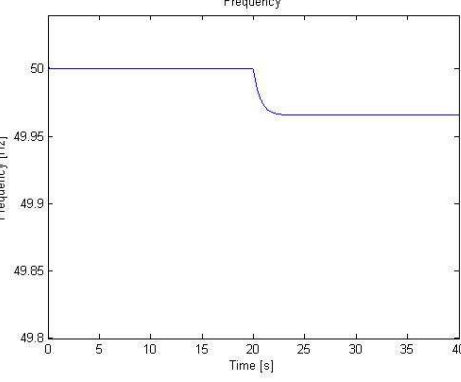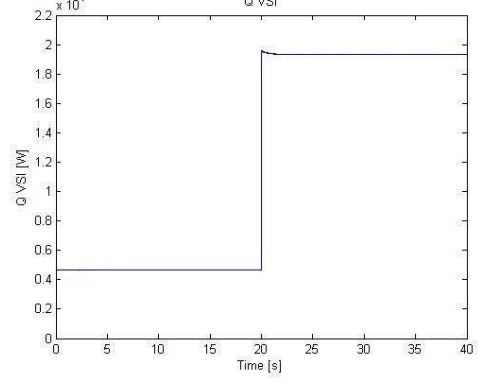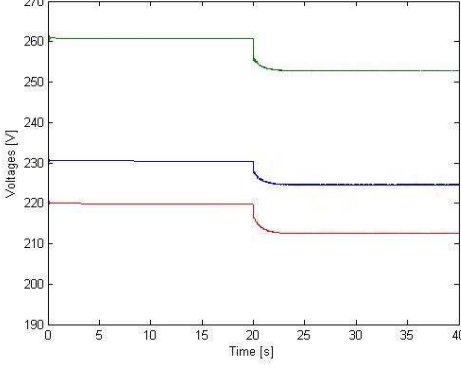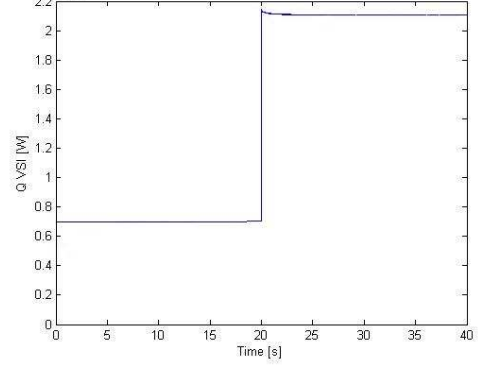
- Inject the deficit of power in the system when their active power is positive (Generation smaller than Load);
- Absorbed the excess of power in the system when their active power is negative (Generation bigger than Load);
- Don't inject or absorbed power in the system when their active power is zero (Generation equal to Load).

For simulations of 90 seconds (horizontal axis) in the scenarios 1.1 and 1.2, and 40 seconds (horizontal axis) in the scenarios 2.1, 2.2 and 2.3, the analysis of the voltages magnitudes in node 15 and VSI reactive power are achieved by the subsequent graphics.

Table 5.6 — Voltages Magnitudes in the Node 15 and VSI Reactive Power Graphics for the First MG configuration with microturbine

	Voltages Magnitudes in the Node 15	VSI Reactive Power
1.1	Figure 5.13 – Time Evolutions of the Voltages in Scenario 1.1 for the node 15.	Figure 5.14 – Time Evolution of the Reactive Power in Scenario 1.1.
1.2	Figure 5.15 – Time Evolutions of the Voltages in Scenario 1.2 for the node 15.	Figure 5.16 –Time Evolution of the Reactive Power in Scenario 1.2.

Table 5.7 — Voltages Magnitudes in the Node 15 and VSI Reactive Power Graphics for the First MG configuration without microturbine

	Voltages Magnitudes in the Node 15	VSI Reactive Power
2.1	Figure 5.17 – Time Evolutions of the Voltages in Scenario 2.1 for the node 15.	Figure 5.18 – Time Evolution of the Reactive Power in Scenario 2.1.
2.2	Figure 5.19 – Time Evolutions of the Voltages in Scenario 2.2 for the node 15.	Figure 5.20 – Time Evolution of the Reactive Power in Scenario 2.2.
2.3	Figure 5.21 – Time Evolutions of the Voltages in Scenario 2.3 for the node 15.	Figure 5.22 – Time Evolution of the Reactive Power in Scenario 2.3.

Analysing the graphics above, for all case scenarios, it is possible to observe the following similarities:

- Through the Voltages Magnitudes in the node 15 that:
    - The voltages are directly proportional to the increasing of generation;

        o   The most significant increase happens in the phases where the generations are connected.

- Through the VSI reactive power that:
  - o   The VSI reactive power rises with the increase of generation, only because the imbalance between the Generation and Load voltages are higher.

The fact that the VSI reactive power injection is not enough for the voltages regulation is related to some MG characteristics. When the MG operate in the emergency mode, their high resistance levels, in comparison with the reactance, and the significant number of single-phase loads and Microsources are the characteristics that aggravate the voltages regulation. Requiring the identification of voltage regulation mechanisms through active power control, thus being a possible conflict with the frequency regulation.

According with the analysis done before, the generation increase has a direct impact on the MG frequency, on the VSI active power and on the voltages magnitudes, especially in the phases connected with the generations. In the VSI reactive power this influence is indirect, because the VSI answer with reactive power when the voltages between the Generation and the Load are unbalanced.

The results and analysis achieved in this section were essential for the construction of the second MG configuration, used in the following sections, and for the definition of their parameters. Therefore, knowing the results of the generation increase in the microgrid the second configuration was built with more drastic conditions, for example larger number of photovoltaic panels with higher power capacity.

Finally, some distortions observed in the graphs are provoked by variations in the simulation algorithms of *MatLab®/Simulink®*. In order to consult the other graphics obtained in this simulations consulate the Appendix B.

5.3 - Impact of Proposed Control Strategies

The Chapter 4 presents and describes the control strategies developed for the MG under study. Therefore, this section discloses the simulations that help build the control strategies and also validate them.

As stated, this section applies for the second MG configuration, having knowledge that this one possesses the best conditions to show the impact of the control strategies developed.

5.3.1 - Electrical Vehicle control Strategies

In this section the EV control capacities are explored, contrarily to the previous section where the EV was used as a load.

As described in the Chapter 4 the EV control strategies are divided by primary frequency control and primary voltage control. The simulations presented below, start to evaluate the primary frequency control, developed in INESC.

Subsequently, based on the EV primary frequency control simulations results, the primary voltage control was built, using the next procedure to achieve the adequate parameters (presented in Chapter 4 and described in detail in the Appendix C):

- **First** using EV frequency control simulation results – the first parameters were determined and was made the first simulation with the EV voltage control;

- **Second** comparing the simulations results from the frequency control and the first voltage control - the second group of parameters were determined and a second simulation with the EV voltage control was done;

- **Third** comparing the simulations results of the first and second voltage controls - the third group of parameters were determined and a third simulation with the EV voltage control was performed;

- **Finally,** comparing the simulations results of the second and third voltage controls - the procedure stopped, because the values were no longer changing significantly.

After this procedure to reach the appropriate parameters for the EV primary voltage control an evaluation was performed for the impact of their control strategy.
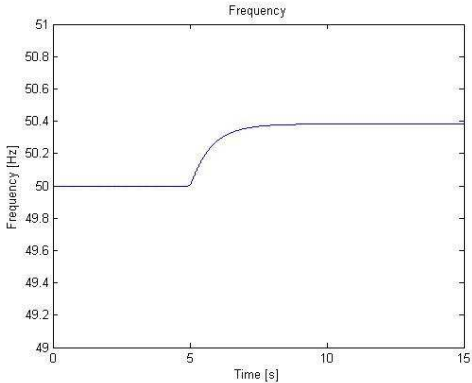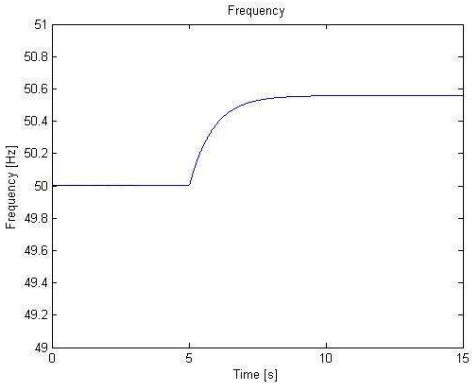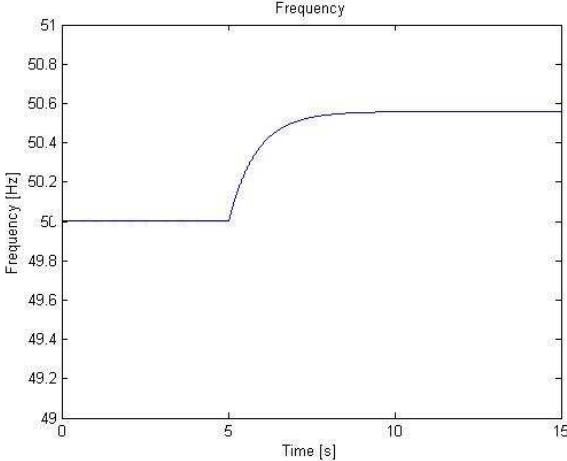
Finally, it was combined and coordinated both strategies, where the EV had to choose which one is more appropriate for the conditions in the MG, comparing the power in each control strategy and choosing the one with lower value.

Thus, the graphics simulations are divided by the following order:

- The **F_Control** - Show the impact of the primary frequency control, already developed**;**

- The **U_Control** - Evaluate the EV primary voltage control impact on MG;

- The **UvsF_Controlo** - Evaluate the coordination between the two EV control Strategies, previously described.

For simulations of 15 seconds (horizontal axis) the analysis of the MG frequency, VSI active and reactive power, Voltages Magnitudes in the Node 69 and EV active Power are reached by the subsequent graphics.

Table 5.8 — Time Evolution of MG Frequency in EV control Strategies

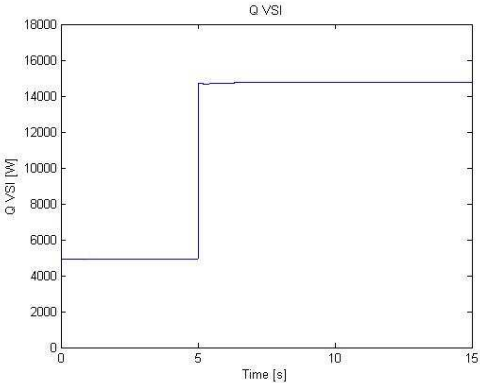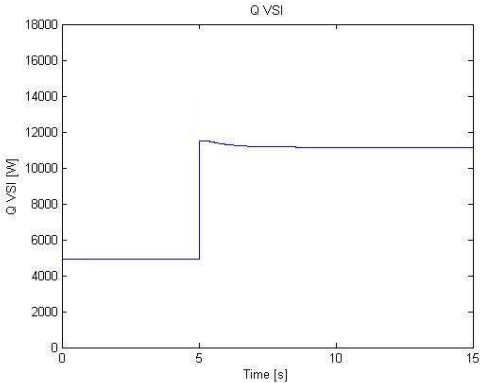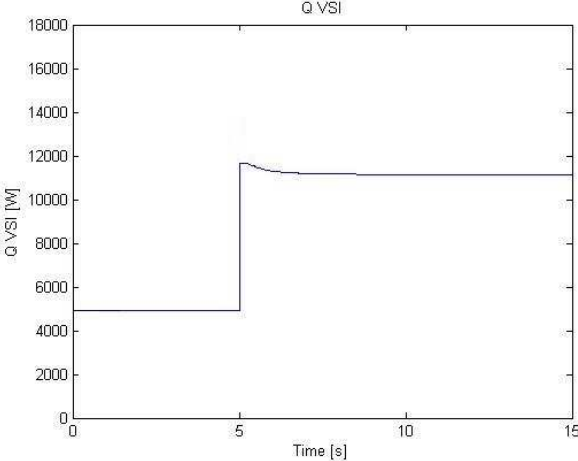| MG frequency	
F_Control	**U_Control**
Figure 5.23 – Time Evolutions of the MG frequency in EV **F_Control**.	Figure 5.24 – Time Evolutions of the MG frequency in EV **U_Control**.
UvsF_Controlo	
Figure 5.25 – Time Evolutions of the MG frequency in EV **UvsF_Control**.	

Interpreting the graphics it is possible to state that:

- In the **F_Control** the frequency value is higher than the nominal value (50 Hz), making the EV increase their charging power and causing a drop in the phase voltage in the node where EV is connected (node 69);

- In the **U_Control** the frequency value is higher than the one in **F_Control,** because the phase voltage is too low and the EV decreases its charging power until a point that it starts injecting power in the MG (V2G mode). Consequently, the phase voltage will increase (where the EV is connected);

- The combination of both controls (**UvsF_Controlo)** is similar to the primary voltage control – meaning that the EV chose the voltage control strategy for the MG conditions (the Voltage power is lower, so the local voltages are the worst case scenario compared to the frequency).

Table 5.9 — Time Evolution of VSI Active Power for the EV control Strategies

VSI Active Power	
F_Control	**U_Control**
Figure 5.26 – Time Evolutions of the VSI active power in EV **F_Control**.	Figure 5.27 – Time Evolutions of the VSI active power in EV **U_Control**.
UvsF_Controlo	
Figure 5.28 – Time Evolutions of the VSI active power in EV **UvsF_Control**.	

Table 5.10 — Time Evolution of VSI Reactive Power for the EV control Strategies
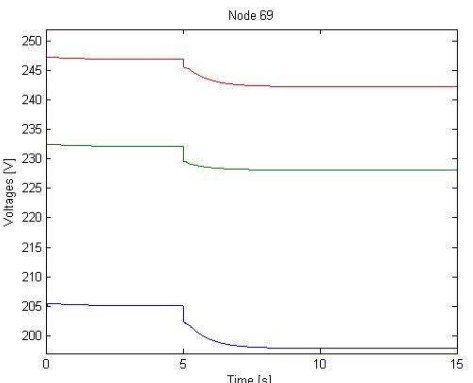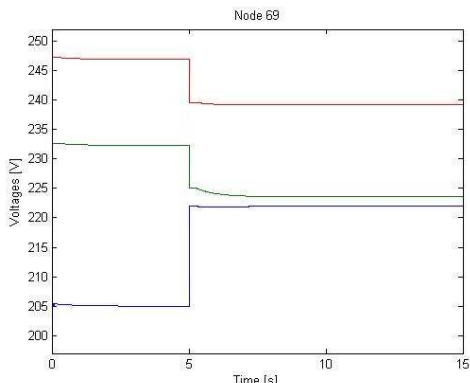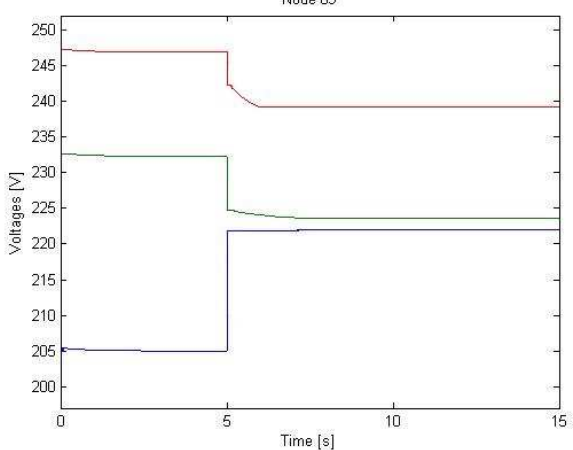
VSI Reactive Power	
F_Control	**U_Control**

Figure 5.29 – Time Evolutions of the VSI reactive power in EV **F_Control**.

Figure 5.30 – Time Evolutions of the VSI reactive power in EV **U_Control**.

UvsF_Controlo

Figure 5.31 – Time Evolutions of the VSI reactive power in EV **UvsF_Control**.

For the same control strategies, the VSI active and reactive power shows an opposite variation, according to their graphics. Consequently:

- The VSI active power, related to the system frequency, decreases when the frequency tends to the nominal value (50 Hz). The best case scenario is the **F_Control**, where the VSI has a lower contribution of active power in the MG;

- The VSI reactive power, related to the unbalance between Generation and Load voltages, decreases when this unbalance is minimum. The best case scenario is the **UvsF_Controlo**, where the VSI has a lower contribution of reactive power in the MG.

Table 5.11 — Time Evolution of Voltages Magnitudes in the Node 69 for the EV control Strategies
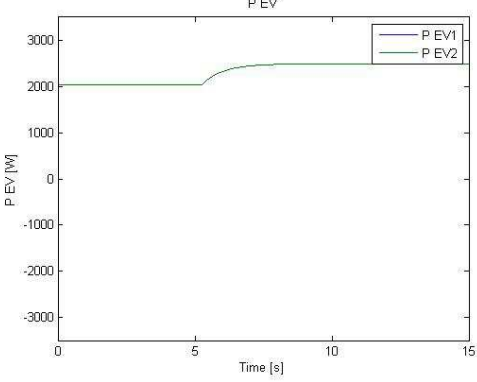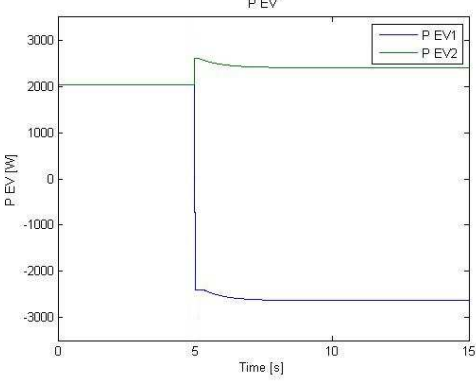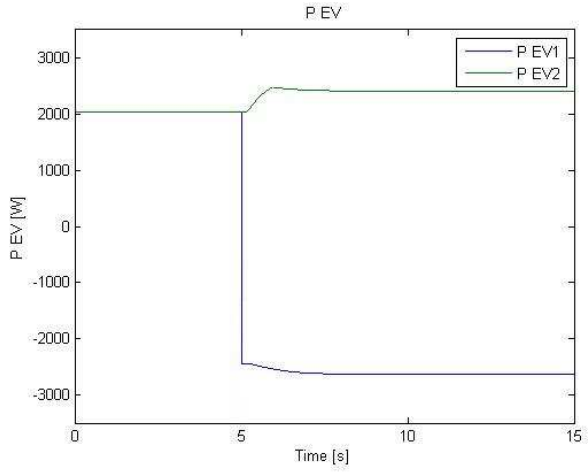
Voltages Magnitudes in the Node 69	
F_Control	**U_Control**
Figure 5.32 – Time Evolutions of the Voltages magnitudes for the node 69 in EV **F_Control**.	Figure 5.33 – Time Evolutions of the Voltages magnitudes for the node 69 in EV **U_Control**.
UvsF_Controlo	

Figure 5.34 – Time Evolutions of the Voltages magnitudes for the node 69 in EV **UvsF_Control**.

As predicted with MG frequency graphics, the phases voltages, where the EV is connected, are the ones with higher variation.

Analysing the graphics above, it is possible to observe:

- The blue Phase (Phase A) has the lowest voltage magnitude, far from the nominal value (230 V) – in the **F_Control** this voltage is more affected compared to the **U_Control** and consequently the **UvsF_Controlo** prioritize the voltage control;

- The green Phase (Phase B) has also a low voltage magnitude, but not so far from the nominal value (230 V) – in the **F_Control,** this voltage is more suitable comparing to the one in **U_Control**, but the **UvsF_Controlo** use voltage control because their value is smaller and consequently also their power;

- The red Phase (Phase C) has a similar behaviour in all strategies, meaning that it does not have any EV connected.

Table 5.12 — Time Evolution of EV Active Power for the EV control Strategies

EV Active Power	
F_Control	**U_Control**
Figure 5.35 – Time Evolutions of the VSI active power in EV **UvsF_Control**.	Figure 5.36 – Time Evolutions of the VSI active power in EV **UvsF_Control**.
UvsF_Controlo	
Figure 5.37 – Time Evolutions of the VSI active power in EV **UvsF_Control**.	

Analysing the graphics it is possible to see that during the isolation the **U_Control** has a similar graphic compared to **UvsF_Controlo.**

Given the fact that the primary frequency control only depends on the frequency system, this control will always have the same behaviour for each EV in the MG.

On the other hand, given the fact that **U_Control** reacts to the phase local magnitude, each EV can have a different behaviour.

The combination of both strategies (**UvsF_Controlo)** proposes the best option to control the MG frequency and the local voltage magnitudes. When the active power is negative the EV is injecting active power in the MG and when it is positive the EV is charging their batteries. Choosing always the worst case scenario: the lowest power.

Based on the simulations results of voltages magnitudes it was possible to construct a group of tables with their precise variation. The tables and their analysis as well as the EV graphics (not shown in this chapter) are presented in the Appendix C.

5.3.2 - **Photovoltaic Panel control Strategies**

Given the results of the previous section, it is possible to realize that the EV control strategies are not enough to mitigate the system frequency deviation from their nominal value.
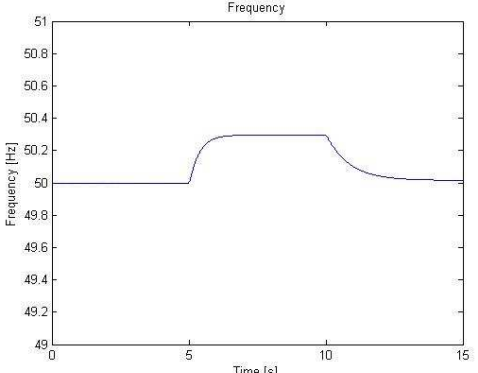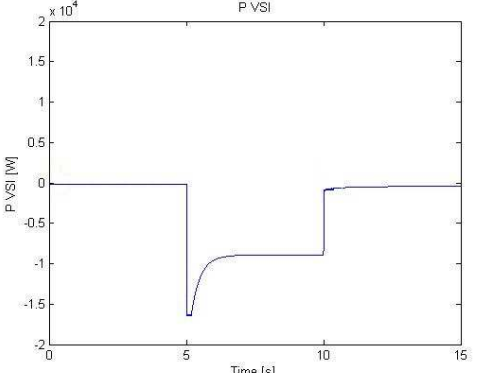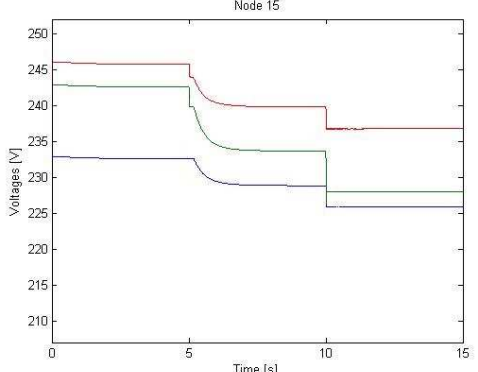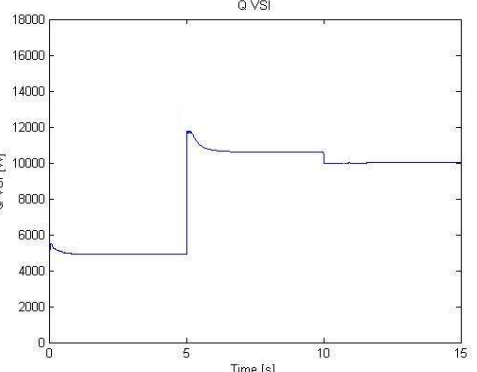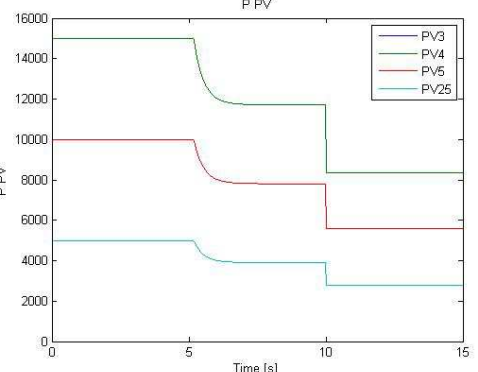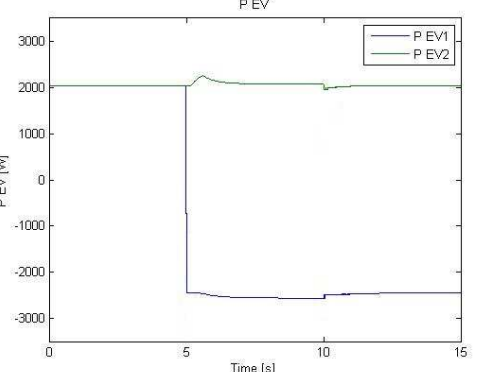
Having Knowledge that the photovoltaic panels (non-controllable MS) give a big contribution for this problem, the next step was to develop their control strategies. Accordingly with the Chapter 4, the PV control strategies have a primary and secondary frequency control. The first idea was to adapt the PV active power injection in function of the system frequency, because they are directly proportional. With the simulations results from the PV primary frequency control, the next idea was to distribute the excess remaining in the VSI active power proportionally throughout the photovoltaic panels, considering their injection capacity.

These control strategies are applied for frequencies deviations above their nominal value (50 Hz). For the opposite situation the photovoltaic panels operate in their maximum power capacity, so the frequency improvement is not done by these microsources.

The simulations for the PV control strategies include the EV control strategies, in order to understand the impact of the PV strategies in the scenario study for the electrical vehicles.

For simulations of 15 seconds (horizontal axis) the analysis of the MG frequency, VSI active and reactive power, Voltages Magnitudes in the Node 15 and EV active Power are reached by the subsequent graphics.

Table 5.13 — PV Control Strategies Graphics

MG Frequency	VSI Active Power
Figure 5.38 – Time Evolutions of the MG frequency in PV control strategies.	Figure 5.39 – Time Evolutions of the VSI active power in PV control strategies.
Phases Voltages Magnitudes node 15	VSI Reactive Power
Figure 5.40 – Time Evolutions of the Voltages magnitudes for the node 15 in PV control strategies.	Figure 5.41 – Time Evolutions of the VSI reactive power in PV control strategies.
PV Active Power	EV Active Power
Figure 5.42 – Time Evolutions of the PV active power in PV control strategies.	Figure 5.43 – Time Evolutions of the EV active power in PV control strategies.

During the 15 seconds of simulations the control strategies occur:

- after the isolation time, between the 5 and 10 seconds - the primary frequency control;
- after the double of the isolation time, between the 10 and 15 seconds - the second frequency control.

Interpreting the graphics in the **primary frequency control** zone, it is possible to state that:

- The voltages in the node 15 decrease – comparing the values before and after the 5 seconds it is possible to see that all voltages decrease in the direction of their nominal value (230 V);
- The VSI active power decreases and consequently also the MG frequency, that is directly related to the VSI active power. Comparing to the MG frequency graphic from the EV **UvsF_Control,** where the value is about 50.5 Hz and with the primary control about 50.4 Hz;
- The PV power injection decrease – the reduction of each power is done depending on the MG frequency and their own capacity.

In the **secondary frequency control** zone, the graphics show that:

- The PV power injection in the grid decrease – the MGCC set, for each PV, their Power injection value, in function of the active power in the VSI during the primary control and proportional to each PV capacity;
- The frequency drop to their nominal value (50 Hz) and the VSI active power contribution is reduce to zero –the distribution of the VSI active power excess for each PV, reducing their power injection, making the frequency return to their nominal value;
- The voltages in the node 15 drop drastically and their value is proportional to the PV power capacity – comparing the values before and after the 10 seconds:
  - in the blue phase (Phase A) and green phase (Phase B) the voltages magnitudes decrease to values bellow the nominal (230 V);
  - in the red Phase (Phase C) the voltage magnitude decrease in the direction of the nominal (230 V);
- The VSI reactive power has a smaller decrease – reflecting an improvement in the balance between generation and load voltages;
- The EV active power remains constant – reflecting that locally, in the node where the electrical vehicles are connected the voltages don't change their value and now only this control need to be prioritise.

The fact that generation is bigger than the load makes necessary that the PV decrease their active power injection.

Making conclusions of the graphics and their analysis it is possible to state that:

- The generation decreasing occurs first with the primary frequency control, which is not sufficient, and then with the secondary frequency control;
- The combination of the two PV controls are suitable, because the frequency tend to their nominal value and the active power is reduced to zero;
- The voltages results are acceptable but still one of the issues to improve, because their phases values could be better and also the VSI reactive power contribution could be reduced.

In order to consult the others graphics obtained in these simulations confer the Appendix D.**Error! Reference source not found.**

5.4 - Impact of the Balancing Unit

After the implementation and validation of the control strategies previously discussed, still need to improve one aspect in MG emergency operation, the unbalanced voltages (represented by the negative and zero-sequence components).

The VSI balancing unit is used to cancel all unwanted negative and zero-sequence voltage-current components. For this study this element was implemented in some cases of Single-phase Generation Impact:

1. MG Base configuration with double generation in all Photovoltaic Panels;
2. MG Base configuration with triple generation in all Photovoltaic Panels.

For simulations of 90 seconds (horizontal axis) the analysis of the voltage unbalance factor ($\%VUF$) for negative and zero sequence voltages are reached by the subsequent graphics.

Table 5.14 — Time Evolution of Voltage Unbalance factor for negative and zero sequence voltages

Node 15	Without Balancing Unit	With Balancing Unit
1.		
2.		
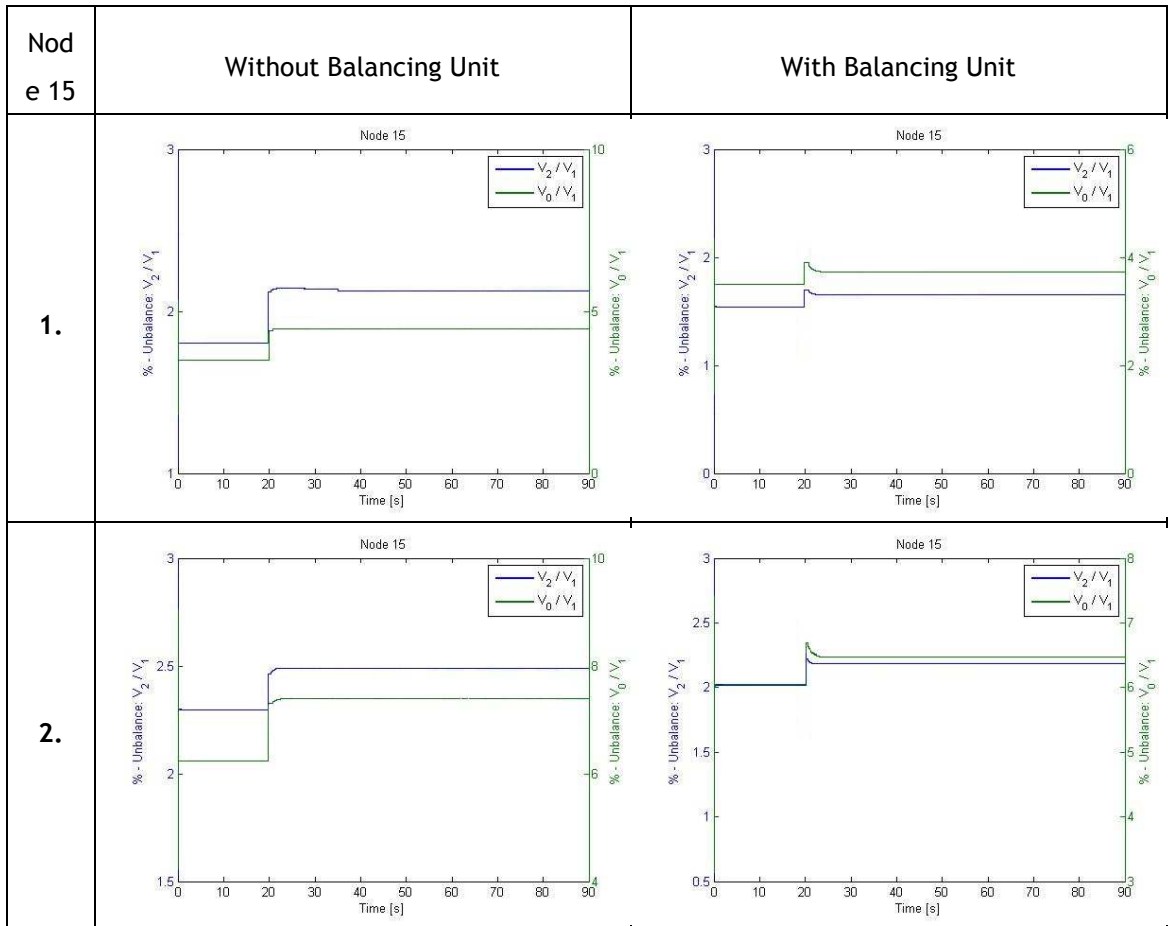
The graphics chosen are those belonging to the node where the major generation variation exists. Therefore, it is possible to observe that both negative and zero-sequence voltage unbalance factor increase with the increasing of generation.

In the first case, the unbalance negative factor (represented in blue) is the only with balancing unit that reduce their value to less than 2%, the normalized value. Although, the other case has their negative and zero-sequence factors values above 2 %, it is possible to recognize that the integration of the balancing unit decrease both unbalanced factors. Consequently, associated to this decrease will be an improvement in the voltages values, reducing the unbalance between them.

5.5 - Summary and Main Conclusions

Throughout the previous chapters, the MG emergency operation, their architecture, their problems and the possible solutions were described. As a result, this chapter reunites the simulations environment that studies the MG emergency operation, their problems with the variation of generation and the solutions developed.

According with the results and analysis done in the impact of the single-phase operation, the generation increasing affects directly the MG frequency and system voltages magnitudes, especially in the phases connected with the generations. Consequently, they progress far from their nominal values.

The VSI acts to improve the frequency value compensating the active power in the system and to balance the voltages between the generation and the load compensating the reactive power in the system. The utilization of the microturbine bring an additional frequency regulation crucial for the systems without control strategies in others components.

As result, and based on INESC researches, the development of control strategies in the Electrical Vehicles and in the Photovoltaic Panels become a good combination of solutions to improve the MG frequency and the local voltages magnitudes. The EV can improve both electrical parameters, depending on which one has a worst case scenario. The PV improves directly the MG frequency and the phase voltages magnitudes, where PV is connected, by adapting their power injection in the MG.

The last improvement in the MG emergency operation is the improvement in the balance between the voltages magnitudes. The Balancing unit plays this role by cancelling the unwanted negative and zero-sequence voltage-current components. In this thesis the balancing unit was not studied for the cases with the control strategies developed. However, given their results in the other cases, it was possible to conclude that this component will be a good answer for the improvement of the voltages magnitudes balance in the system. This problem, after the combination of EV and PV control strategies, still is a relevant issue to solve.

Chapter 6

Conclusions

6.1 - Main Conclusions

In the near future, the power system planning and operation will focus on the LV distribution networks, followed by the increasing penetration of distributed generation.

An efficient solution to deal with the DER integration acting is their local control and management, being able to provide a coordinated response to the upstream distribution grid. This also can be understood as a Smart Grid paradigm that could be dealt by the microgrid concept.

The microgrid concept presented in this dissertation tried to provide additional answers to the MG when it is operating in emergency conditions. However, the studies were developed to respond to any type of microgrid, many parameters have been adapted to MG in question.

According to the objectives of this dissertation, it was possible to study and adapt the dynamic models of the MG elements provided by INESC.

The MG hierarchical architecture and communication infrastructure are indispensable for the emergency operation. The single master operation approach was used in the MG, where the VSI (acting as master: MGCC) is used as voltage and frequency reference and all other inverters are operated in PQ mode. These PQ inverters receive the MGCC information and control the LC and update their one set-point.

The MG can be seen as a three-phase LV distribution system with neutral, bringing unbalanced conditions of operation. Additionally to that, for a MG emergency operation, the single-phase MS and loads bring problems in maintaining suitable voltage and frequency levels at the system.

Particularly the increasing of the power production cause several effects in these two electrical grid parameters (the system frequency and voltages magnitudes). In this thesis, the first MG approach to mitigate this effect was the utilization of the microturbine and the VSI.

The microturbine regulate the system frequency and control the local voltages, through the adaptation of their power injection. The VSI regulate the system frequency by the active power compensation and mitigate the unbalance between the generation and load voltages magnitudes through the reactive power compensation. However, the VSI capacity to inject or absorb the active and reactive power (the MG compensation) is limited by its storage capacity.

For a case scenario with a large number of microsources such as photovoltaic panels, with some electrical vehicles and excluding the microturbine, it was more appropriate a regulation done by the PV and EV. Therefore, through simulations it was possible to build and validate the control strategies projected for EV and PV.

The combination of EV primary frequency and voltage control improve significantly the local voltages and consequently the system frequency. However, through the validation of these strategies it was possible to notice that the system frequency has to be improved.

Given the direct relation between the frequency system and the PV power injection, the next step is to adapt this power injection, using a primary and secondary frequency control.

The combination of the EV and PV control strategies, for the MG under study, improves expressively the frequency in the system, being possible to achieve their nominal value (50 Hz). This fact was also noticed in the VSI active power contribution that returns to zero. The voltages magnitudes were improved more significantly in the nodes where the EV and PV were connected. The VSI reactive power value shows that the balance between the generation and load voltages could be improved.

However the balancing unit was not integrated in the MG with all the control strategies developed, I t is possible to conclude that their contribution would be an improvement in the voltages balance and the best case scenario.

Concluding, the results obtained in this dissertation, confirm that a big difference between the generation and load causes severe problems to the stability of the grid (unbalanced operation with high power production and low load), particularly to the system frequency and voltages magnitudes. The utilization of the Matlab/Simulink allowed to identify more precisely the potential causes of the unbalance operation. At the same time it was possible to build and validated the potential control strategies that bring adequate values of frequency and voltages in the microgrid operating in emergency conditions. Summarising, this study allow the exploration of the potential benefits that DG and other DER management may provide with their potential integrations.

This study represents a good contribution to future and present researches at INESC Porto in Smart or Microgrid area.

6.2 - Suggestions for Future Work

As mentioned, the study presented in this dissertation provides an insight on MG management and control issues. The research developed is a start for a complex study, particularly in a future implementation. Therefore, some suggestions could be made to continue and improve this research:

- Implementation of Balancing Unit with the control strategies developed;
- Implement the developed system in experimental environment;
- Study the single-phases loads behaviour in the control strategies developed;
- Study a possible integration of other Microsources such as Micro-wind turbine and Fuel Cells, assessing their impact;
- Study the possibility of integration of batteries in the PV technologies.

Bibliographic References

[1] "Microgrids: The next logical step for the military", SmartGridNews.com, http://www.smartgridnews.com/artman/publish/Delivery_Microgrids/Microgrids-The-next-logical-step-for-the-military-6327.html#.UzGq9_l_uPt.

[2] N. Hatziarguriou, H. Asano, R. Iravani and C. Marnay, "Microgrids", IEEE Power and Energy Magazine, vol.5, July/August 2007.

[3] J. A. Peças Lopes, C. L. Moreira and A. G. Madureira, "Defining Control Strategies for Microgrids Islanded Operation", IEEE Transactions on Power Systems, vol.21, no.2, May 2006.

[4] C. Gouveia, C. Moreira (Supervisor) and J. A. P. Lopes (Co-Supervisor), "Experimental Validation of Microgrids: Exploiting the role of Plug-in Electrical Vehicles, active load control and micro-generation units", Thesis Research Plan, Faculty of Engineering of the University of Porto.

[5] "Technology Roadmaps: Smart Grids", International Energy Agency (IEA), 2011. Available at: http://www.iea.org/publications/freepublications/publication/name,3972,en.html (Last Consulted on November 2012).

[6] C.Gouveia, D. Rua, C. L. Moreira and J. A. Peças Lopes, "Coordinating Distributed Energy Resources During Microgrid Emergency Operation", Book: "Renewable Energy Integration", pp. 259-303, 2014

[7] J.A.P. Lopes, F.J. Soares, P.M.R. Almeida, "Integration of Electric Vehicles in the Electric Power System", Proceedings of the IEEE, vol.99, no.1, pp.168-183, Jan. 2011

[8] F.C. Schweppe, R.D. Tabors, J.L. Kirtley, H.R.Outhred, F.H. Pickel, A.J. Cox, "Homeostatic Utility Control," IEEE Transactions on Power Apparatus and Systems, vol.PAS-99, no.3, pp.1151-1163, May 1980

[9] J.A. Short, D.G. Infield, L.L. Freris,"Stabilization of Grid Frequency Through Dynamic Demand Control," IEEE Transactions on Power Systems, vol.22, no.3, pp.1284-1293, Aug. 2007.

[10] K. Samarakoon, J. Ekanayake, N. Jenkins, "Investigation of Domestic Load Control to Provide Primary Frequency Response Using Smart Meters," IEEE Transactions on Smart Grid, vol.3, no.1, pp.282-292, March 2012.

[11] S.A. Pourmousavi, M.H. Nehrir, "Real-Time Central Demand Response for Primary Frequency Regulation in Microgrids", IEEE Transactions on Smart Grid, vol.3, no.4, pp.1988-1996, Dec. 2012.

[12] T.C. Green, M. Prodanovic, "Control of inverter-based micro-grids", Electric Power Systems Research, vol. 77, no. 9, pp. 1204-1213, July 2007.

[13] Márcio Lunardelli Ribeiro, Phd C. Moreira(Supervisor) and Phd Fernanda Resende (Co-Supervisor), "Estratégia de Reposição de Serviço utilizando Micro-Redes", Master Thesis develop in the context of Master in Electrical and Computer Engineering Major Energy, Faculty of Engineering of the University of Porto, June 2010.

[14] Carlos Coelho Leal Moreira and J. A. Peças Lopes (Supervisor), "Identification and Development of Microgrids Emergency Control Procedures", Dissertation for the degree of Doctor of Philosophy, Faculty of Engineering of the University of Porto, July 2008.

[15] J. A. Peças Lopes, Silvan A. Polenz, C.L. Moreira, Rachid Cherkaoui, "Identification of control and management strategies for LV unbalanced microgrids with plugged-in electric vehicles", Electric Power Systems Research, vol. 80, no. 8, pp. 898-906, August 2010.

[16] Prabha Kundur, "Power System Loads", in Power System Stability and Control, Ed. McGraw-Hill Education, 1994, ch.7, pp.279-305.

[17] J. V. Mierlo, P. V. d. Bossche, and G. Maggetto, "Models of energy sources for EV and EHV: fuel cells, batteries, ultracapacitors, flywheels and engine-generators." Journal of Power Sources, vol. 128, no. 1, pp. 76-89, March 2004.

Appendix

A. Test System simulation Parameters

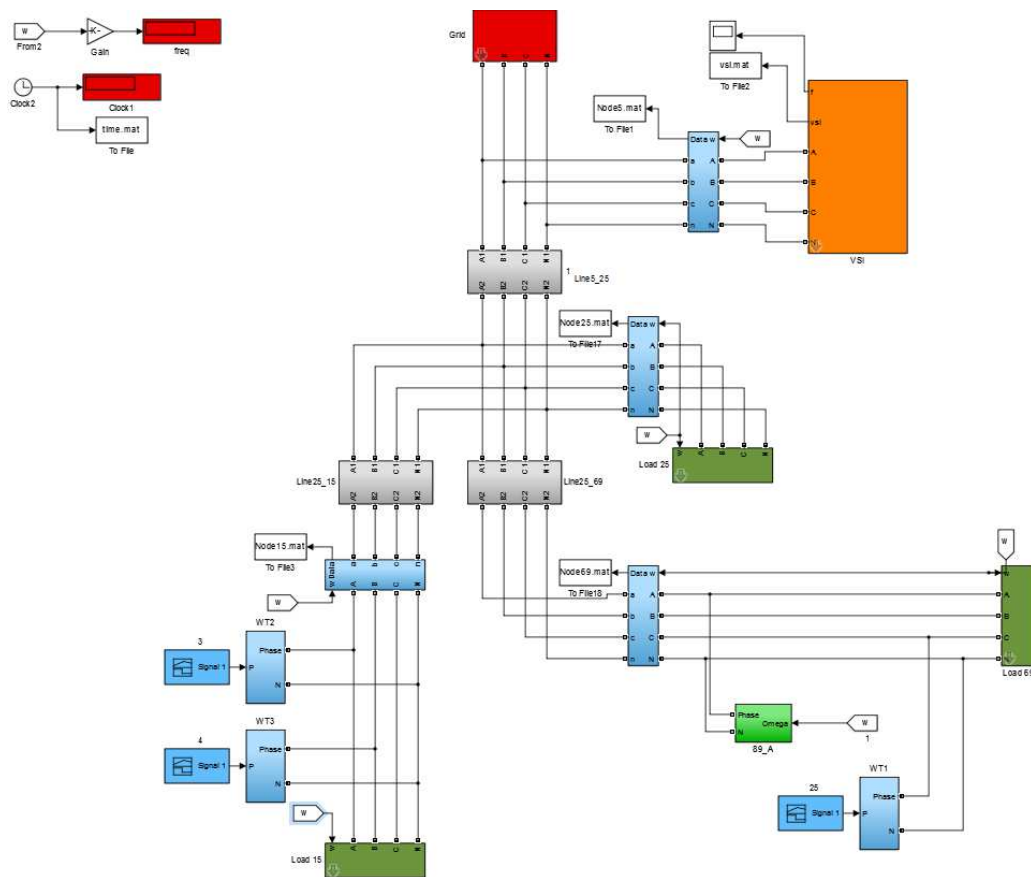First MG configuration topology without SSMT simulated in Matlab®/Simulink®.

Figure A.1 –First MG configuration topology without SSMT simulated in MatLab/Simulink.

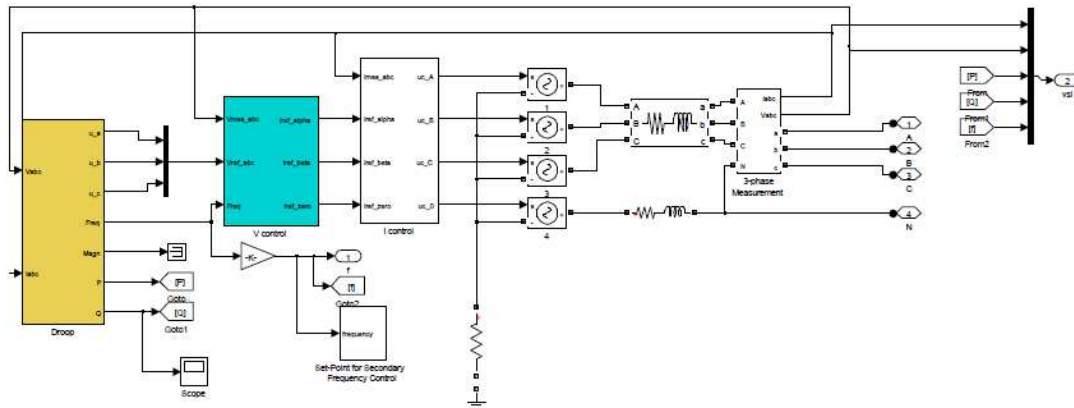Balancing Unit topology simulated in Matlab®/Simulink®.

Figure A.2 – Balancing Unit topology simulated in Matlab®/Simulink®.

B.   Single-phase Generation Graphics

Thus, the study cases and their predicted results are:

1.   The first MG configuration using microturbine:

   1.1.   With double generation in all Photovoltaic Panels;

   1.2.   With triple generation in all Photovoltaic Panels;

2.   The first configuration without microturbine:

   2.1.   With double generation in all Photovoltaic Panels;

   2.2.   With triple generation in all Photovoltaic Panels;

   2.3.   With quadruple generation in all Photovoltaic Panels.

Table A.1 — SSMT Active and Reactive Power Graphics for the First MG configuration with microturbine

1.1	1.2
Figure A.3 – Time Evolutions of the SSMT active and reactive power in Scenario 1.1.	Figure A.4 – Time Evolutions of the SSMT active and reactive power in Scenario 1.2.
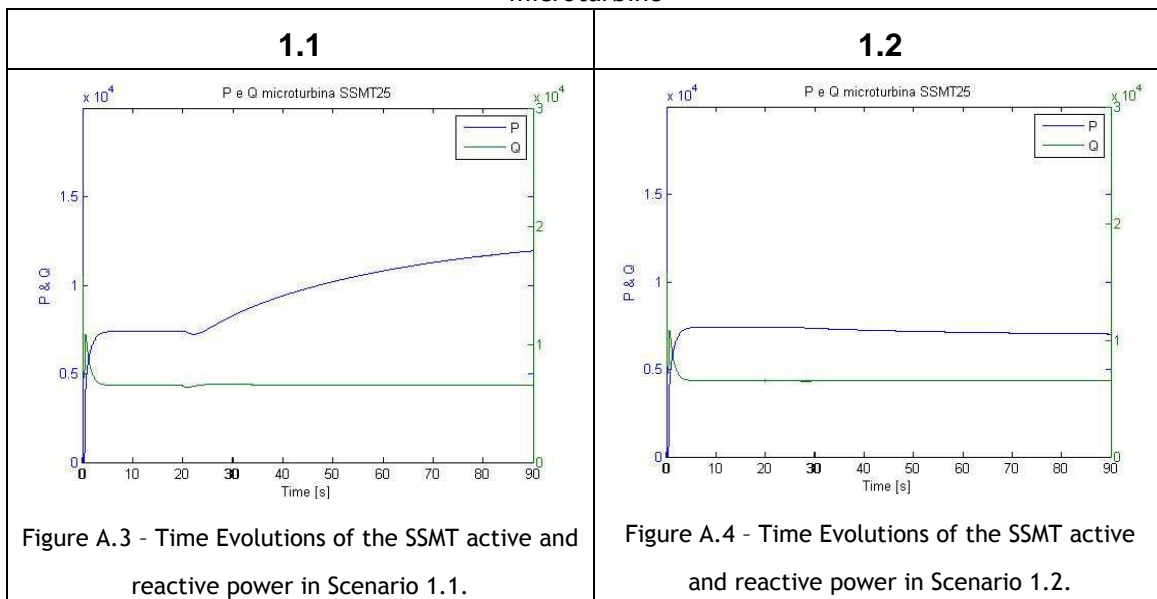
Table A.2 — Node 5 and 25 Voltages Magnitudes Graphics for the First MG configuration with microturbine
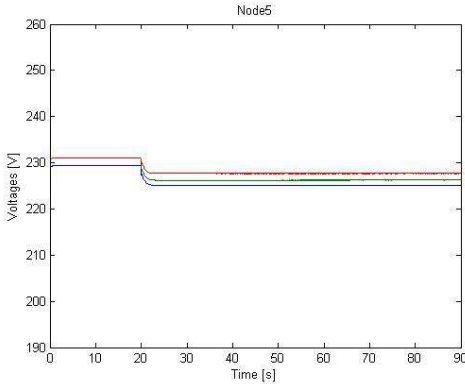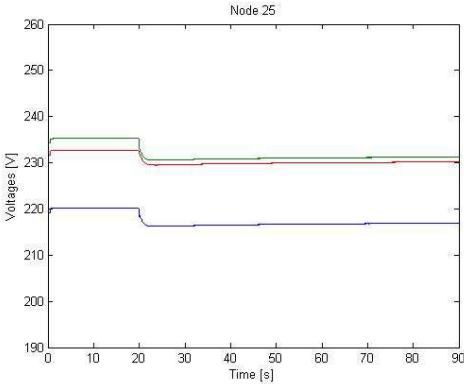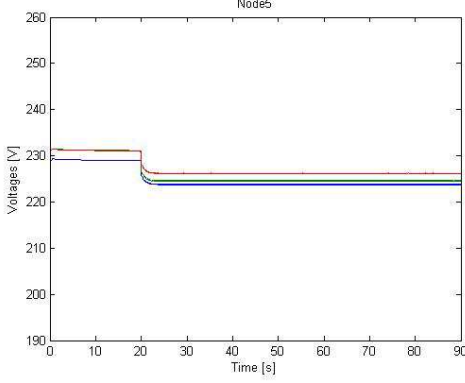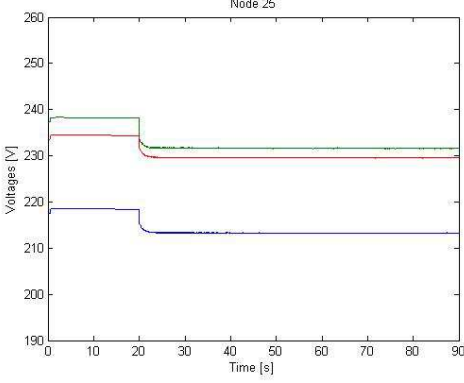
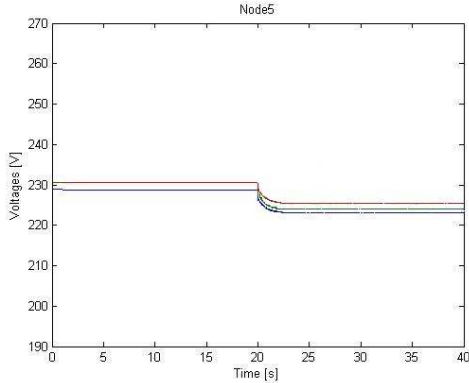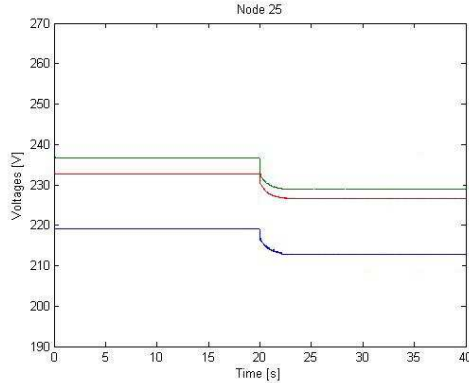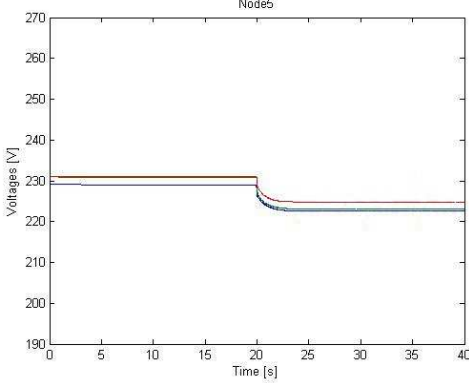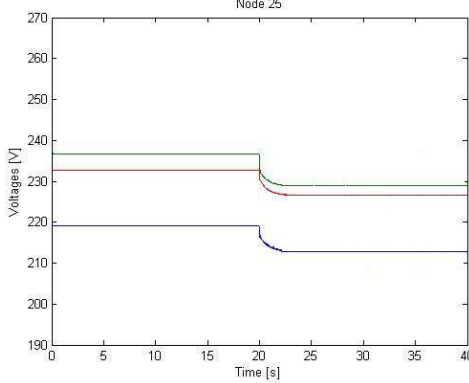|	Node 5 Voltages Magnitudes	Node 25 Voltages Magnitudes
1.1	Figure A.5 – Time Evolutions of the node 5 voltages in Scenario 1.1.	Figure A.6 – Time Evolutions of the node 25 voltages in Scenario 1.1.
1.2	Figure A.7 – Time Evolutions of the node 5 voltages magnitudes in Scenario 1.2.	Figure A.8 – Time Evolutions of the node 25 voltages magnitudes in Scenario 1.2.

Table A.3 — Node 5 and 25 Voltages Magnitudes Graphics for the First MG configuration without microturbine
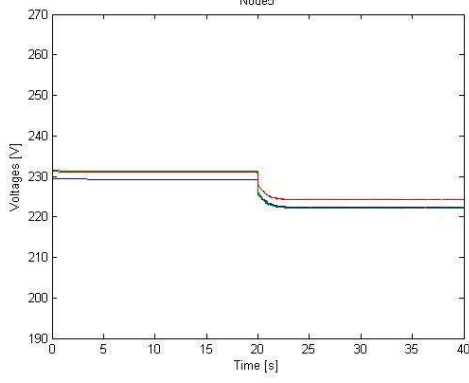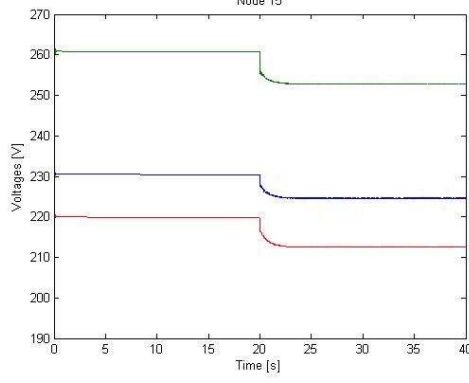
	Node 5 Voltages Magnitudes	Node 25 Voltages Magnitudes
2.1	Figure A.9 – Time Evolutions of the node 5 voltages magnitudes in Scenario 2.1.	Figure A.10 – Time Evolutions of the node 25 voltages magnitudes in Scenario 2.1.
2.2	Figure A.11 – Time Evolutions of the node 5 voltages magnitudes in Scenario 2.2.	Figure A.12 – Time Evolutions of the node 25 voltages magnitudes in Scenario 2.2.
2.3	Figure A.13 – Time Evolutions of the node 5 voltages magnitudes in Scenario 2.3.	Figure A.14 – Time Evolutions of the node 25 voltages magnitudes in Scenario 2.3.

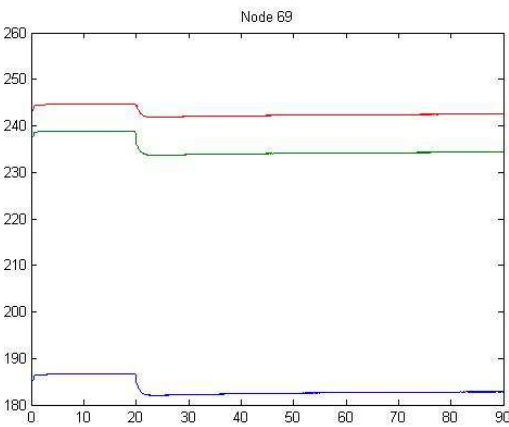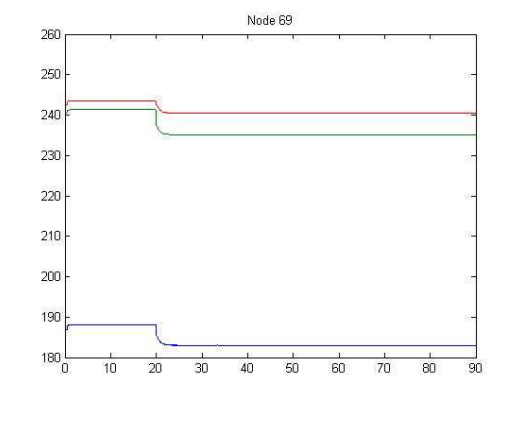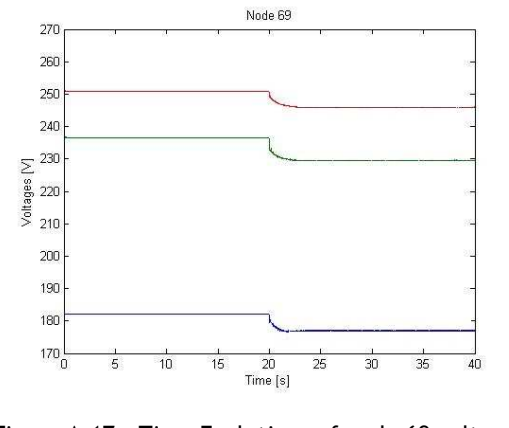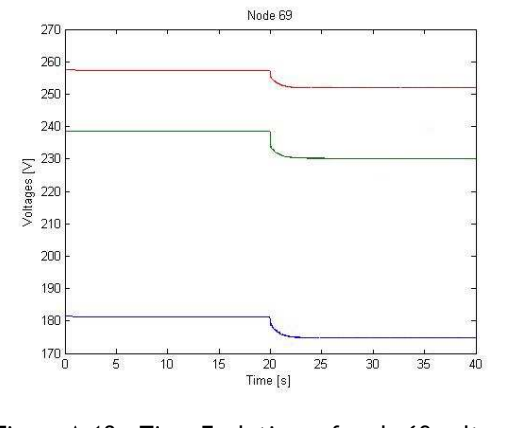Table A.4 — Node 69 Voltages Magnitudes Graphics for the First MG configuration with and without microturbine

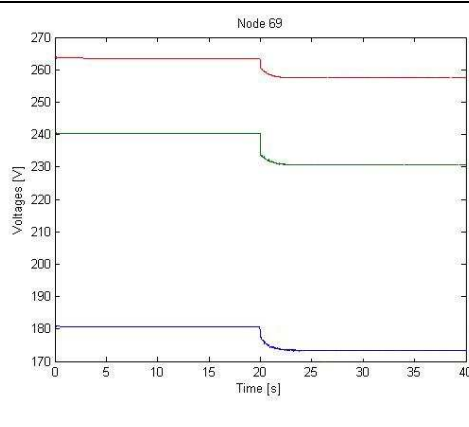| 1.1	1.2
Figure A.15 – Time Evolutions of node 69 voltages magnitudes in Scenario 1.1.	Figure A.16 – Time Evolutions of node 69 voltages magnitudes in Scenario 1.2.
2.1	**2.2**
Figure A.17 – Time Evolutions of node 69 voltages magnitudes in Scenario 2.1.	Figure A.18 – Time Evolutions of node 69 voltages magnitudes in Scenario 2.2.

2.3

Figure A.19 – Time Evolutions of node 69 voltages magnitudes in Scenario 2.3.

Table A.5 — Node 5 and 15 Time Evolution of Voltage Unbalance factor for negative and zero sequence voltages for the First MG configuration with microturbine

	Node 5 voltage unbalance factor for negative and zero sequence voltages	Node 15 voltage unbalance factor for negative and zero sequence voltages
1.1	Figure A.20 – Time Evolutions of node 5 voltages unbalance factors in Scenario 1.1.	Figure A.21 – Time Evolutions node 15 voltages unbalance factors in Scenario 1.1.
1.2	Figure A.22 – Time Evolutions of node 5 voltages unbalance factors in Scenario 1.2.	Figure A.23 – Time Evolutions of node 15 voltages unbalance factors in Scenario 1.2.

Table A.6 — Node 5 and 15 Time Evolution of Voltage Unbalance factor for negative and zero sequence voltages for the First MG configuration without microturbine
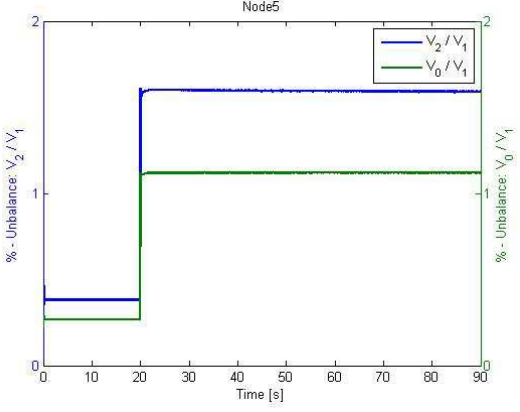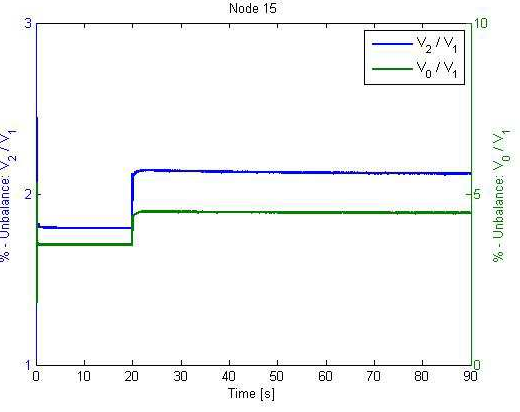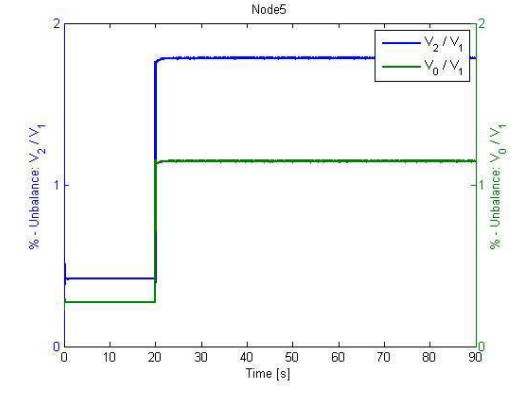
	Node 5 voltage unbalance factor for negative and zero sequence voltages	Node 15 voltage unbalance factor for negative and zero sequence voltages
2.1	Figure A.24 – Time Evolutions of node 5 voltages unbalance factors in Scenario 2.1.	Figure A.25 – Time Evolutions of node 15 voltages unbalance factors in Scenario 2.1.
2.2	Figure A.26 – Time Evolutions of node 5 voltages unbalance factors in Scenario 2.2.	Figure A.27 – Time Evolutions of node 15 voltages unbalance factors in Scenario 2.2.
2.3	Figure A.28 – Time Evolutions node 5 voltages unbalance factors in Scenario 2.3.	Figure A.29 – Time Evolutions of node 15 voltages unbalance factors in Scenario 2.3.

Table A.7 — Node 25 and 69 Time Evolution of Voltage Unbalance factor for negative and zero sequence voltages for the First MG configuration with microturbine
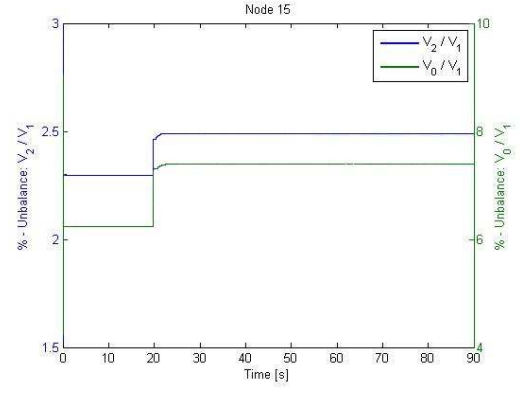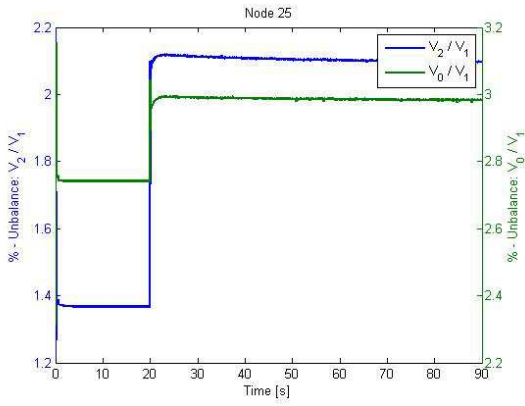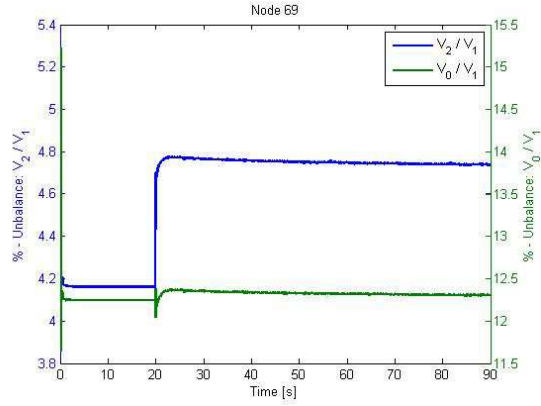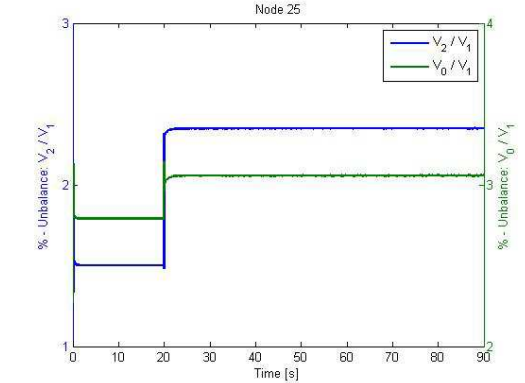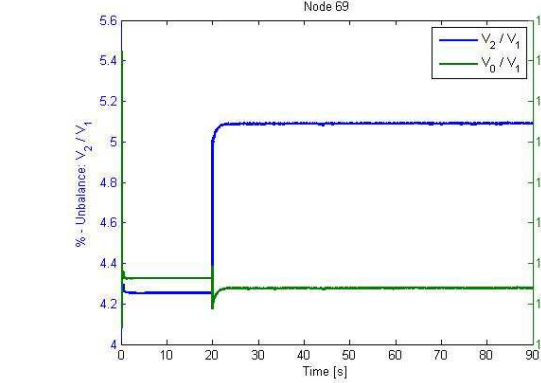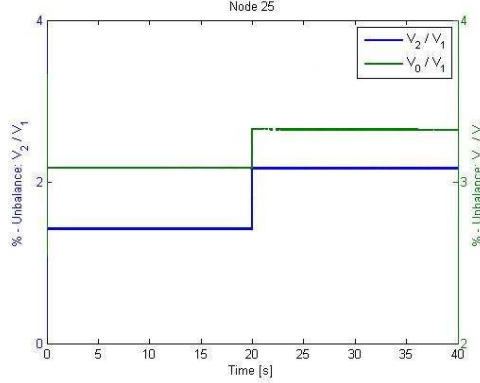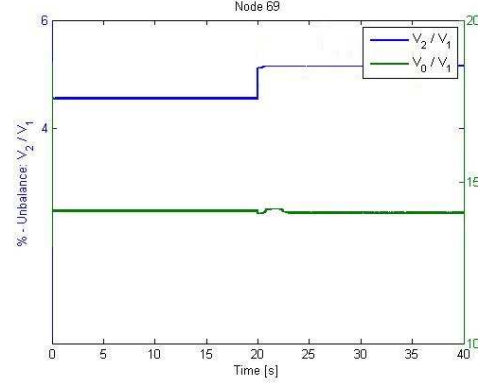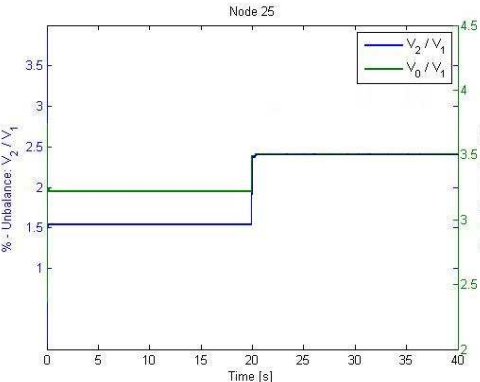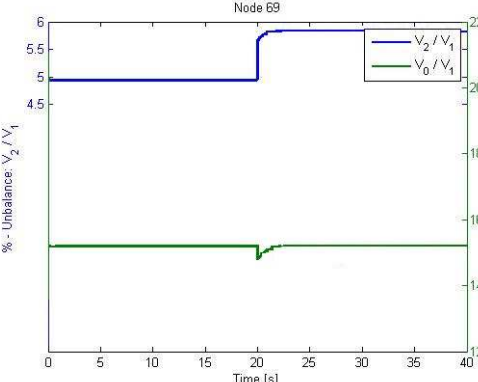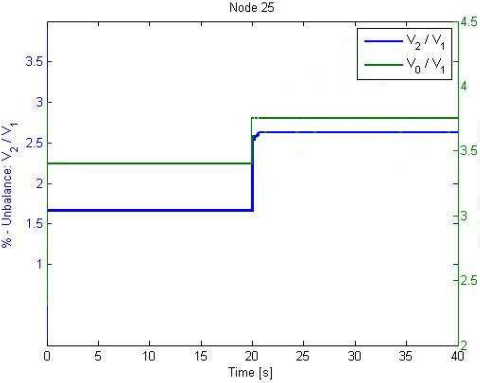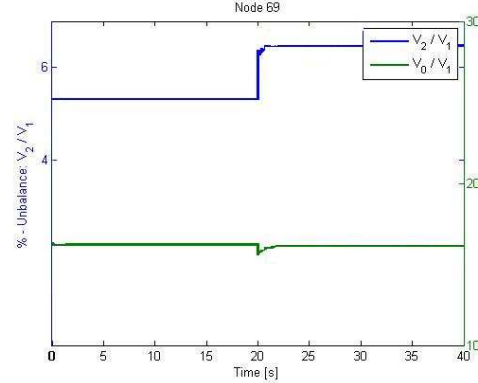
	Node 25 voltage unbalance factor for negative and zero sequence voltages	Node 69 voltage unbalance factor for negative and zero sequence voltages
1.1	Figure A.30 – Time Evolutions of node 25 voltages unbalance factors in Scenario 1.1.	Figure A.31 – Time Evolutions node 69 voltages unbalance factors in Scenario 1.1.
1.2	Figure A.32 – Time Evolutions of node 25 voltages unbalance factors Scenario 1.2.	Figure A.33 – Time Evolutions of node 69 voltages unbalance factors in Scenario 1.2.

Table A.8 — Node 25 and 69 Time Evolution of Voltage Unbalance factor for negative and zero sequence voltages for the First MG configuration without microturbine
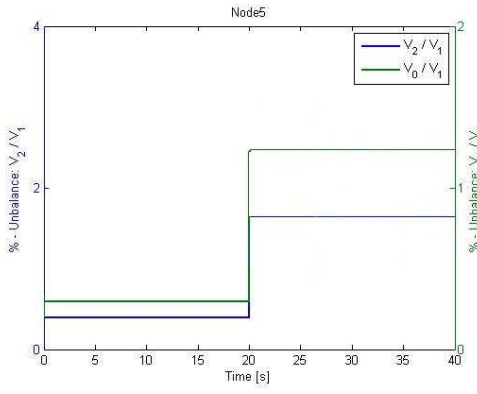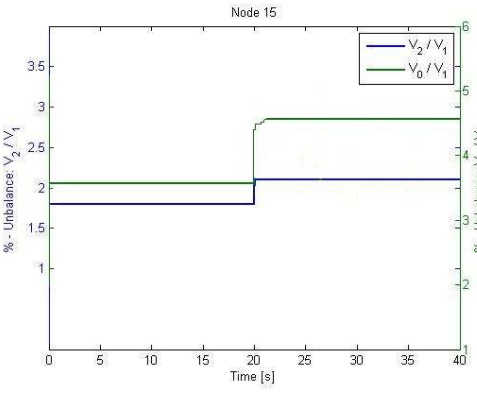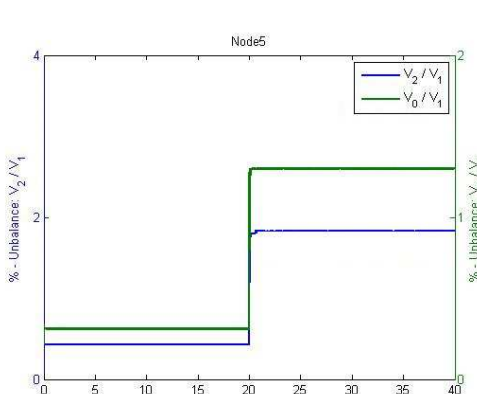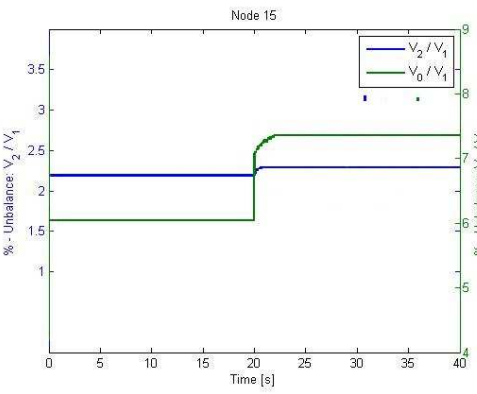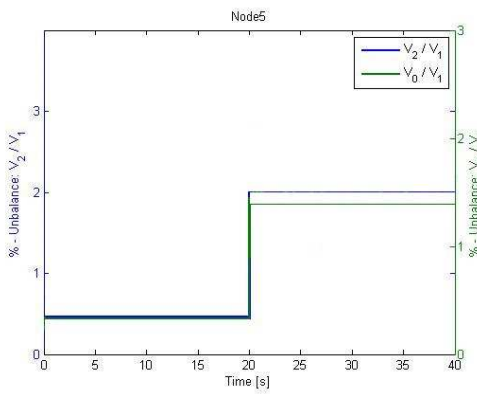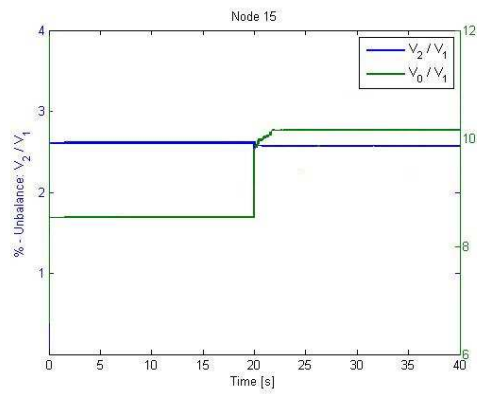
	Node 25 voltage unbalance factor for negative and zero sequence voltages	Node 69 voltage unbalance factor for negative and zero sequence voltages
2.1	Figure A.34 – Time Evolutions of node 25 voltages unbalance factors in Scenario 2.1.	Figure A.35 – Time Evolutions of node 69 voltages unbalance factors in Scenario 2.1.
2.2	Figure A.36 – Time Evolutions of node 25 voltages unbalance factors in Scenario 2.2.	Figure A.37 – Time Evolutions of node 69 voltages unbalance factors in Scenario 2.2.
2.3	Figure A.38 – Time Evolutions node 25 voltages unbalance factors in Scenario 2.3.	Figure A.39 – Time Evolutions of node 69 voltages unbalance factors in Scenario 2.3.

C.   EV control Strategy

EV primary voltage Control

To reach the correct parameters used in the EV primary voltage control there was made 3 simulations. However, only the results of the two first ones will be presented, because the second represent the ones used.

- **EV frequency control simulation:**

VSI Q (Var)	F (Hz)	Scenario	EV1 P	EV2 P	Microgrid
14763	50.38	Load (kW)	2491.5	2491.5	28799
		Generation (kW)	0	0	40000
-	-	Total (kW)	-	-	**11200.72**

Node	5	15	25	69	Max	Min
Phase A (V)	223.80	227.55	218.21	**197.85**	227.55	197.85
Phase B (V)	224.58	238.79	228.41	228.12	238.79	224.58
Phase C (V)	226.13	241.69	232.33	**242.25**	242.25	226.13

Based in the results it is possible to determine:

- Dead band (db)- analysing node 5, lower variation:
    - Minimum (Maximum Phases Voltages)≈ 227 V and Maximum (Minimum Phases Voltages)≈ 226 V
    - $db = 8\,V;\ U_{db} = [228\,;\,232]$
- Maximum, Minimum Voltages and U0 (limit value to the power injection) - analysing the 15, 25 e 69 nodes, with bigger variation:
    - $Umax\ e\ Umin\ +/-6\% * Unominal$, because 243 it is the maximum:
        - $Umax \approx 253\,V$ ≥ maximum (Maximum Phases Voltages) ≈ 243 V;
        - $Umin \approx 207\,V$ ≤ minimum (Minimum Phases Voltages) ≈ 199 V;
    - U0 will be the Maximum (values smaller then 226) ≈ 224 V.

- **1 EV voltage control Simulation:**

VSI Q (Var)	F (Hz)	Scenario	EV1 P	EV2 P	Microgrid
11471	50.54	Load (kW)	0	2212.3	26029
		Generation (kW)	1814.1	0	41814
-	-	Total (kW)	-	-	**15785.52**

Node	5	15	25	69	Max	Min
Phase A (V)	224.72	231.15	222.39	**218.35**	231.15	218.35
Phase B (V)	225.50	239.02	228.47	224.21	239.02	224.21
Phase C (V)	227.05	**242.54**	232.96	240.36	242.54	227.05

Based in the results it is possible to determine:

- Dead band (db)- analysing node 5, lower variation:
  - Minimum (Maximum Phases Voltages)≈ 231 V e Maximum (Minimum Phases Voltages)≈ 227 V
  - $231 - 227 = 4\,V, so\ db = 4\,V;\ U_{db} = [228\,;\,232]$
- Maximum, Minimum Voltages and U0 (limit value to the power injection) - analysing the 15, 25 e 69 nodes, with bigger variation:
  - $Umax\ e\ Umin\ +/-\ 6\%\ *\ Unominal$, because 243 it is the maximum:
    - $Umax \approx 244\,V$ ≥ maximum (Maximum Phases Voltages) ≈ 243 V;
    - $Umin \approx 216\,V$ ≤ minimum (Minimum Phases Voltages) ≈ 218 V;
  - U0 will be the Maximum (values smaller then 228) ≈ 227 V.

- **2 EV voltage control Simulation:**

VSI Q (Var)	F (Hz)	Scenario	EV1 P	EV2 P	Microgrid
11151	50.56	Load (kW)	0	2407.2	26223
		Generation (kW)	2634.7	0	42635
-	-	**Total** (kW)	-	-	**16411.22**

Node	5	15	25	69	Max	Min
Phase A (V)	224.83	231.76	223.04	**221.95**	231.76	221.95
Phase B (V)	225.60	239.00	228.41	223.57	239.00	223.57
Phase C (V)	227.16	**242.47**	232.87	239.15	242.47	227.16

Based in the results it is possible to determine:

- Dead band (db)- analysing node 5, lower variation:
  - Minimum (Maximum Phases Voltages)≈ 231 V e Maximum (Minimum Phases Voltages)≈ 227 V
  - Equal situation $, so\ db = 2\,V;\ U_{db} = [229\,;\,231]$
- Maximum, Minimum Voltages and U0 (limit value to the power injection) - analysing the 15, 25 e 69 nodes, with bigger variation:
  - $Umax\ e\ Umin\ +/-\ 5\%\ *\ Unominal$, because 243 it is the maximum again:
    - $Umax \approx 242\,V$ ≥ maximum (Maximum Phases Voltages) ≈ 243 V;
    - $Umin \approx 219\,V$ ≤ minimum (Minimum Phases Voltages) ≈ 222 V;
  - U0 will be the maximum (values smaller then 228) ≈ 228 V.

Node	5	15	25	69	VSI Q	f	VSI P
Phase A (V)	0.11	0.61	0.65	3.60			
Phase B (V)	0.11	-0.03	-0.06	-0.64	-320	0.02	689
Phase C (V)	0.11	-0.08	-0.09	-1.21			

Legend:
- **Green** values: voltage portion increased approaching the nominal value;
- **Red** Values: voltage portion increased moving away from the nominal value;
- **Orange** Values: voltage portion decreased moving away from the nominal value;
- **Dark-green** values: voltage portion decreased approaching the nominal value.

Analysing the previous table its possible to see that the second solution improve the voltages magnitudes.

EV Control Strategies Parameters:

- **Primary frequency control Strategies (F_control):**

Scenario	Phase A (kW)	Phase B (kW)	Phase C (kW)	EV1 P (kW)	EV2 P (kW)	Microgrid (kW)	VSI Q (Var)	F (Hz)
Load	14950	7942	5907	2491.5	2491.5	28799		
Generation	10000	15000	15000	0	0	40000	14763	50.38
Total	-4950	7058	9093	2491.5	2491.5	**11200.72**		

- **Primary voltage control Strategies (U_control):**

Scenario	Phase A (kW)	Phase B (kW)	Phase C (kW)	EV1 P (kW)	EV2 P (kW)	Microgrid (kW)	VSI Q (Var)	F (Hz)
Load	12458	7942	5823	0	2407.2	26223		
Generation	12636	15000	15000	2635.5	0	42636	11151	50.55
Total	177	7058	9177	-	-	**16412.02**		

- **Combination of Primary frequency and voltage control Strategies (UvsF_control):**

Scenario	Phase A (kW)	Phase B (kW)	Phase C (kW)	EV1 P (kW)	EV2 P (kW)	Microgrid (kW)	VSI Q (Var)	F (Hz)
Load	12458	7942	5823	0	2407.2	26223		
Generation	12635	15000	15000	2634.6	0	42635	11151	50.56
Total	176	7058	9177	2634.6	2407.2	**16411.12**		

EV Control Strategies Graphics:

Table A.9 — Time Evolution of Node 5 Voltages Magnitudes for the EV control Strategies

Node 5 Voltages Magnitudes	
F_Control	**U_Control**
Figure A.**40 – Time Evolutions of the** Node 5 Voltages Magnitudes in EV **F_Control**.	Figure A.41 – Time Evolutions of **the** Node 5 Voltages Magnitudes in EV **U_Control**.
UvsF_Controlo	
Figure A.42 – Time Evolutions of **the** Node 5 Voltages Magnitudes in EV **UvsF_Control**.	

Table A.10 — Time Evolution of Node 15 Voltages Magnitudes for the EV control Strategies

Node 15 Voltages Magnitudes	
F_Control	**U_Control**

Figure A.43 – Time Evolutions of **the** Node 15 Voltages Magnitudes in EV **F_Control**.

Figure A.44 – Time Evolutions of **the** Node 15 Voltages Magnitudes in EV **U_Control**.

UvsF_Controlo

Figure A.45 – Time Evolutions of **the** Node 15 Voltages Magnitudes in EV **UvsF_Control**.

Table A.11 — Time Evolution of Node 25 Voltages Magnitudes for the EV control Strategies

Node 25 Voltages Magnitudes	
F_Control	**U_Control**
Figure A.46 – Time Evolutions **the** Node 25 Voltages Magnitudes in EV **F_Control**.	Figure A.47 – Time Evolutions of **the** Node 25 Voltages Magnitudes in EV **U_Control**.
UvsF_Controlo	
Figure A.48 – Time Evolutions of **the** Node 25 Voltages Magnitudes in EV **UvsF_Control**.	

Table A.12 — Time Evolution of Node 5 Voltages Unbalance Factors for the EV control
Strategies

Node 5 Voltages Unbalance Factors	
F_Control	**U_Control**
Figure A.49 – Time Evolutions **the** Node 5 Voltages unbalance factors in EV **F_Control**.	Figure A.50 – Time Evolutions of **the** Node 5 Voltages unbalance factors in EV **U_Control**.
UvsF_Controlo	
Figure A.51 – Time Evolutions of **the** Node 5 Voltages unbalance factors in EV **UvsF_Control**.	

Table A.13 — Time Evolution of Node 15 Voltages Unbalance Factors for the EV control Strategies

Node 15 Voltages Unbalance Factors	
F_Control	**U_Control**
Figure A.52 – Time Evolutions **the** Node 15 Voltages unbalance factors in EV **F_Control**.	Figure A.53 – Time Evolutions of **the** Node 15 Voltages unbalance factors in EV **U_Control**.
UvsF_Controlo	
Figure A.54 – Time Evolutions of **the** Node 15 Voltages unbalance factors in EV **UvsF_Control**.	

Table A.14 — Time Evolution of Node 25 Voltages Unbalance Factors for the EV control Strategies

Node 25 Voltages Unbalance Factors	
F_Control	**U_Control**
Figure A.55 – Time Evolutions **the** Node 25 Voltages unbalance factors in EV **F_Control**.	Figure A.56 – Time Evolutions of **the** Node 25 Voltages unbalance factors in EV **U_Control**.

UvsF_Controlo
Figure A.57 – Time Evolutions of **the** Node 25 Voltages unbalance factors in EV **UvsF_Control**.
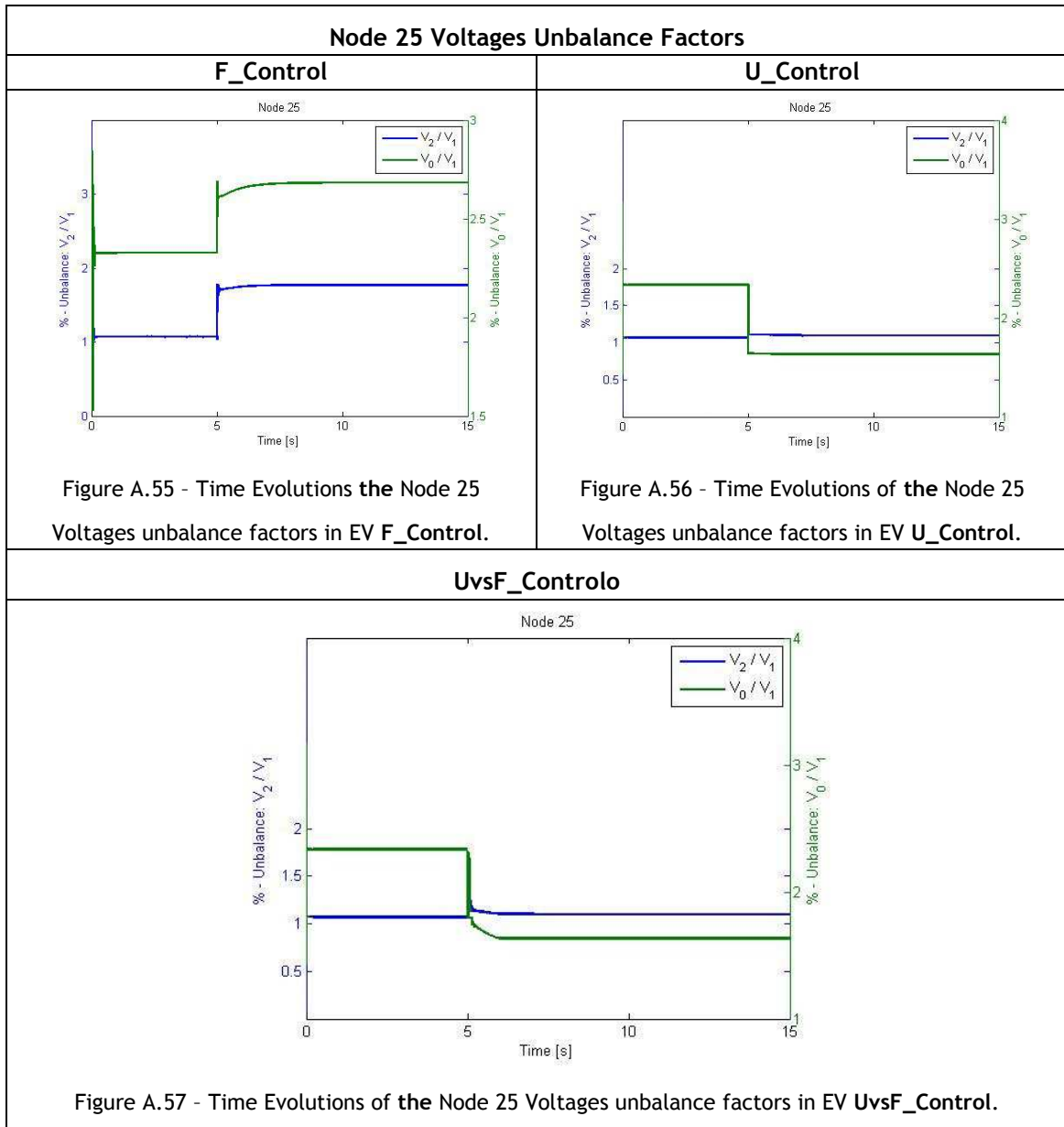
Table A.15 — Time Evolution of Node 69 Voltages Unbalance Factors for the EV control Strategies
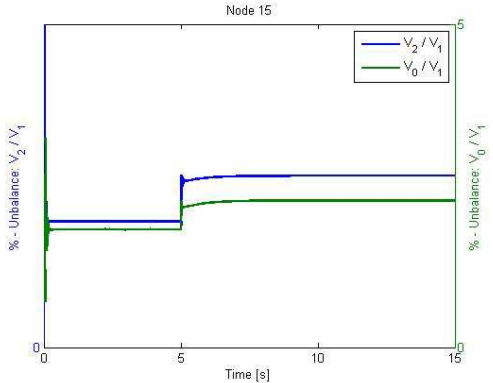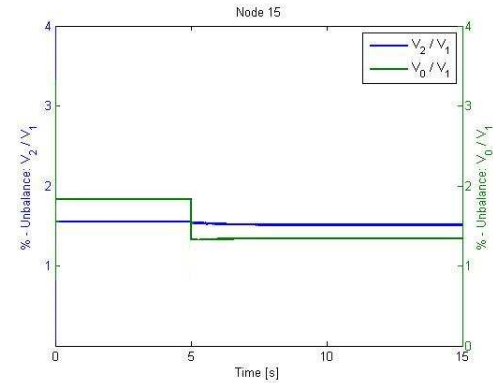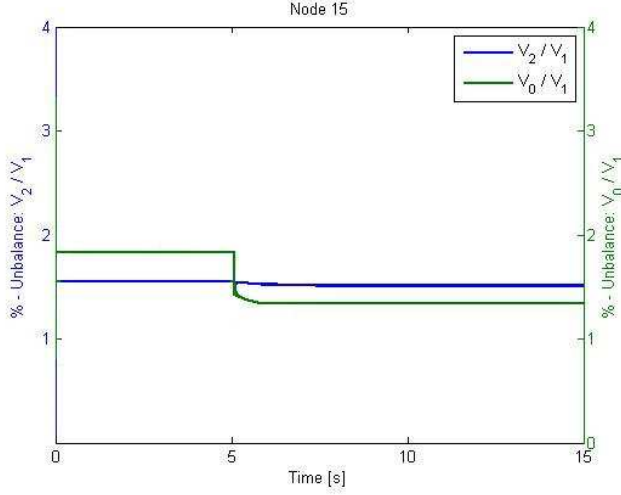
Node 69 Voltages Unbalance Factors	
F_Control	**U_Control**
Figure A.58 – Time Evolutions **the** Node 69 Voltages unbalance factors in EV **F_Control**.	Figure A.59 – Time Evolutions of **the** Node 69 Voltages unbalance factors in EV **U_Control**.
UvsF_Controlo	
Figure A.60 – Time Evolutions of **the** Node 69 Voltages unbalance factors in EV **UvsF_Control**.	
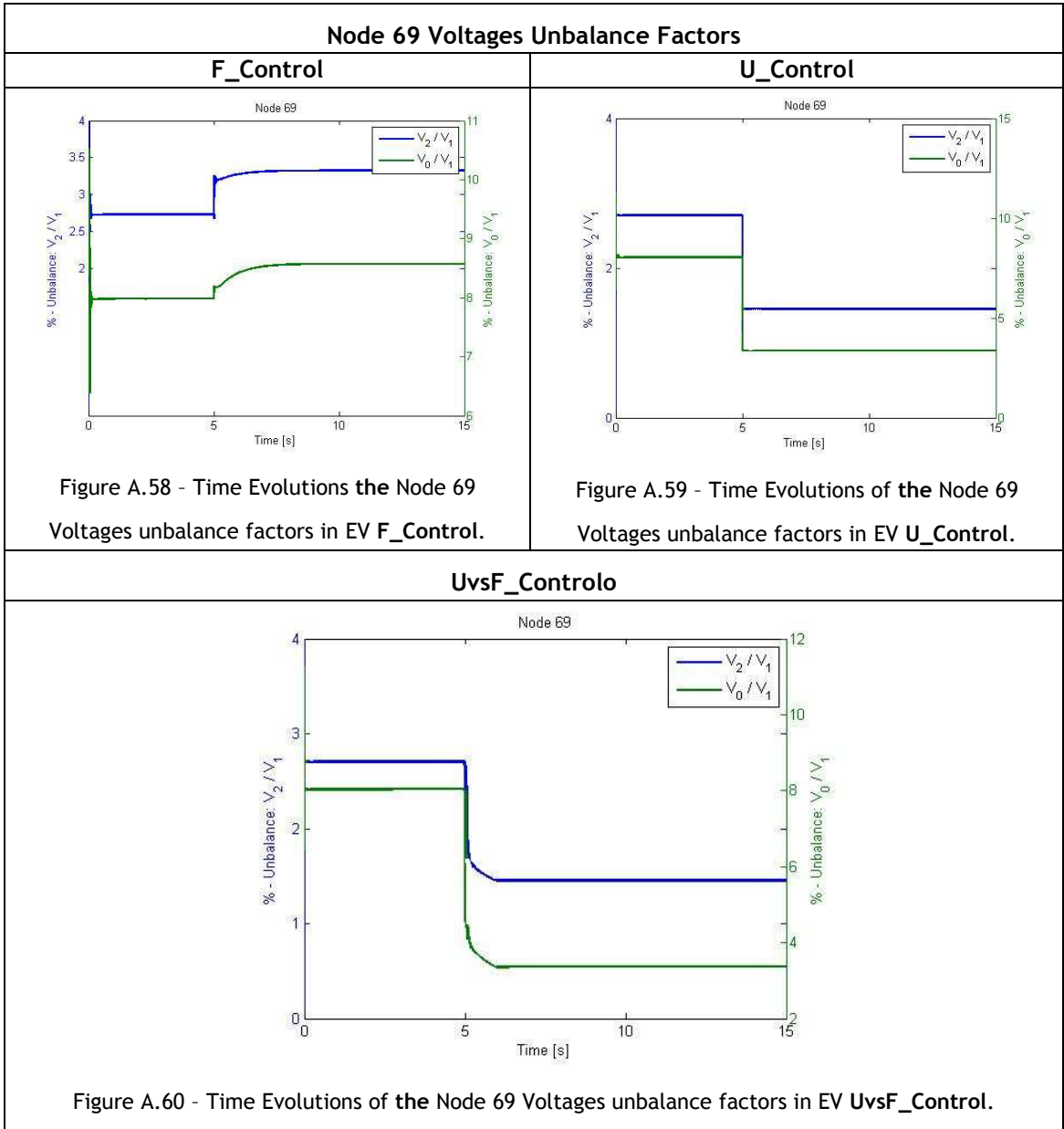
EV Control Strategies Voltages Values:

Table A.16 — Primary frequency control Voltages (F_control)

Node	5	15	25	69	Max	Min
Phase A (V)	223.80	227.55	218.21	**197.85**	227.55	197.85
Phase B (V)	224.58	238.79	228.41	228.12	238.79	224.58
Phase C (V)	226.13	241.69	232.33	242.25	242.25	226.13

For a first analysis it possible to realize that the voltages highlighted in green and red correspond to the highest and lowest voltage magnitude in MG. They are in the same node, the 69, and their values are significantly far from the nominal value (230 V).

As mentioned in the previous chapter through simulations it was possible to achieve the appropriate parameters to regulate the local voltages magnitudes that can be found in the Appendix C.

Table A.17 — Primary voltage control Voltages (U_control)

Node	5	15	25	69	Max	Min
Phase A (V)	224.82	231.80	223.06	**221.92**	231.80	221.92
Phase B (V)	225.60	239.04	228.44	223.76	239.04	223.76
Phase C (V)	227.16	242.55	232.90	239.19	242.55	227.16

The combination of both control strategies results in the following table values.

Table A.18 — Primary frequency and voltage control Voltages Predictions (UvsF_control)

Node	5	15	25	69	Max	Min
Phase A (V)	224.83	231.75	223.06	**221.95**	231.75	221.95
Phase B (V)	225.60	239.00	228.44	223.57	239.00	223.57
Phase C (V)	227.17	242.50	232.90	239.16	242.50	227.17

The following table compare the relevant parameters between the frequency and voltage primary control strategies.

Table A.19 — Comparison between primary voltage and frequency control strategies

Node	5	15	25	69	VSI Q	f	VSI P
Phase A (V)	0.92	3.61	4.17	20.51			
Phase B (V)	0.92	0.23	0.06	-3.91	-3292	0.17	4593
Phase C (V)	0.92	0.86	0.63	-1.90			

Legend:
- **Green** values: voltage portion increased approaching the nominal value;
- **Red** Values: voltage portion increased moving away from the nominal value;
- **Orange** Values: voltage portion decreased moving away from the nominal value;
- **Dark-green** values: voltage portion decreased approaching the nominal value.

At this point with the values of the two primary control strategies it is possible to see that with the voltage control the frequency increase slightly, but the voltages magnitudes become

more acceptable. However, the maximum has increased this happened in another node, meaning that the desired voltage local control is working.

The next two tables compare the combination of the two controls, first with the frequency control and second with the voltage control.

Table A.20 — Comparison between the Combination of the two controls and primary frequency control strategy

Node	5	15	25	69	VSI Q	f	VSI P
Phase A (V)	1.03	4.21	4.85	24.11			
Phase B (V)	1.03	0.21	0.04	-4.55	-3608	0.18	5273
Phase C (V)	1.03	0.81	0.57	-3.10			

Table A.21 — Comparison between the Combination of the two controls and primary voltage control strategy

Node	5	15	25	69	VSI Q	f	VSI P
Phase A (V)	0.01	-0.05	0.01	0.04			
Phase B (V)	0.01	-0.05	0.01	-0.20	4	0.01	-9
Phase C (V)	0.01	-0.05	0.00	-0.03			

Analysing the two tables it is possible to see that mainly the combination of the two controls bring wiser electric magnitudes. This case has a closer behaviour to the primary voltage control showing better values, even if the frequency has not the same improvement it is inside the limits. It is also easily recognized the progress of the local voltages magnitudes in the node of EV, one of the biggest concerns.

D. PV control Strategy

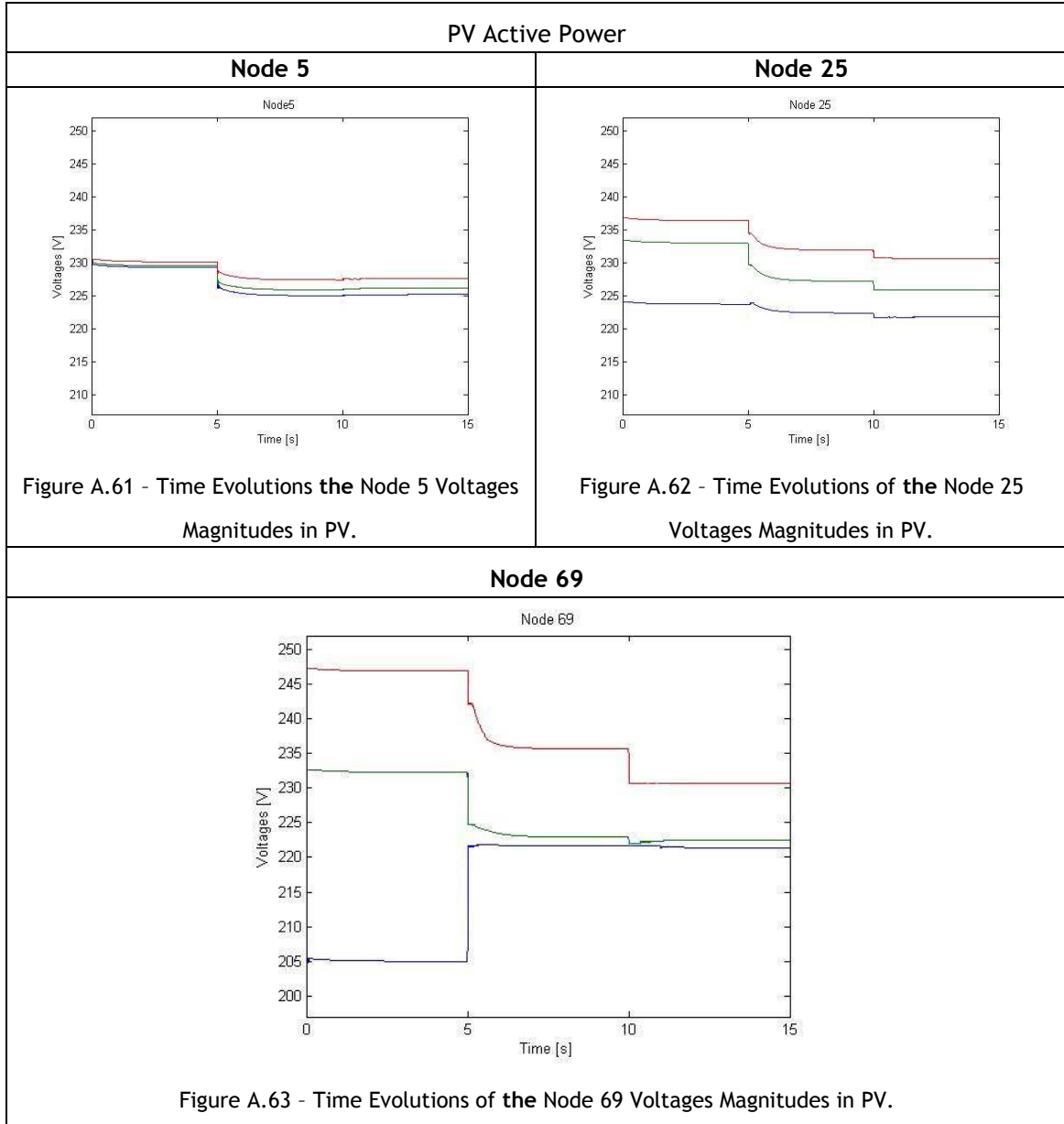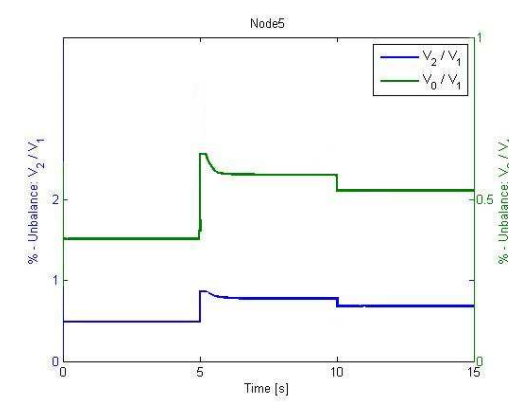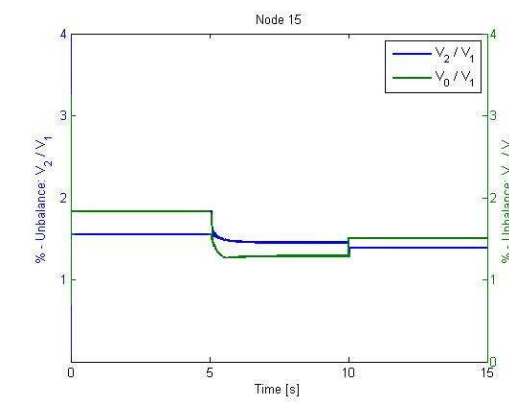Table A.22 — Time Evolution of Node 5 Voltages Magnitudes for the PV control Strategies
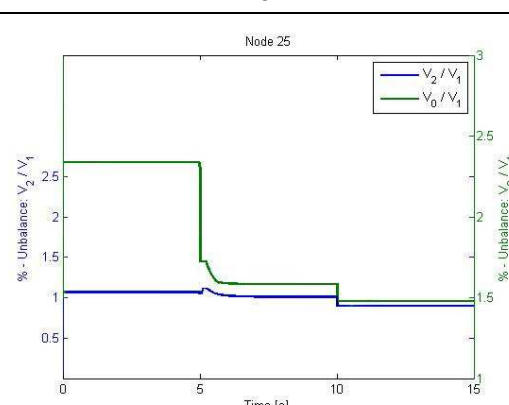
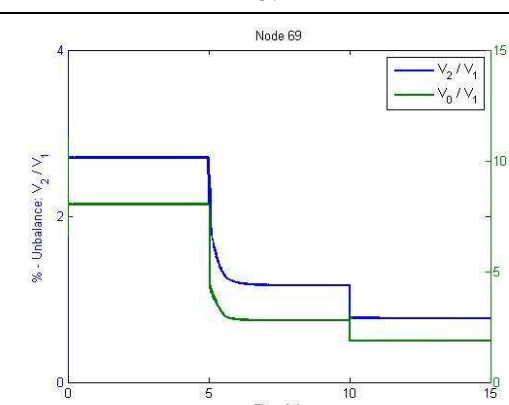| PV Active Power	
Node 5	**Node 25**
Figure A.61 – Time Evolutions **the** Node 5 Voltages Magnitudes in PV.	Figure A.62 – Time Evolutions of **the** Node 25 Voltages Magnitudes in PV.
Node 69	
Figure A.63 – Time Evolutions of **the** Node 69 Voltages Magnitudes in PV.	

Table A.23 — Time Evolution of Voltages Unbalance Factors for the PV control Strategies

5	15
Figure A.64 – Time Evolutions node 5 voltages unbalance factors in PV.	Figure A.65 – Time Evolutions node 15 voltages unbalance factors in PV.
25	**69**
Figure A.66 – Time Evolutions node 25 voltages unbalance factors in Scenario 2.3.	Figure A.67 – Time Evolutions node 69 voltages unbalance factors in PV.